ADVANCED OBJECT CHARACTERIZATION AND MONITORING TECHNIQUES USING POLARIMETRIC IMAGING

A Thesis

Presented to

The Graduate Faculty of The University of Akron

In Partial Fulfillment

of the Requirements for the Degree

Master of Science

Bharath Kumar Reddy Mandadi

August, 2009

ADVANCED OBJECT CHARACTERIZATION AND MONITORING TECHNIQUES USING POLARIMETRIC IMAGING

Bharath Kumar Reddy Mandadi

Thesis

Approved:	Accepted:
______________________	______________________
Advisor Dr. George C. Giakos	Department Chair Dr. Alex De Abreu Garcia
______________________	______________________
Faculty Reader Dr. Malik Elbuluk	Dean of the College Dr. George K. Haritos
______________________	______________________
Faculty Reader Dr. Michael McGarry	Dean of the Graduate School Dr. George R. Newkome
	______________________
	Date

ABSTRACT

The main purpose of this research study was to explore the potential application of polarimetric principles in characterization and monitoring of space materials. Space monitoring and collision avoidance between space vehicles and inter-space debris has become a major concern for space agencies and authorities maintaining satellites, space shuttles and stations. Inter-space debris can be man-made or natural. As the quantity of space debris increases, tracking and collision avoidance becomes a critical issue.

The novelty of this study consists in the single pixel analysis of back scattered optical polarimetric signatures from various space materials. Surface characterization of different materials was performed by analysis of their polarization response. The study employed single-pixel detection of back scattered laser beam polarimetric signatures obtained from different materials. The back scattered optical polarimetric signatures contained major information related to geometry, texture and composition of the material.

The DOLP (Degree of Linear Polarization) algorithm was applied to analyze polarization response from the different materials used in this study. Different materials used in space vehicle design were examined and the DOLP ratio was calculated at different material and detector orientations. On examining Teflon, which is a soft polymer material used in space vehicle design, we observed high depolarization of light. This was due to the “Diffuse reflectance” nature of Teflon at different object orientations.

Hence, Teflon can be identified as a “Lambertian surface” exhibiting high depolarization of light. The polarization response exhibited by materials such as windowless polysilicon solar panel and a wooden stick painted in white color mixed with titanium dioxide was found to be similar to the response exhibited by Teflon. It was observed that the extent of depolarization exhibited by different materials was found to be distinct and depended on material composition.

Materials such as Kapton and shiny aluminum foil exhibited sharp backscattered intensity distributions with high polarization of light at different orientations. The sharp back scattered intensity distributions of Kapton and shiny aluminum foil indicated their high polarization and “Specular reflectance” nature. Different metallic materials such as roughened aluminum, molybdenum and stainless steel were examined. It was observed that the backscattered distributions exhibited by roughened aluminum, molybdenum and stainless steel were broadened curves with distinct depolarization signatures. The depolarization exhibited by roughened aluminum was due to discontinuities present on its surface.

Windowed solar panels made of amorphous silicon and polysilicon materials were tested and it was observed that both of the panels exhibited similar sharp backscattered distributions. It was observed that the amorphous silicon solar panel exhibited higher depolarization of light than the polysilicon solar panel.

The experimental results indicated that single pixel polarimetric imaging can effectively sense and characterize various space materials based on the amount of optical depolarization and backscattered intensity distributions; suggesting its potential application in space research and sensing, with emphasis on the monitoring of space objects.

ACKNOWLEDGEMENTS

My foremost gratitude goes to my advisor Dr. Giakos for allowing me to work under him. It has been a great opportunity and joy working with Dr. Giakos. He has been very helpful to me since 2 years especially during laboratory experiments. I have learnt many things about life from Dr. Giakos. He has been more than an advisor for me. I cannot forget the moments I had with Dr. Giakos. He is truly an inspiring and energetic human I have ever seen. Thank you very much for all that you have provided me.

I would like to thank Dr. McGarry and Dr. Elbuluk for their support as my committee members. I am greatly indebted to my department chair Dr. Alex for providing me departmental assistantship. I take this opportunity to thank all teaching and non-teaching staff of Electrical and Computer Engineering department for their support since 2 years.

I dedicate every success in my life to my parents. They always encouraged me towards success. My sister has been very supportive and good friend of me since childhood. Her sweet kids, my nephew’s sai and abhi have always loved me and wished for my success, thank you for your love and support. I thank all my friends at Akron for their kind support.

TABLE OF CONTENTS

LIST OF TABLES

LIST OF FIGURES

CHAPTER I

INTRODUCTION

1.1 Overview of Optical Imaging

Over the past two decades, there has been a growing interest among the research community in the areas of optical imaging and opto-electronics. A plethora of applications in fields such as optical fibers, lasers, biomedical, space monitoring and homeland security has made optical imaging a promising technology among different imaging modalities.

1.2 Optical Imaging Using Polarization Principles

Polarization properties of light have been used by many researchers over the last few years for the purpose of diagnostic imaging, surface characterization and object detection. Optical polarimetric imaging using polarization properties of light offers unparalleled advantages for characterization and detection problems in real time systems. Polarization imaging can produce high sensitivity and high specificity images under low light conditions [16-21]. Imaging of polarimetric back scattered optical signatures from the material can be used for material characterization in terms of its orientation, texture, molecular and chemical composition [6].

Optical imaging technique is highly preferred over other techniques such as x-rays, ultrasound and digital radiography because of its non-contacting and non-destructive nature [30]. The ability of polarimetric imaging to detect and characterize materials depends on the conservation of backscattered signatures and also on the assumption of maintenance of initial polarization state by weakly scattered light [18]. The polarization of backscattered light depends on a number of physical and geometrical factors. Table 1.1 describes factors affecting polarization of backscattered light [18].

Table 1.1 Factors affecting backscattered polarization

Factors Affecting Polarization State of the Scattered Light Radiation
Incident polarization state
Size of the scatterer
Shape of the scatterer
Concentration of the scatterer
Refractive indexes of the scatterer and the surrounding medium

1.3 Problem Definition

Space monitoring and collision avoidance between space vehicles has become a major concern for space agencies and authorities maintaining satellites, space shuttles and stations. “According to NASA a massive cloud of approximately 19,000 objects including satellite debris currently pollute the low and high orbit space around the planet"

[22]. “NASA database details 1,951 debris impacts to the space shuttle through 2006, requiring windows and radiators to be replaced”. The U.S. Space Command tracks 13,943 orbiting objects 4 inches or larger out of which only 900 are active satellites [23].

The above mentioned figures explain the intensity of collision problem between space vehicles and inter-space debris which can be either man-made or natural. As the quantity of space debris increases, tracking and collision avoidance becomes a critical issue.

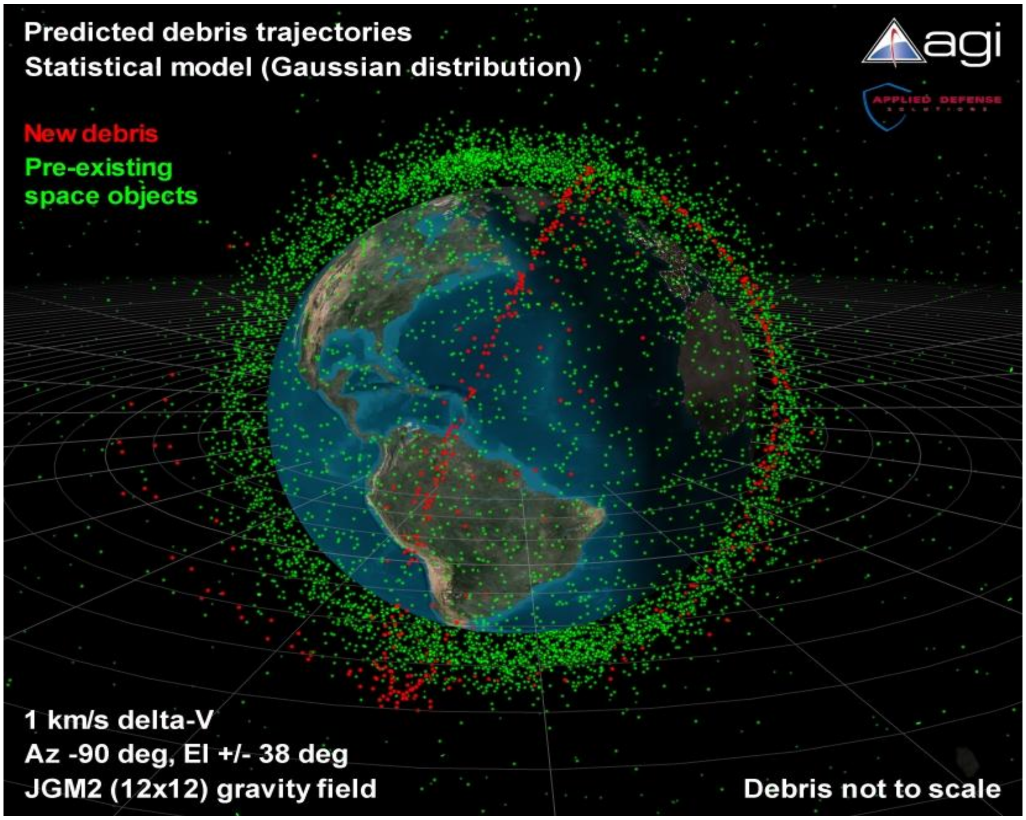

Figure 1.1 Picture depicting space debris distribution [33]

1.4 Proposed Methodology

The proposed technique makes use of optical imaging to sense polarization signatures on a pixel basis from different scattering surfaces. The obtained polarization signatures can serve as markers for object shape, orientation and composition.

The study utilized an efficient polarimetric imaging technique at different sensing positions and imaging the polarization response of objects at different orientations. The proposed single pixel detection algorithm based on polarimetric imaging makes use of depolarization characteristics of different materials for the purpose detection, identification and classification of different space materials. The advantages of single pixel detection include [6]:

a) Ability to concentrate on desired pixels on target enabling extraction of minute details pertaining to object.
b) High scatter rejection imaging for detection of unresolved objects from clutter.
c) High sensitivity
d) Enhanced discrimination capabilities
e) Reduced noise from interfering signals of adjacent pixels.

1.5 Objectives of The Study

a) To develop an optical imaging system capable of sensing polarimetric signatures at different scattering and object orientations.
b) To examine the depolarization characteristics of different materials by analyzing the DOLP (Degree of Linear Polarization) ratio of the backscattered optical signatures.

1.6 Null Hypotheses of The Study

a) The optical polarimetric backscattered signatures contained no significant information about different materials; therefore all the materials are indistinguishable from each other.

b) There is no significant difference in the polarization response exhibited among different man-made or natural space materials.

1.7 Alternate Hypotheses of The Study

a) A significant amount of information regarding material texture, orientation and composition can be obtained by examining backscattered optical polarimetric signatures.

b) There is significant difference in the polarization response exhibited by different space materials either man-made or natural.

1.8 Limitations of The Study

a) The experiment was performed using single wavelength laser source operating at 830 nm. Multispectral interrogation of objects is desirable.

b) An automatic positioning of the receiver detector is highly desirable.

c) Degree of polarization (DOP) study of the backscattered polarimetric signatures is desirable.

1.9 Organization of The Study

The rest of this thesis is organized as follows. Chapter 2 briefly describes the work carried out by researchers in the field of optical imaging. Chapter 3 describes basic principles of light, polarimetry, Stokes parameters and Mueller matrices. Chapter 4 presents the experimental procedure, calibration of components and error analysis. Chapter 5 describes the equipment used in the study and their specifications. Chapter 6 presents a detailed study of the results obtained through the experiment. Finally, in chapter 7, conclusions drawn from the study and future works are discussed.

CHAPTER II

LITERATURE REVIEW

2.1 Optical Imaging Using Polarimetric Principles

Optical imaging has been a major area of interest over the last few years. A significant number of research studies were performed in the areas of biomedical, object detection and remote sensing. Most of the studies used polarization properties of light for various classification problems. This chapter briefly describes the work carried out by researchers in the field of optical imaging.

2.2 Optical Imaging through Scattered Media

Rowe et al [3] developed a polarization difference imaging technique to enhance the surface visibility of targets suspended in scattering media. The system used CCD camera to image the aluminum disk target suspended in dilute milk. The technique captured the two orthogonal linear polarization images of scene and computed the difference pixel by pixel and rescaled the resultant difference image. The images obtained through polarization difference imaging technique showed an increased visibility of targets in scattering media.

Das et al [1] developed an ultrafast time-gated optical detection system to image a translucent object hidden in a highly scattered media. The proposed detection method separates snake photons from the diffuse and used obtained snake photons to image the hidden object with different optical properties. The study demonstrated that a 2.5-mm-thick fat tissue embedded inside a 40-mm-thick chicken breast tissue can be detected using ultrafast time-gated optical system.

Bucher et al [2] experimented propagation of light pulse through atmospheric clouds. The study consisted of interrogating multi path propagation effects of light through clouds focusing on loss factors in the optical communication. The experiments used a Q-switched ruby laser producing 30 nsec light pulses as transmitter. The received pulse duration was 1-10 microseconds when there was a cloud in the transmission path. The study attributed the multipath time lengthening of light pulses to multiple scattering of light inside the cloud.

Lewis et al [4] employed a method for increasing target contrast in a turbid environment. The polarization state of scattered light was utilized for calculating target contrast. It was shown that discrimination based on detection of cross-polarized intensities is more efficient and effective than total intensity information.

2.3 Optical Polarimetric Analysis

Giakos [5] proposed a multispectral, multifusion, optical imaging system based on polarimetric principles. The study was based on interrogation of target in a scattered media using Mueller matrix, rotating retarder, fusion of dual-energy subtraction principles. The results of the study indicated that high contrast images can be obtained by backscattered photons from the target embedded in scattered media.

Giakos et al [6] explored multispectral polarimetric space surveillance techniques for improving ladar performance. The results of the study indicated that an enhanced signal-to-noise ratio of backscattered signals can be obtained using polarimetric techniques, thus improving ladar range accuracy.

Giakos et al [7] developed a novel optical imaging technique for detection, classification and monitoring of semiconductor, microelectronic components, and space craft defects. Cadmium Zinc Telluride (CdZnTe) and Pentium chip were used as test subjects in the study. The image contrast was significantly improved by DOLP polarimetric images over the average polarimetric image.

Breugnot and Clemenceau [8] demonstrated a novel polarization active imager operating at wavelength of 806 nm. An imaging system operating in monostatic configuration was developed using laser to illuminate a target and a CCD camera was used to acquire intensity and polarization degree. The method actively detected targets buried under ground with same reflectivity but different polarization degree. It was also demonstrated that a polarization imager can increase image contrast and detection performance.

Alouini et al [9] developed an active polarimetric multispectral imaging system for target detection and discrimination. Targets of various kinds like synthetic foam, wood, metallic plane, and sand blasted aluminum, stone were used in the study. Different objects are classified through their degree of polarization and reflectance information which is obtained from orthogonal state contrast images. The study proved that polarimetric and multispectral imaging significantly increased target detection capabilities.

Duggin et al [10] studied polarization analysis of targets in differing albedo and shadow depth. The study demonstrated that the polarization is strongly dependent on scene radiation at the sensor over a dynamic range of radiance values. A Kodak digital camera was used for obtaining intensity and polarization images. The degree of polarization was calculated at near infrared, green and red bands and it was proved that scene radiance values depended strongly on target illumination, shadow depth, albedo and type of target. These factors affected polarization state as polarization is strongly related to scene radiation.

2.4 Depolarization Analysis

Deboo et al [11] studied the polarization properties of light scattered or diffusely reflected by various man-made surfaces. A Mueller matrix imaging polarimeter at fixed bistatic configuration was used for the purpose of target analysis. Depolarization indices of different targets were found at varying target angles. The results of this study concluded that depolarization degree was minimal at specular reflection and increased with increase of scatter which relating to angle of incidence. It was also shown that circular polarization states were more depolarized than linear states.

Egan et al [12] investigated depolarization properties of various complex surfaces like basalt, volcanic ash, wet and dry sand, gravel, silt and different foliage. The study determined that the depolarization degree increases with decrease in individual particle size, increase of surface roughness, porosity and increase of water level (wetness of surface). It was also shown that dryness of surface increases depolarization index. The outcome of this study has been mainly useful for surface characterization through depolarization properties of different materials.

2.5 Target Classification Using Polarimetry

Chun and Sadjadi [13] developed a laser radar target classification system based on optical polarimetric principles. The study used a combination of attributes to determine the build and composition of target instead of using conventional range value at target pixel to determine target's 3-D shape. The tools used for this purpose were intensity, range and degree of polarization. Target identification and classification efficiency was improved using polarization components of reflected light. This technique effectively resolved the discrimination problems arising from ambiguity between targets of the same class.

Lavigne et al [14] proposed an enhanced military target classification methodology using active and passive polarization imaging. The study indicated that there was a significant enhancement in the target contrast when the polarization state of the reflected light from the ambient light sources like sun and moon was added to active imaging using direct polarized laser source. A set of polarimetric signatures of various military targets were acquired during differing climate conditions were recorded. The images encoded with degree of polarization enabled discrimination of different man-made targets from the natural background.

2.6 Conclusion

A review of literature pertaining to optical imaging was done. Optical imaging using polarization properties of light has been used by researchers for solving many classification and detection problems. Researchers have mainly used linear, circular polarization state analysis of light with Stokes parameters and Mueller matrices for purpose of target identification and contrast enhancement. It can be observed from various studies that polarimetric principles are mainly applied towards identification of objects which are embedded in scattered media and buried underground. The application of polarimetric principles for classification of space materials using the proposed method is a novel technique. The proposed highly sensitive single pixel technique uses DOLP analysis for classification and monitoring of space materials. The proposed methodology is discussed in more detail in the later chapters of this thesis.

CHAPTER III

POLARIMETRIC THEORY

3.1 Wave Nature of Light

The wave-like behavior describes light as an electromagnetic wave consisting of electric and magnetic fields. An electromagnetic wave can be completely predicted by classical "Maxwell's equations" [24]. The Maxwell's equations for an electromagnetic wave are given by:

$$\nabla.\vec{E} = \frac{\rho}{\varepsilon_0} \tag{3.1}$$

$$\nabla.\vec{B} = 0 \tag{3.2}$$

$$\nabla \times \vec{E} = -\frac{\partial \vec{B}}{\partial t} \tag{3.3}$$

$$\nabla \times \vec{B} = \left(\vec{J} + \varepsilon_0 \frac{\partial \vec{E}}{\partial t} \right) \tag{3.4}$$

Where E is the electric field, B is the magnetic field, μ_0 and ε_0 are permeability and permittivity of vacuum respectively, ρ and $\vec{J}$ are the volume charge and current density respectively [24].

3.2 Polarized Light

Light is described as an electromagnetic wave comprising of oscillating electric and magnetic fields. The electric field of an electromagnetic wave can be decomposed into two orthogonal components of specific amplitude and phase. One of the fundamental properties of light is its polarization which is described as the process of converting unpolarized light into polarized light. Polarized light waves are those whose oscillations take place in a single plane. The polarization direction is defined by the electric field vector.

A wave propagating along y-axis is said to be linearly polarized (i.e. the two orthogonal components are in phase) in vertical direction if the electric field oscillates along the z-axis and horizontally polarized if the electric field lies along the x-axis (figure 3.1). If the angle between the two orthogonal components is 45° then the light is said to be linearly polarized with phase angle of 45° degrees (figure 3.2). As the projection of polarization along axes determines the amplitude of two components, light polarized at 45° will have equal amplitude and phase for both vertical and horizontal polarizations [25]. Light is said to be circularly polarized (figure 3.3) when two orthogonal components have phase difference of 90° and elliptically polarized (figure 3.4) for any phase difference other than 90° [25].

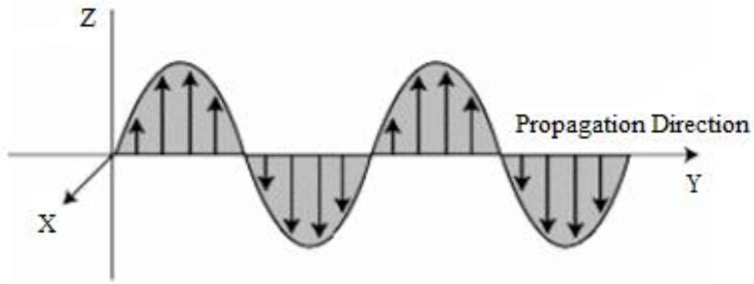

Figure 3.1 Linear polarization of light [25]

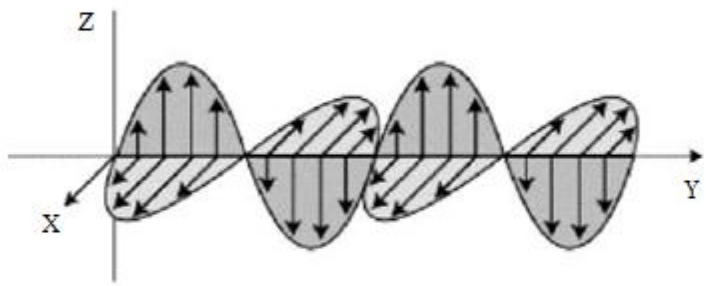

Figure 3.2 Linear polarization of light at 45 Degrees [25]

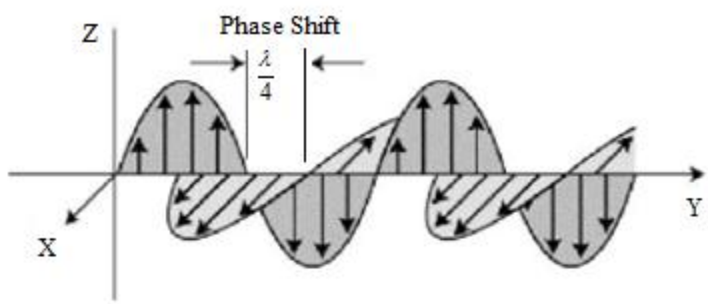

Figure 3.3 Circular polarization of light [25]

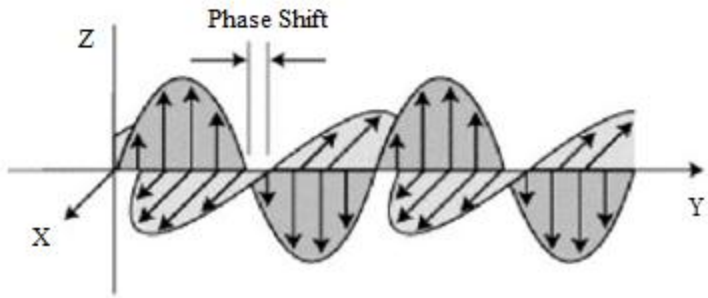

Figure 3.4 Elliptical polarization of light [25]

3.3 Polarimetry

Polarizer is one of the basic optical elements in polarimetry. A polarizer transmits light with electric field component parallel to its transmission axis with a desired polarization state independent of incident polarization state and rejects all other planes. The maximum transmission occurs when electric field component of incident beam is parallel to the polarization axis [27]. The maximum intensity beam when passed through a polarizer whose axis is perpendicular to incident beam transmits light with some intensity; this is very low and indicates non-perfect nature of polarizer. The non-perfect nature of polarizer is known as “Depolarization” due to which polarized light is turned to unpolarized light [27].

Retarder is another basic element in polarimetry which is used to shift the phase between two orthogonal fields of light wave. This principle of change of phase between two orthogonal components is known as “Retardance’’ or “Phase Retardance”. A retarder produces a predetermined phase difference between the two orthogonal waves independent of incident polarization state [27].

A technique used to measure polarization state of light and response of different materials to polarization is known as “Polarimetry”. The response of different materials is generally in terms of diattenuation, retardance and depolarization which can be determined by knowing the polarization state of incident and transmitted, reflected or backscattered light from material. [26]

Polarimetry deals with polarization generation and analysis [26]. A polarization generator produces a beam of known polarization state. It mainly consists of a light source (most common source is a laser beam), optical elements (optical chopper, filter, beam expander) and polarization elements (polarizer, retarder). A polarization analyzer analyses the polarization states of the backscattered optical signals from different materials. It mainly consists of optical elements such as lenses, polarizers, retarders and a detector.

3.4 Stokes Parameters

The Stokes parameter describes the polarization state of an electromagnetic wave [28-29]. The Stokes parameters were described in terms of two orthogonal electric field components as:

For a plane wave,

$$S_0 = E_{0x}^2 + E_{0y}^2 \tag{3.5}$$

$$S_1 = E_{0x}^2 - E_{0y}^2 \tag{3.6}$$

$$S_2 = 2E_{0x}E_{0y}\cos\delta \tag{3.7}$$

$$S_3 = 2E_{0x}E_{0y}\sin\delta \tag{3.8}$$

E_{0x} , E_{0y} are the two orthogonal electric field amplitudes and δ represent the phase difference between them.

Table 3.1 Description of Stokes Parameters [28-29]

Parameter	Description
S_0	Total intensity of light
S_1	Amount of linear horizontal or vertical polarization
S_2	Amount of linear $+45^\circ$ or -45° polarization
S_3	Amount of right or left circular polarization within the beam

For any polarization state of light, the stokes parameters always satisfy the relation

$$S_0^2 \geq S_1^2 + S_2^2 + S_3^2 \tag{3.9}$$

The equality in the above relation holds good for a completely polarized light and the inequality applies to partially polarized light or unpolarized light [28-29].

The Stokes vector is given by:

$$S = \begin{pmatrix} S_0 \\ S_1 \\ S_2 \\ S_3 \end{pmatrix} = \begin{pmatrix} E_{0x}^2 + E_{0y}^2 \\ E_{0x}^2 - E_{0y}^2 \\ 2E_{0x}E_{0y}\cos\delta \\ 2E_{0x}E_{0y}\sin\delta \end{pmatrix} \tag{3.10}$$

The Stokes vectors for some common polarization states of light are given by [28-29]:

For linearly polarized light (horizontal), $$S = \begin{pmatrix} 1 \\ 1 \\ 0 \\ 0 \end{pmatrix} \tag{3.11}$$

For linearly polarized light (vertical), $$S = \begin{pmatrix} 1 \\ -1 \\ 0 \\ 0 \end{pmatrix} \tag{3.12}$$

For linearly polarized light ($+45^0$), $$S = \begin{pmatrix} 1 \\ 0 \\ 1 \\ 0 \end{pmatrix} \tag{3.13}$$

For linearly polarized light (-45^0), $$S = \begin{pmatrix} 1 \\ 0 \\ -1 \\ 0 \end{pmatrix} \tag{3.14}$$

For left-handed circularly polarized light, $$S = \begin{pmatrix} 1 \\ 0 \\ 0 \\ 1 \end{pmatrix} \tag{3.15}$$

For right-handed circularly polarized light, $$S = \begin{pmatrix} 1 \\ 0 \\ 0 \\ -1 \end{pmatrix} \tag{3.16}$$

For unpolarized light, $$S = \begin{pmatrix} 1 \\ 0 \\ 0 \\ 0 \end{pmatrix} \tag{3.17}$$

3.5 Mueller Matrices

The study of polarization states include interaction of polarized light with various polarization elements which assume a change of polarization state at every interaction. Mueller matrices in combination with stokes parameters can be used to study the change of polarization state due to interaction of light with various elements or materials.

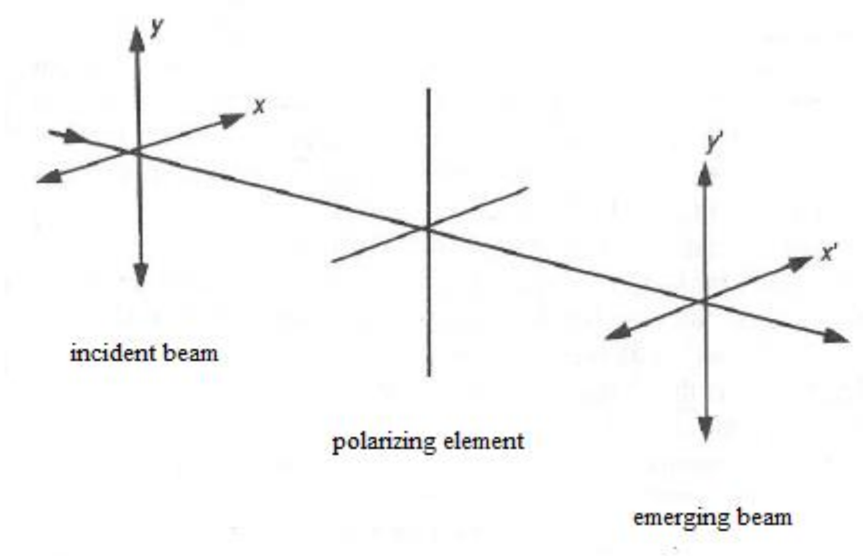

Figure 3.5 Change of polarization state as light interacts with elements [28]

A plane polarized light beam characterized by Stokes parameters $S_{0,}S_{1,}S_{2,}S_3$ when interacts with a polarizing element produces a beam with a polarization state given by Stokes parameters $S_0^{'}, S_1^{'}, S_2^{'}, S_3^{'}$ [28-29]. The relationship between incident beam and the emerging beam is given by [28-29]:

$$\begin{pmatrix} S_0^{'} \\ S_1^{'} \\ S_2^{'} \\ S_3^{'} \end{pmatrix} = \begin{pmatrix} m_{00} & m_{01} & m_{02} & m_{03} \\ m_{10} & m_{11} & m_{12} & m_{13} \\ m_{20} & m_{21} & m_{22} & m_{23} \\ m_{30} & m_{31} & m_{32} & m_{33} \end{pmatrix} \begin{pmatrix} S_0 \\ S_1 \\ S_2 \\ S_3 \end{pmatrix} \tag{3.11}$$

The equation can be simply represented as $S^{'} = M * S$. The 4×4 matrix M is known as Mueller matrix. The Mueller matrix of the linear horizontal polarizer is given by [28-29]:

$$M = \begin{pmatrix} 1 & 1 & 0 & 0 \\ 1 & 1 & 0 & 0 \\ 0 & 0 & 0 & 0 \\ 0 & 0 & 0 & 0 \end{pmatrix} \qquad (3.12)$$

The Stokes parameters of emerging beam can completely describe the polarization state of light and can be used to derive important parameters useful in polarimetric characterization of the materials. Some of the important parameters obtained from Stokes parameters are given by [28-29]:

Degree of Polarization,

$$\text{DOP} = \frac{\sqrt{S_1^2 + S_2^2 + S_3^2}}{S_0} \qquad 0 \le DOP \le 1 \qquad (3.12)$$

Degree of Linear Polarization,

$$\text{DOLP} = \frac{\sqrt{S_1^2 + S_2^2}}{S_0} \qquad 0 \le DOLP \le 1 \qquad (3.13)$$

Degree of Circular Polarization,

$$\text{DOCP} = \frac{S_3}{S_0} \qquad 0 \le DOCP \le 1 \qquad (3.14)$$

Ellipticity,

$$\text{e} = \frac{S_3}{S_0 + \sqrt{S_1^2 + S_2^2}} \qquad (3.15)$$

CHAPTER IV

METHODS AND PROCEDURES

4.1 Experimental Setup

The experiment was performed using an 830 nm continuous wave single mode laser source, set of polarizer's, an optical chopper, optical filter, lock-in-amplifier, oscilloscope and a nirvana detector. A variety of space materials were interrogated in back scattering geometry. The experiment was performed on optical tabletop and arranged as shown in the following figure 4.1.

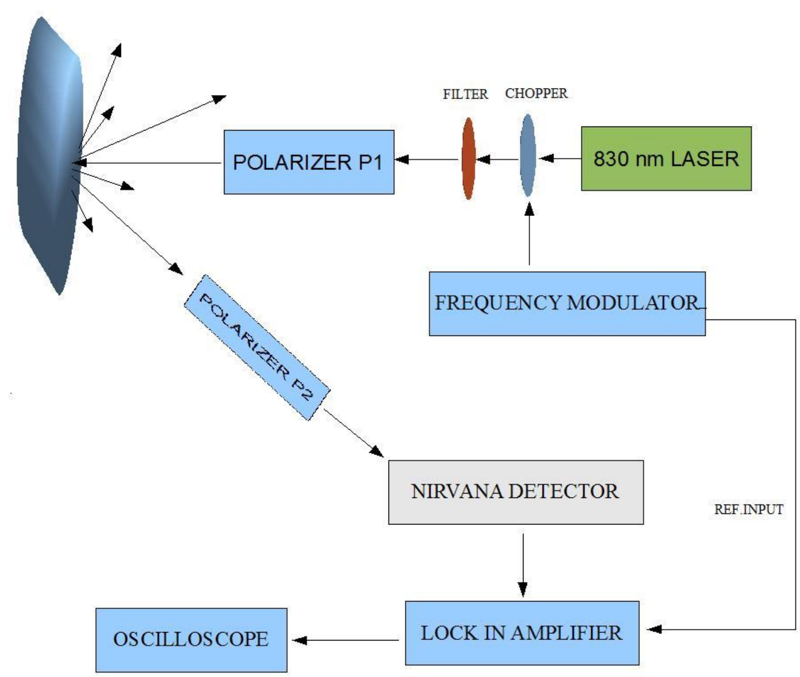

Figure 4.1 Experimental Setup

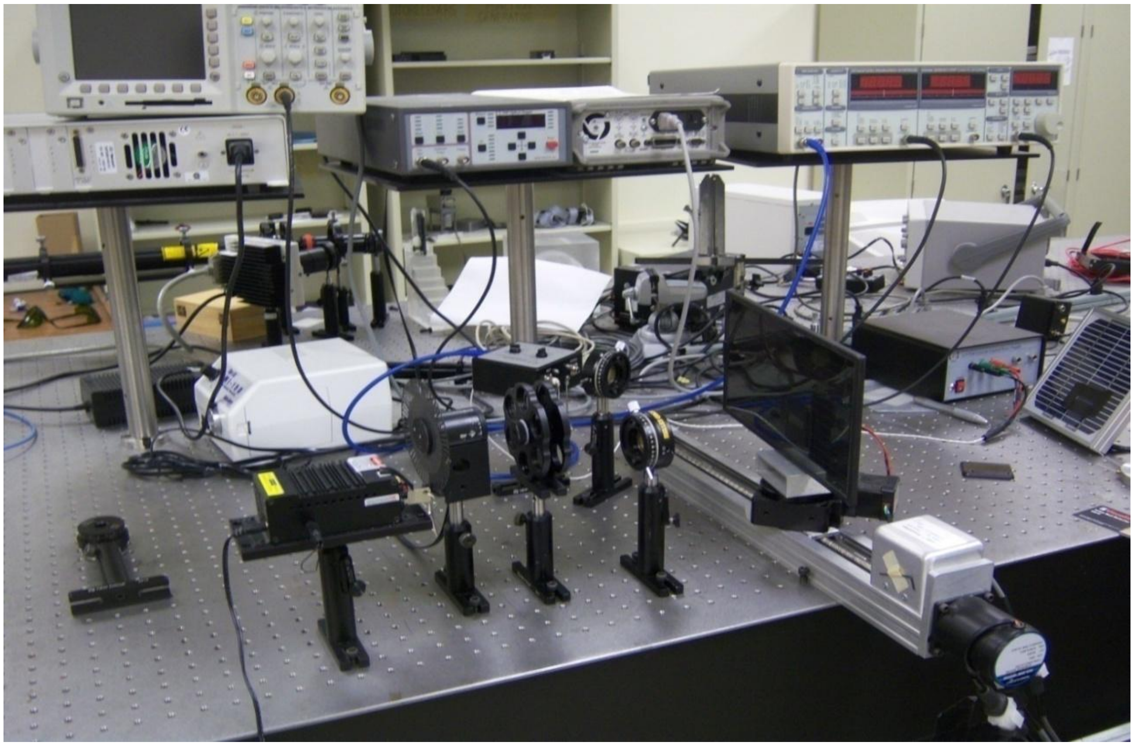

Figure 4.2 Photograph of experimental setup in laboratory

4.2 Experimental Procedure

Based on the experimental geometry [6], the light from the laser source was passed through the neutral density filter to reduce its intensity. An optical chopper was used for modulating purpose. The modulated light was passed through a polarizer P1 oriented along its maximum transmission axis to pass 100% of light. The linearly polarized light was used to illuminate the target. The receiver branch consisted of polarizer P2 and a nirvana detector. The backscattered light incident on polarizer P2 was made to be incident on the nirvana detector for effective single pixel detection. The detected signal intensities were observed on an oscilloscope. The analyzer polarizer P2 was placed in both parallel, perpendicular orientations to the generating polarizer P1 and corresponding signal intensities were observed. The output of the nirvana detector is connected to the lock-in-amplifier to recover the signal in presence of high noise conditions. This arrangement has provided high sensitivity. The response of lock-in-amplifier was observed on oscilloscope. The distance of the object and the laser source was 45 cm and the detector was placed 27 cm away from the object. The distance between components was kept fixed during the entire experiment. Figure 4.3 shows the orientation of object and detector movement directions of the experimental arrangement.

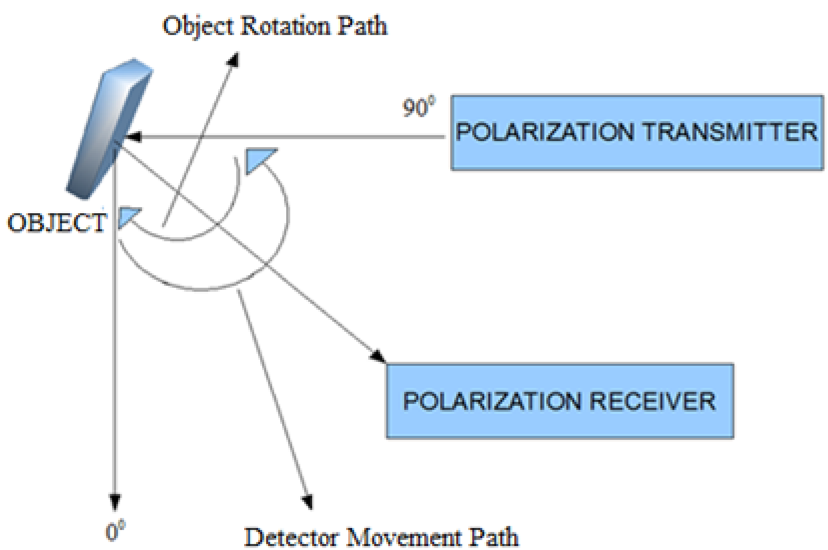

Figure 4.3 Object and Detector Rotation Directions

The co-polarized and cross polarized signal intensities (peak to peak voltage) were obtained when the analyzer polarizer P2 was placed in parallel and perpendicular orientations to the generating polarizer P1 respectively. The DOLP (Degree of Linear Polarization) was calculated using the formulae given by equation 4.1.

$$DOLP = \frac{V_{(p-p)Parallel} - V_{(p-p)Perpendicular}}{V_{(p-p)Parallel} + V_{(p-p)Perpendicular}} \qquad (4.1)$$

4.3 Calibration of Components

The two key parameters in any measurement are precision and accuracy. The components used in the experiments were calibrated to minimize or avoid any measurement errors [31]. A detailed calibration procedure of components is discussed in this section.

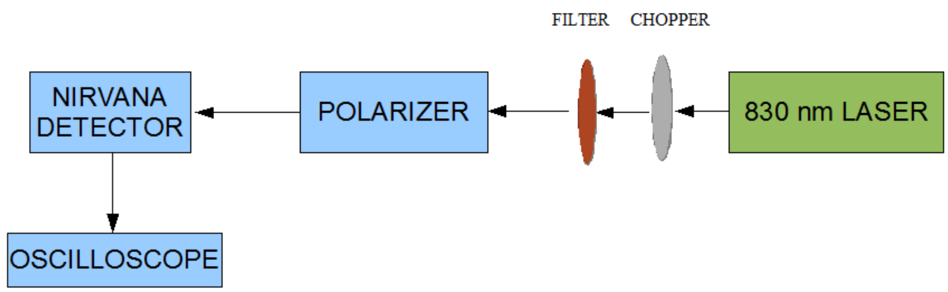

Figure 4.4 Calibration of Polarizers

The polarizer needs special attention while calibration procedures as the experiment deal with the polarimetric principles. The polarizer was calibrated using the setup as shown in Figure 4.4. An optical tabletop was used for mounting all the components. The light from 830 nm laser source was passed through chopper for modulation at 3 KHz frequency. An optical filter was placed after chopper to reduce laser beam intensity. The light was passed through the polarizer and the output signal of polarizer was detected by a nirvana detector. The axis of polarizer was rotated 0° through 360° and corresponding signal was observed on oscilloscope. The maximum and minimum signal levels were observed. The axis angles at which maxima and minima occur was recorded and these angles were used to adjust light polarization.

4.4 Error Analysis

Experimental results need a measure of dispersion. Standard deviation and standard error of mean were calculated for whole data set to represent variations in the obtained measurements. The degree of linear polarization (DOLP) ratio was calculated using three sets of observations at every step. The three measurements included a set of 3 co-polarized and set of 3 cross-polarized intensities. A set of 3 DOLP's were obtained using co-polarized and cross-polarized light intensities using the formulae given by equation 4.1. The standard deviation of three DOLP's is calculated using the formulae given by equation 4.2. The calculation of error statistics is presented in APPENDIX. If $d_1, d_{2,} d_3$ are assumed DOLP's and $\bar{d}$ is average DOLP, the standard deviation is given by

$$S_N = \sqrt{\frac{1}{N}\sum_{i=1}^{N}(d_i - \bar{d})^2} \qquad (4.2a)$$

Number of data sets obtained (N) is 3. The standard deviation of 3 DOLP's is given by:

$$S_3 = \sqrt{\frac{1}{3}\sum_{i=1}^{3}(d_i - \bar{d})^2} \qquad (4.2b)$$

The allowable error in the data can be calculated using standard error of mean (SEM) given by:

$$SE_n = \frac{S}{\sqrt{n}} \qquad (4.3a)$$

As the number of observations taken is 3, the standard error of mean becomes

$$SE_3 = \frac{S}{\sqrt{3}} \qquad (4.3b)$$

CHAPTER V

EQUIPMENT USED IN THE STUDY

5.1 Optical Tabletop

The experiment was conducted on an optical tabletop from MELLES GRIOT. The components used in the experiment were mounted on the tabletop. The important parameters influencing the experiment were thermal fluctuations, acoustic noise, and electromagnetic interference from different sources [32]. An optical tabletop was able to address above mentioned issues along with stiffness, flatness and surface quality factors [32]. The image of optical table top is shown in figure 5.1.

Figure 5.1 Optical tabletop used in the experiment

5.2 Laser Source

An 830 nm continuous wave single mode laser source (IS 830-100C Intelite Inc, Minden, NV) was used as light source for the experiment. Figure 5.2 shows the laser source used in experiment and the specifications of the laser source are given below:

Figure 5.2 Laser source

Table 5.1 Specifications of Laser source

Wavelength	830 nM
Output power	100 mW
Beam Diameter	Adjustable circular beam
Laser head size	45 x 60 x 120mm
Power Stability	< 2%
LED emission indicator	ON/OFF SWITCH
Operating Voltage	5VDC / Max. 1.3mA
Power Input	100 - 240 VAC, 50 -60Hz
Power output	5 VDC, Max. 1,6A

5.3 Lock-In-Amplifier

A high performance DSP lock-in-amplifier (SR-830, Stanford Research Systems) is used to recover the signal in the presence of high noise background and also to obtain high resolution measurements. The output of nirvana detector is connected to input of lock in amplifier and the Sync. Input of frequency modulator is taken as reference for lock-in-amplifier. The lock-in-amplifier essentially multiplies its input signal and reference to produce a highly sensitive signal which can be observed on oscilloscope. For this purpose the frequency of chopper and lock-in-amplifier were both set to 3.00 KHz during experiment. Figure 5.3 shows the lock-in-amplifier used in the experiment and specifications are described below in table 5.2.

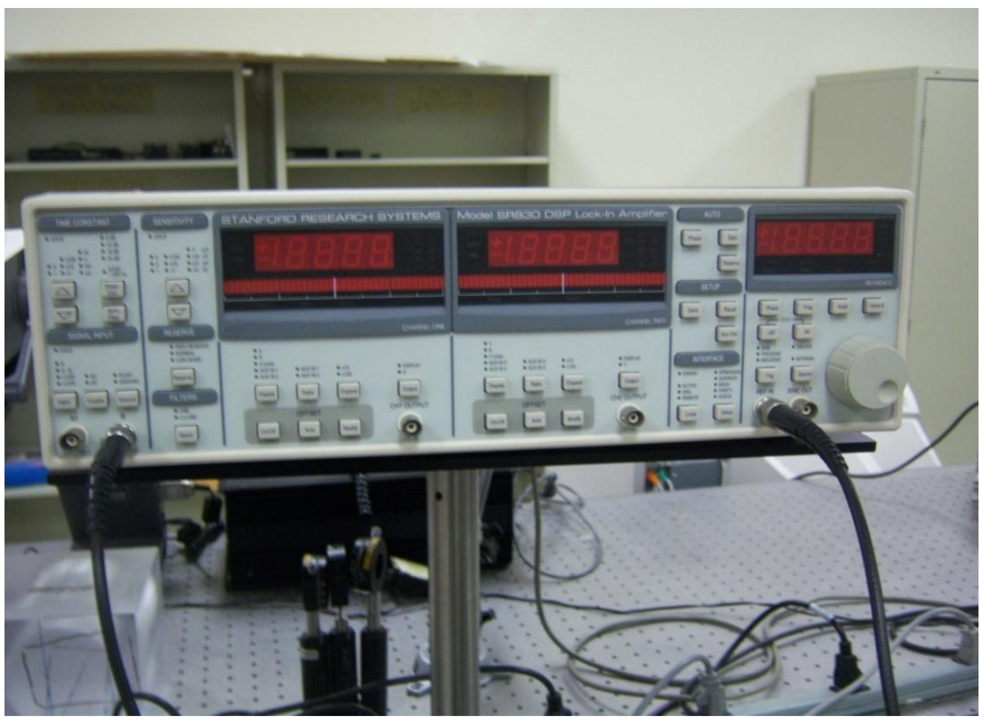

Figure 5.3 Lock-in-amplifier

Table 5.2 Specifications of DSP SR-830 Lock-in-amplifier

Single Channel	
Voltage inputs	Single-ended or differential
Sensitivity	2 nV to 1 V
Current input	106 or 108 V/A
Input impedance Voltage: Current:	 10 MΩ + 25 pF, AC or DC coupled 1 kΩ to virtual ground
Gain accuracy	±1 % (±0.2 % typ.)
Noise (typ.)	6 nV/√Hz at 1 kHz , 0.13 pA/√Hz at 1 kHz (106 V/A) , 0.013 pA/√Hz at 100 Hz (108 V/A)
Line filters	50/60 Hz and 100/120 Hz (Q = 4)
CMRR	100 dB to 10 kHz, decreasing by 6 dB/oct above 10 kHz.
Dynamic reserve	>100 dB (without prefilters)
Stability	<5 ppm/°C
Reference Channel	
Frequency range	0.001 Hz to 102.4 kHz
Reference input	TTL or sine (400 mVpp min.)
Input impedance	1 MΩ, 25 pF
Phase resolution	0.01° front panel, 0.008° through computer interfaces
Absolute phase error	<1°
Relative phase error	<0.001°
Orthogonality	90° ± 0.001°
Phase noise Internal ref. External ref.	Synthesized, <0.0001° rms at 1 kHz 0.005° rms at 1 kHz (100 ms time constant, 12 dB/oct)
Phase drift	<0.01°/°C below 10 kHz, <0.1°/°C above 10 kHz
Harmonic detection	2F, 3F ... nF to 102 kHz (n < 19,999)
Acquisition time	(2 cycles + 5 ms) or 40 ms, Whichever is larger.
Stability	Digital outputs and display: no drift
Analog outputs:	<5 ppm/°C for all dynamic reserve settings
Harmonic rejection	−90 Db

Table 5.2 Specifications of DSP SR-830 Lock-in-amplifier (continued)

Time constants	10 μs to 30 ks (6, 12, 18, 24 dB/oct rolloff). Synchronous filters available below 200 Hz.
Range	1 mHz to 102 kHz
Frequency accuracy	25 ppm + 30 μHz
Frequency resolution	4½ digits or 0.1 mHz, whichever is greater.
Distortion	−80 dBc (f <10 kHz), −70 dBc (f >10 kHz) @ 1 Vrms amplitude
Amplitude	0.004 to 5 Vrms into 10 kΩ (2 Mv resolution), 50 Ω output impedance,50 mA maximum current into 50 Ω
Amplitude accuracy	1 %
Amplitude stability	50 ppm/°C
Outputs	Sine, TTL (When using an external reference, both outputs are phase locked to the external reference.)
Channel 2	4½-digit LED displays with 40-segment LED bar graph. Y, θ, noise, Aux 3 or Aux 4. The display can also be any of these quantities divided by Aux 3 or Aux 4.
Offset	X, Y, R can be offset up to ±105 of full scale.
Expand	X, Y, R can be expanded by 10× or 100×.
Reference	4½-digit LED display.
CH1 output	X, R, X-noise, Aux 1 or Aux 2, (±10 V), updated at 512 Hz
CH2 output (SR830)	Y, θ, Y-noise, Aux 3 or Aux 4, (±10 V), updated at 512 Hz
X, Y outputs (rear panel)	In-phase and quadrature components (±10 V), updated at 256 kHz.
Aux. A/D inputs	4 BNC inputs, 16-bit, ±10 V, 1 mV resolution, sampled at 512 Hz
Aux. D/A outputs	4 BNC outputs, 16-bit, ±10 V, 1 mV resolution
Sine out	Internal oscillator analog output
TTL out	Internal oscillator TTL output
Data buffer	The SR810 has an 8k point buffer. The SR830 has two 16k point buffers. Data is recorded at rates to 512 Hz and read through the computer interfaces
Trigger in (TTL)	Trigger synchronizes data recording

Table 5.2 Specifications of DSP SR-830 Lock-in-amplifier (continued)

Remote preamp	Provides power to the optional SR550, SR552 and SR554 preamps
General	
Interfaces	IEEE-488.2 and RS-232 interfaces standard. All instrument functions can be controlled and read through IEEE-488.2 or RS-232 interfaces.
Power	40 W, 100/120/220/240 VAC,50/60 Hz
Dimensions	17" × 5.25" × 19.5" (WHD)
Weight	23 lbs.

5.4 Nirvana Detector

A highly sensitive auto balanced photo receiver was used for detection of signal at the receiver side after polarizer P2. The use of nirvana detector (Model #2007 New focus, USA) enabled shot noise limited performance. Figure 5.4 shows picture of nirvana detector used in the experiment and specifications are given in Table 5.3.

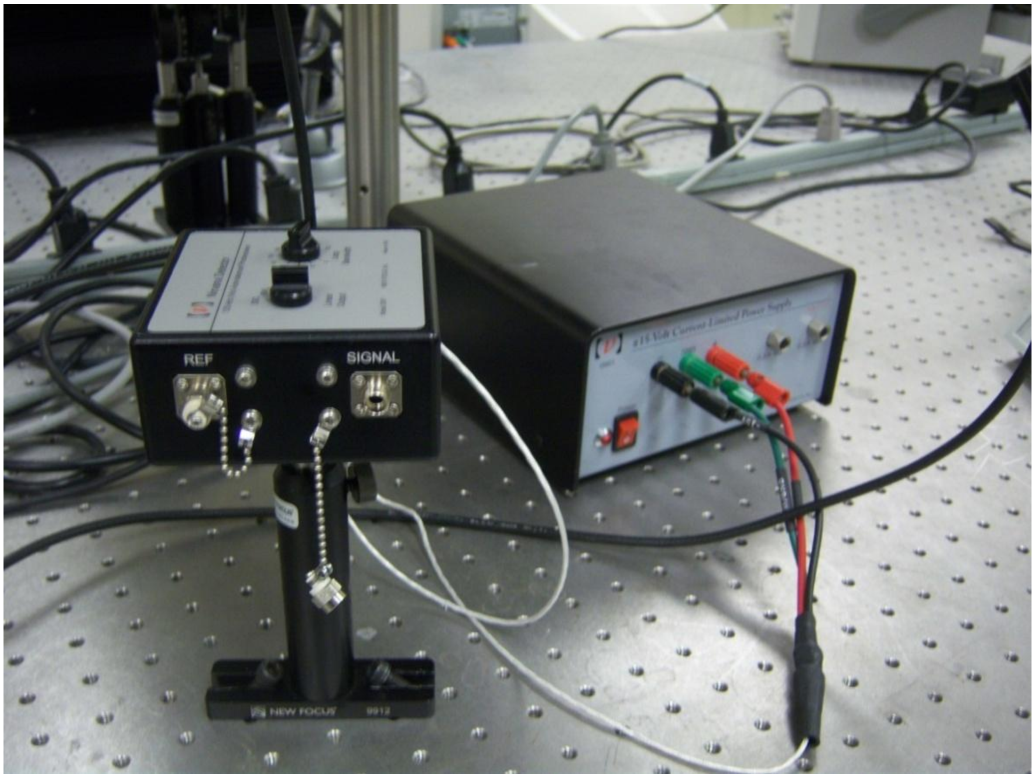

Figure 5.4 Nirvana detector and its power supply

Table 5.3 Specifications of Nirvana Detector

Wavelength Range	400-1070 nm
Common Mode Rejection Ratio (CMRR)	50 dB
Detector Diameter	2.5 mm
Rise Time	3 µs
3-dB Bandwidth	Typical 125 kHz
Maximum Conversion Gain	5.2×10^5 V/W
Typical Maximum Responsivity	0.5 A/W
Maximum Transimpedance Gain	1×10^6 V/A
Output Impedance	100 Ω
Saturation Power	1 mW
Detector Material/Type	Si/PIN
Minimum NEP	<3 pW/sqrt(Hertz)
Power Requirements	±15 V DC, <300mA
Optical Input	FC & Free Space
Electrical Output	BNC

5.5 Optical Chopper

An optical chopper (Model 3501 Optical Chopper, New Focus) was used in front of laser source for purpose of modulation. The function of chopper is to interrupt the laser beam periodically. The optical chopper consists of wheel which rotates according to the frequency generated by external oscillator. Figure 5.5 shows the chopping wheel and figure 5.6 shows function generator. The specifications of modulator and chopper wheel are given in Tables 5.4 and 5.5 respectively.

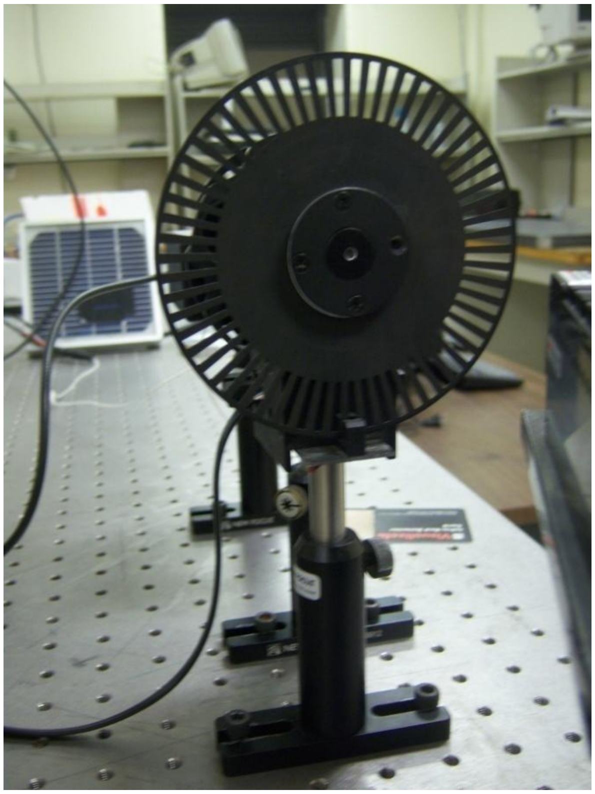

Figure 5.5 Optical chopping wheel

Figure 5.6 Optical modulator

Table 5.4 Specifications of Model 3501 Optical Chopper

Internal Synthesizer	
Stability	100 ppm after one hour warm-up.
Drift	Less than 10 ppm/°C
Accuracy	< 1/5 of least significant digit.
Resolution	4.00 Hz - 99.9 kHz, 3 significant digits.
Range limits (INT)	Upper: [Highest wheel frequency]·S/H. Lower: [Lowest wheel frequency]·S/H.
Range limits (EXT)	4.00 Hz - 99.9 kHz.
General	
Dimensions:	8.5 x 4 x 14.5 inches
Weight:	14 pounds
Power:	90-240 V AC, 50-60 Hz, 35 W
Reference Output	
Sync Out	TTL level square wave may be used as free running oscillator when using EXT+, EXT- or Vext sync.
F_{outer}	TTL level square wave at the chopping frequency

Table 5.4 Specifications of Model 3501 Optical Chopper (continued)

OUT1	TTL level pulse: 5·Fouter in NORMAL mode, Fouter - Finner in +/- mode [H/S] ·Fouter in H/S mode.
OUT2	TTL level pulse: Finner in NORMAL mode Fouter+ Finner in +/- mode. [H/(7·S)]·Fsync- H/S mode.
Phase Shifter	
Range	-180.0° to +179.0°
Resolution	0.1°, increasing to 0.25° at 6.4 kHz.
Harmonic Locking	
Sub harmonic (S):	1 – 15
Harmonic (H) S and H may be set in any combination.	1 – 15
External Voltage Control	0 to -10.0 V DC for 0 to 100% of maximum chopping frequency

Table 5.5 Frequency Specifications of Chopper Wheel

	Chopping Frequency			
Wheel	Min. Freq.	Max. Freq.	Jitter (μs p-p)	
	(F_{outer})	(F_{outer})	@ Min. Freq.	@ Max. Freq.
60	120 Hz	6.40 kHz	60	2
42/30	84 Hz	4.48 kHz	50	2
7/5	14 Hz	746 Hz	500	3
2	4 Hz	213 Hz	500	5

5.6 Polarizers

Polarizers were used in the experiment for generating linearly polarized light. Two polarizers one on transmitter side and other on receiver side were used in the study. For this purpose two high contrast dichroic polarizers (03 FPC 011, Melles Griot, Rochester, NY) were used. Figure 5.7 shows the picture of polarizers used in the experiment and specifications of polarizers were described in Table 5.6.

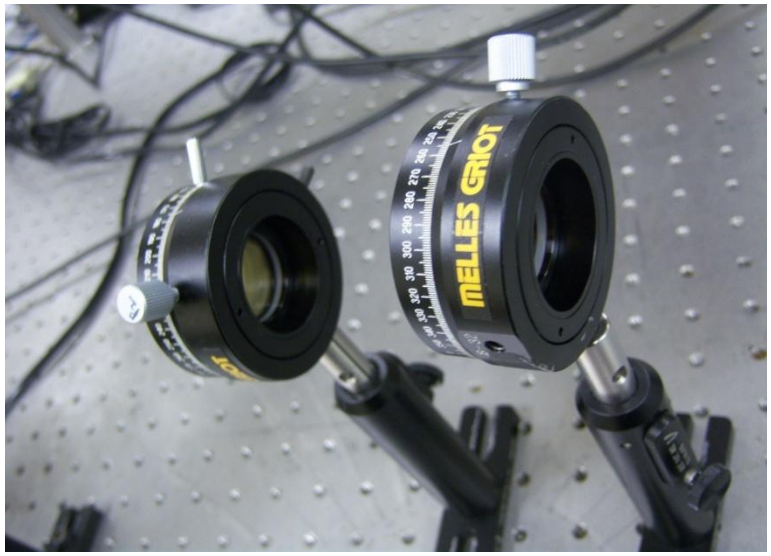

Figure 5.7 Two dichroic polarizers used in the study

Table 5.6 Specifications of the polarizer

Diameter	25.0 +0 / -0.2mm
Thickness	2.0 ± 0.2mm
Clear Aperture	22.5mm
Material	Soda Lime
Wavelength	600-1000nm
Extinction Ratio	600-850nm: >10000:1 600-1000nm: >1000:1
Transmission	600-850nm: 78%-81% 600-1000nm: >78%-88%
Operating Temperature	-20oC to +120oC
Acceptance Angle	±20o
Shape	Round

5.7 Oscilloscope

The output voltage generated across the nirvana detector was observed on a digital oscilloscope. For this purpose a digital phosphor oscilloscope (Tektronix, TDS 3052) was used. The peak to peak voltage of the waveform generated on oscilloscope was taken down as signal intensity. Figure 5.8 shows an image of Tektronix oscilloscope. The electrical specifications of TDS 3052 model were described in Table 5.7.

Figure 5.8 Tektronix digital oscilloscope

Table 5.7 Electrical Specifications of TDS 3052 Oscilloscope

Bandwidth	500 MHz
Channels	2
Sample Rate on Each Channel	5 GS/s
Maximum Record Length	10K points
Vertical Resolution	9–bits
Vertical Sensitivity (/div)	1 mV-10 V
Vertical Accuracy	±2%
Max Input Voltage (1 megaohm)	150V RMS CAT I
Position Range	±5 div
BW Limit	20, 150 MHz
Input Coupling	AC, DC, GND
Input Impedance Selections	1 megaohm in parallel with 13 pF, or 50 ohm
Range (/div)	1 ns - 10 s/div
Accuracy	200 ppm
Display Monitor	Color LCD

5.8 Object Mount

Different materials used in the experiment were mounted on a trans-rotating mount (Unislide Assemblies). The use of mount enabled flexible translational and rotational movement of materials. This feature of mount helped in interrogating materials in different orientations. Figure 5.9 shows an image of trans-rotational mount used in the study.

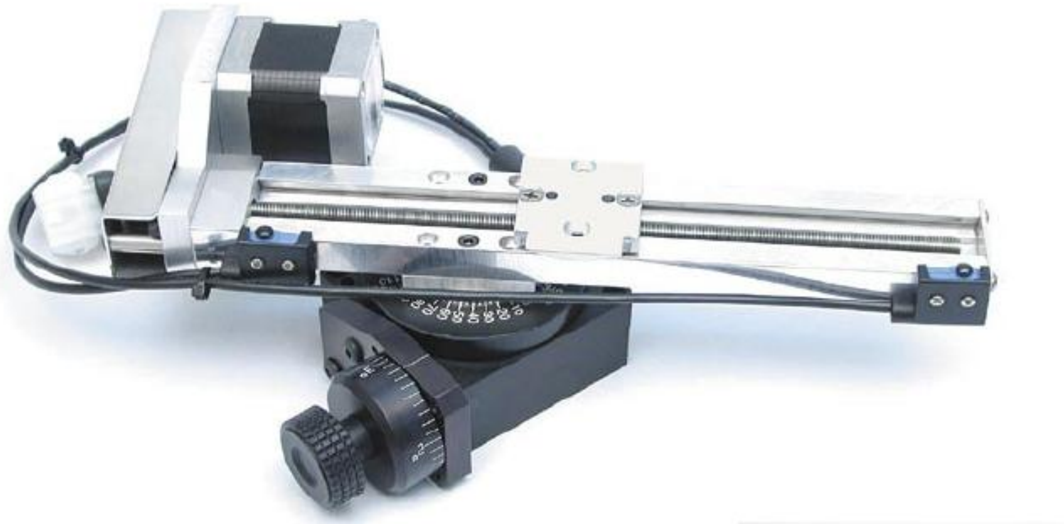

Figure 5.9 Object mount

5.9 Stepper Motor Controller

The rotation control of the mount was performed using a Velmex VP9000 stepper motor controller. The stepper controller enabled rotation of materials at specific angles. The transitional movement of the materials was useful when aligning the system before experiment and also during the angular interrogation of various materials. Figure 5.9 shows a picture of stepper controller used in the experiment. The specifications of controller are given below.

Figure 5.10 Velmex stepper motor controller

Specifications of Stepper Motor Controller:

Functional

- Packaged Controller/Driver, 400 steps per revolution (0.9o step angle) resolution. Operates one to four (dependent on model) motors, one-at-a-time. Bi-level motor drives, settable holding torque for motor one. Interactive limit switch inputs (TTL), (CW and CCW for each axis).
- User input 1 active high (0V to +3V min., -25V to +25V max.), Input 2 is TTL active low, and two user outputs (0 or +5V, 10 mA sinking and 3 mA sourcing capability).
- Wide viewing angle, 2 line x 24 character, backlit, super-twist LCD readout for motor position display and data selection.

- Six key calculator quality keyboard for cursor control, display selection, and 0 entry.
- Front panel programmable or through a full-duplex three wire RS-232-C; 300,1200,4800,9600 Baud (settable), 7 Data bits, Even parity, 2 Stop bits, ASCII.
- User available NVRAM for program storage is 7936 bytes.
- Remote Run, Reset, Two Interrupt input.
- Inputs to count quadrature converted pulses from multiplexed encoder.
- Ten-foot motor and limit switch cables with connectors.

Electrical Requirements

- 90-130 VAC, 50/60 Hz operation standard.
- 190-260 VAC, 50/60 Hz operation is optional.

Motor Compatibility

- American Precision: 23D-6108A, 23D-6209A, 23D-6309A, 34D-9109A, 34D-9209A, 34D-9311A
- Bodine Electric: 2430, 2530, 2431, 2531, 2411, 2511, 2433, 2533, 2434, 2534, 2435, 2535
- Superior Electric: MO61-LS08, MO62-LS09, MO63-LS09, MO91-FD09, MO92-FD09, MO93-FD11
- Vexta: PX245-01, PX245M-01, PX245-02, PX245M-02, PK245-01, PK245M-01
- Other motors on request

Physical

- Weight: 22 lbs. (10 kg)
- Height: 5.2 inches (13.2 cm)

- Width (without handles): 8.5 inches (21.6 cm)
- Depth (without handles): 14.3 inches (36.3 cm)

Environmental -35o to 95o F (2o to 35o C) Convection cooled

5.10 Neutral Density Filter

The intensity of laser beam was reduced by using a neutral density filter (Coherent Inc., Auburn, CA). A filter of diameter 25mm was used in the study. Figure 5.11 shows an image of neutral filter selection set used in the experiment.

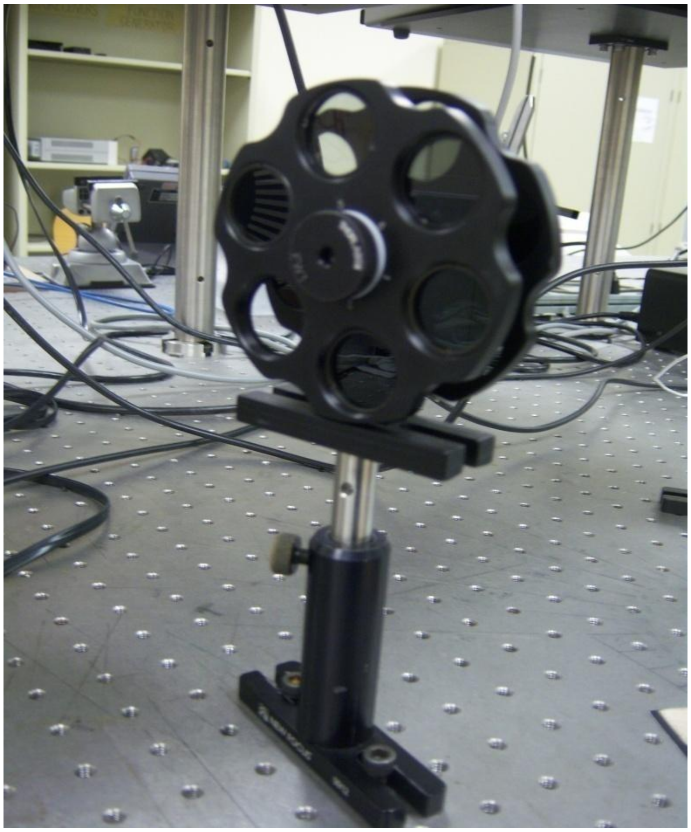

Figure 5.11 Neutral density filter selection wheel

CHAPTER VI

RESULTS AND DISCUSSIONS

Experimental results of the research and a detailed analysis of observations is presented in this chapter. DOLP (Degree of Linear Polarization) was calculated for different materials with varying orientations and detector positions. The backscattered optical polarimetric signatures were captured to calculate polarization ratio of each material. Polar plots representing DOLP as function of varying object orientation angles are used to describe polarization characteristics of different materials. The results were categorized according to materials used in the experiment.

6.1 Teflon

Teflon is a lightweight, soft polymer material used for spacecraft design. Teflon sample was interrogated to obtain its polarization characteristics. It was observed that Teflon exhibited high depolarization of light. The flat DOLP curves shown in polar plots 6.1-6.7 indicates the "Diffuse reflectance" nature of Teflon, therefore it can be identified as a "Lambertian surface" exhibiting high depolarization of light. It can be observed that the amount of polarization exhibited by Teflon remained almost same at all detector positions from 0 deg. through 60 deg. It can also be observed that the flatness of DOLP curves increased as the detector position was moved from 0 deg. to 60 deg. The depolarization ratios observed under all detector positions were around 85%-95%.

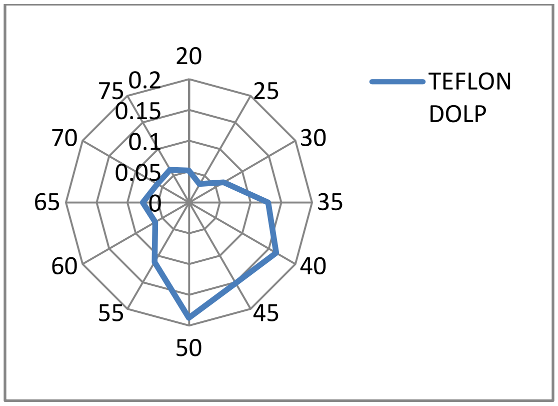

Figure 6.1 Detector at 0 Deg

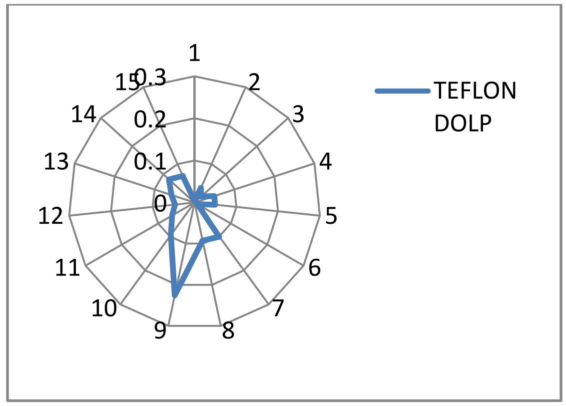

Figure 6.2 Detector at 10 Deg

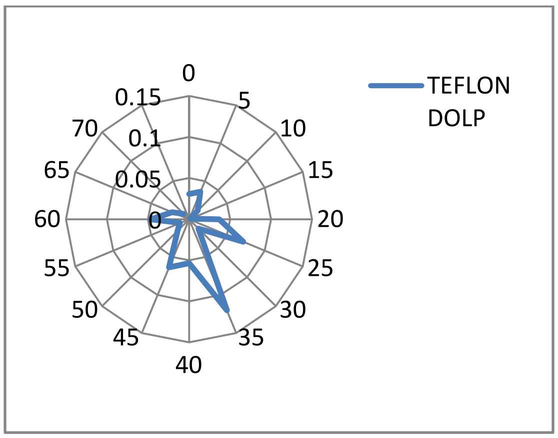

Figure 6.3 Detector at 20 Deg

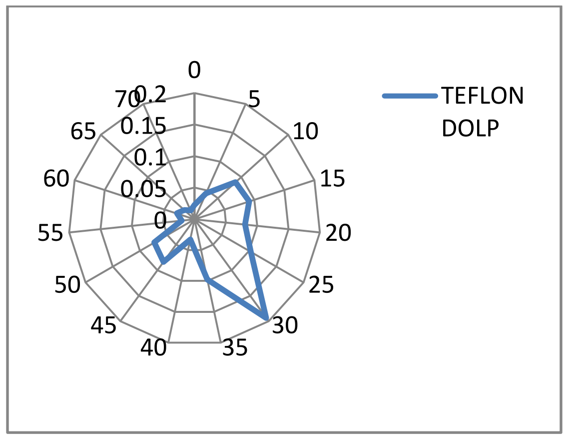

Figure 6.4 Detector at 30 Deg

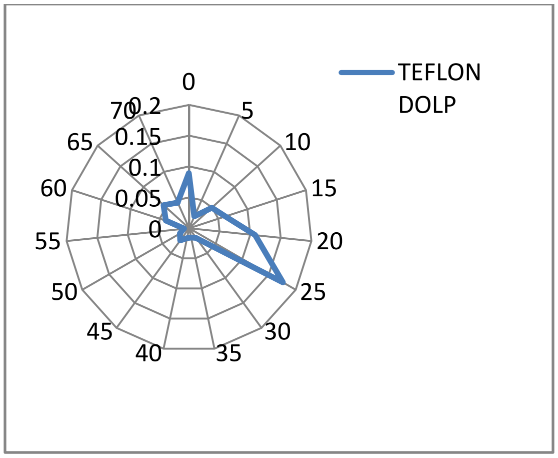

Figure 6.5 Detector at 40 Deg

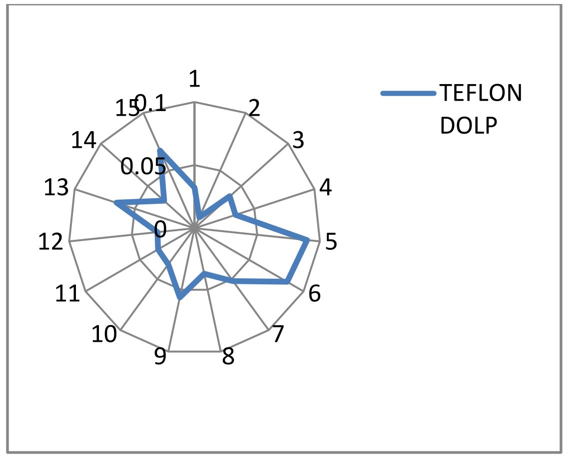

Figure 6.6 Detector at 50 Deg

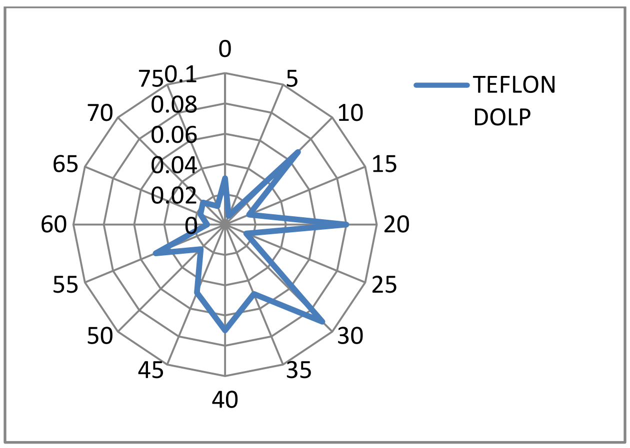

Figure 6.7 Detector at 60 Deg

6.2 Kapton

Kapton is a highly durable, temperature stable, lightweight and soft polymer material used for space applications especially as insulated wiring for civil and military aircrafts. Kapton is also used for space suit design. The obtained backscattered intensity distributions of Kapton material were found to be very sharp indicating strong specular reflectance. The sharp backscattered intensity distributions can be observed from plots 6.8-6.14. It can be observed that the amount of polarization increased as the detector position was moved from 0 deg to 60 deg. The polarization curve at detector position 60 deg showed perfect specular reflectance characteristics with high polarization degree. The amount of depolarization produced by Kapton was found to be less compared to Teflon and was around 60%-90%.

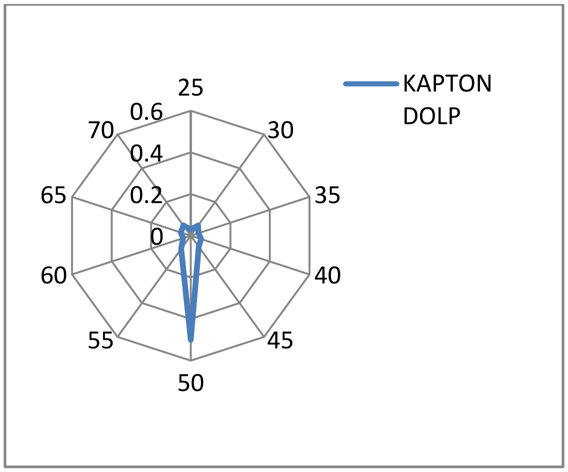

Figure 6.8 Detector at 0 Deg

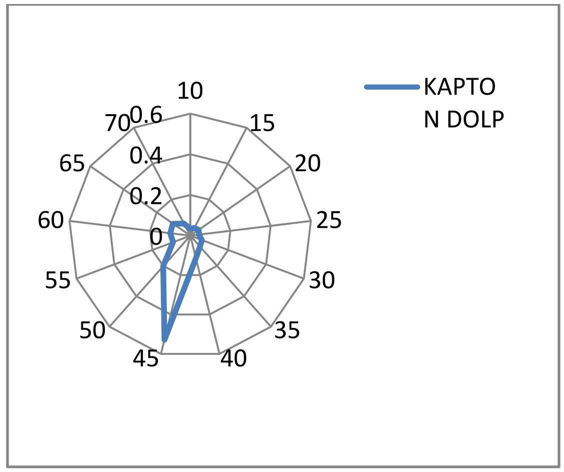

Figure 6.9 Detector at 10 Deg

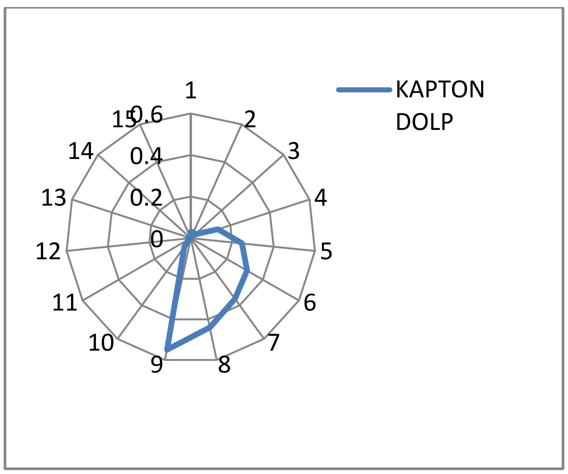

Figure 6.10 Detector at 20 Deg

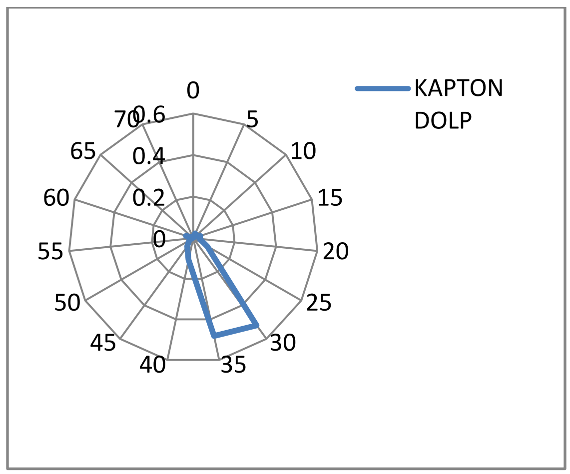

Figure 6.11 Detector at 30 Deg

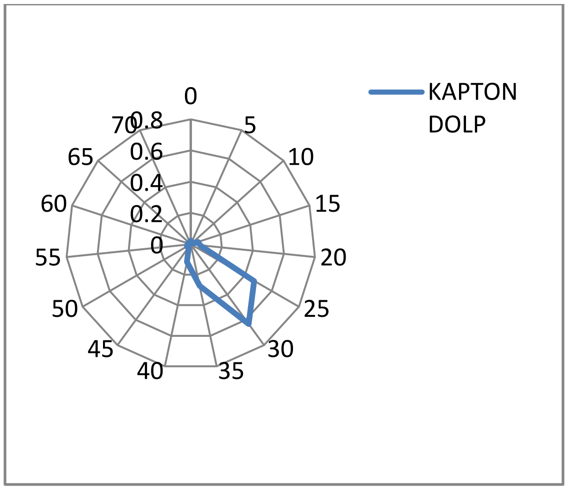

Figure 6.12 Detector at 40 Deg

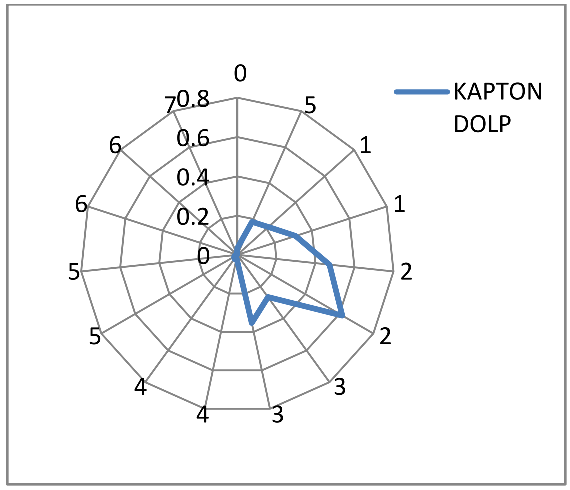

Figure 6.13 Detector at 50 Deg

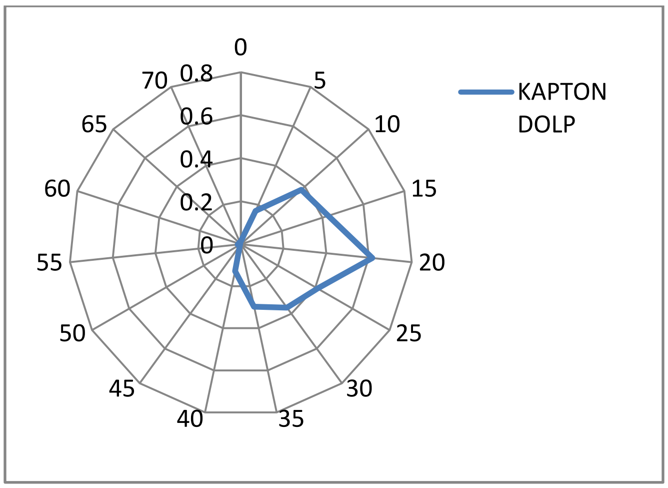

Figure 6.14 Detector at 60 Deg

6.3 Shiny Aluminum

A sample of shiny aluminum foil was interrogated to obtain its polarization response. The obtained backscattered intensity distributions of shiny Aluminum foil were found to be very sharp and similar to Kapton indicating its specular reflectance characteristics. The sharp backscattered intensity distributions can be observed from plots 6.15-6.21. The amount of polarization increased as the detector was moved from 0 deg. to

60 deg. A very sharp reflectance curve can be observed at detector position 60 deg. The DOLP was around 90% when the object and detector were oriented at angle of spectral reflection. The amount of depolarization produced by shiny aluminum foil was found to be very less compared to Kapton and was around 10%-50%.

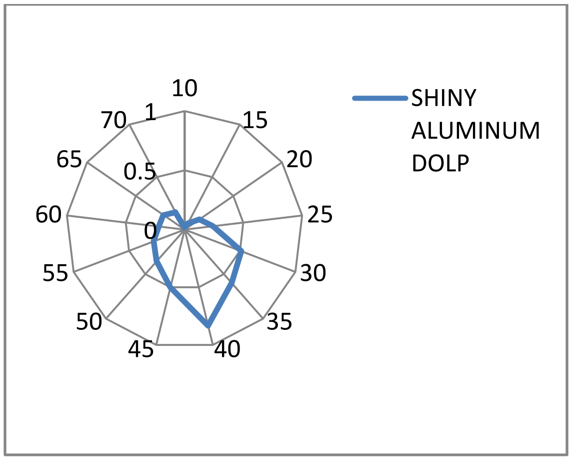

Figure 6.15 Detector at 0 Deg

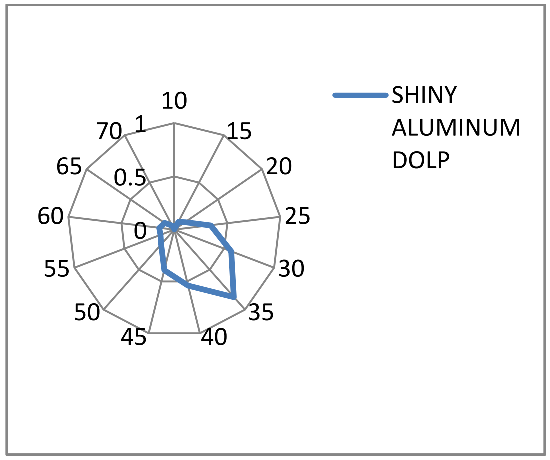

Figure 6.16 Detector at 10 Deg

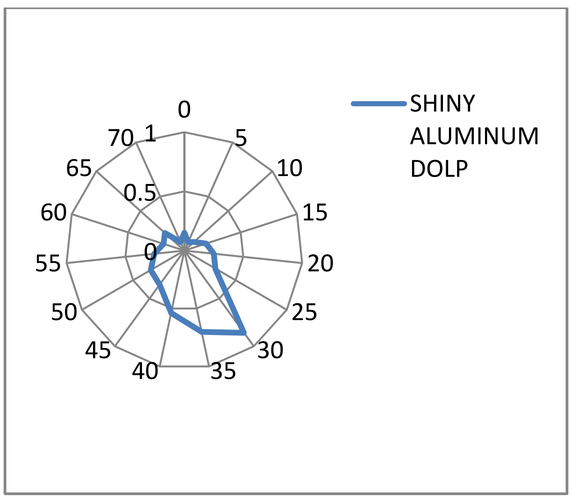

Figure 6.17 Detector at 20 Deg

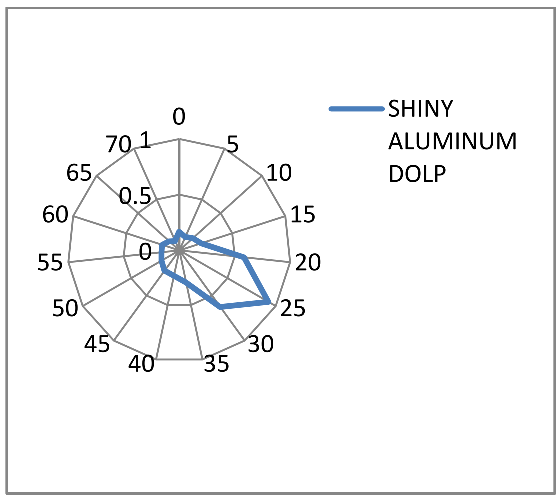

Figure 6.18 Detector at 30 Deg

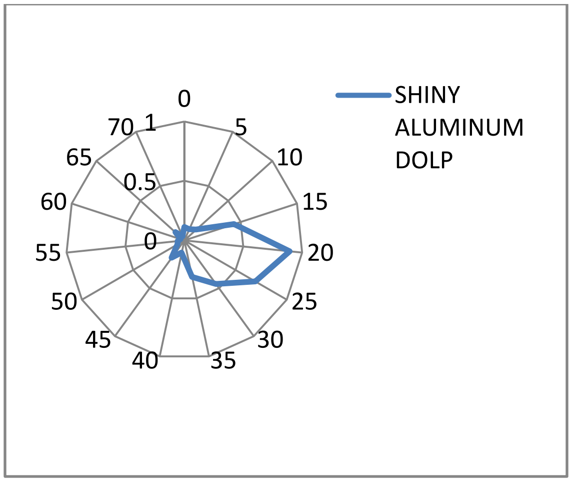

Figure 6.19 Detector at 40 Deg

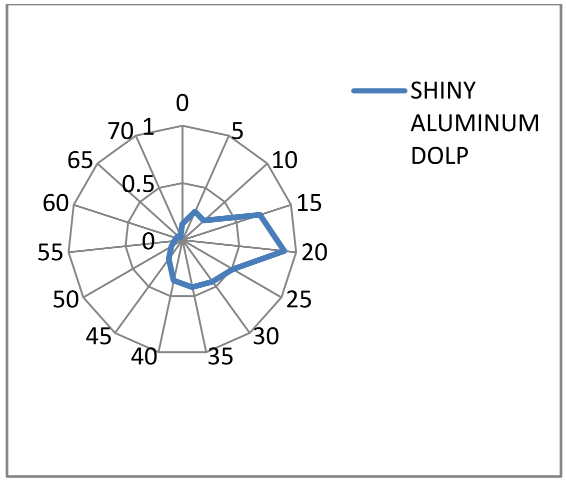

Figure 6.20 Detector at 50 Deg

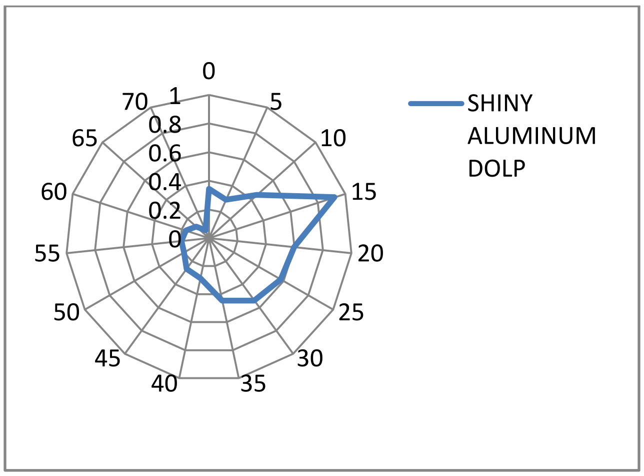

Figure 6.21 Detector at 60 Deg

6.4 Roughened Aluminum

Aluminum is a lightweight, soft, durable metal having numerous applications including space and aircraft. A sample of aluminum was sandblasted to increase its surface roughness. The depolarization characteristics of aluminum can be attributed to the presence of randomly oriented spheroids on flat surfaces [15]. The obtained backscattered distributions were broadened reflectance curves with high depolarization signatures compared to shiny aluminum; this is due to large number of discontinuities on roughened surface. It can be observed that DOLP was more at 40 deg, 50 deg, 60 deg detector positions compared to 0 deg, 10 deg and 20 deg positions. The DOLP curve at 60 deg detector position has sharp distribution due to high polarization. The depolarization ratios observed were around 50%-80%; this indicates stronger depolarization of light due to surface roughness. The polar plots 6.22-6.28 shows DOLP curves at different detector positions.

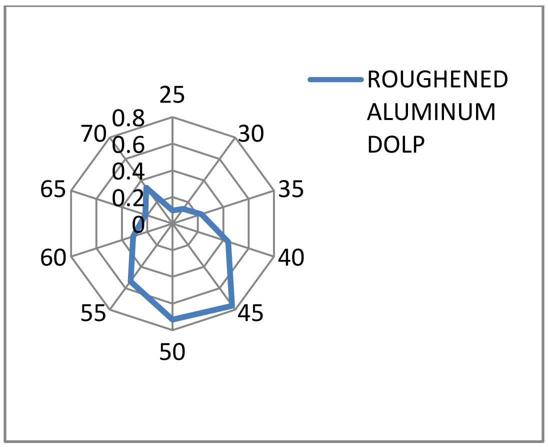

Figure 6.22 Detector at 0 Deg

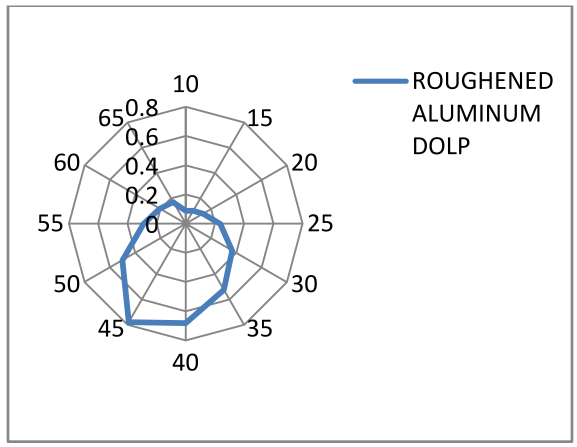

Figure 6.23 Detector at 10 Deg

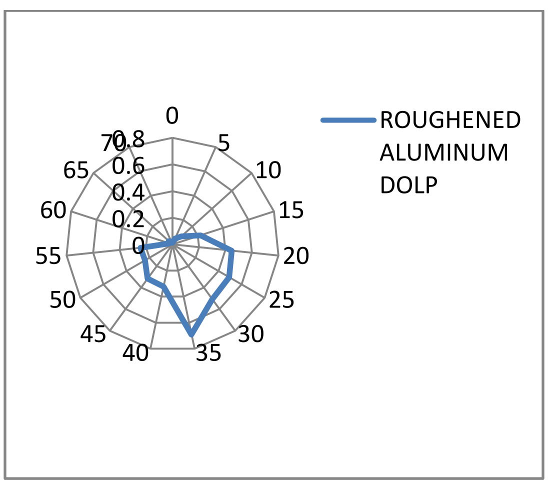

Figure 6.24 Detector at 20 Deg

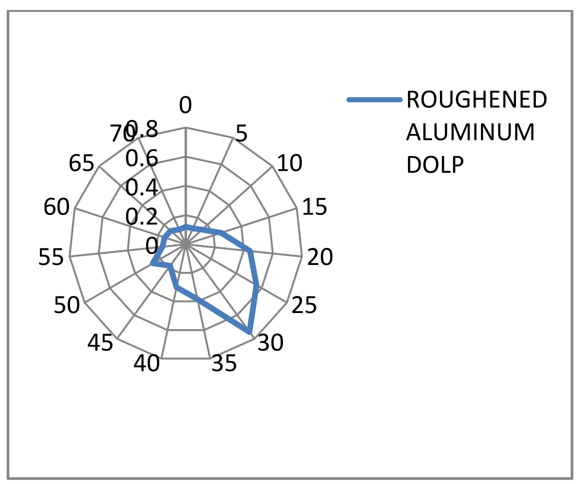

Figure 6.25 Detector at 30 Deg

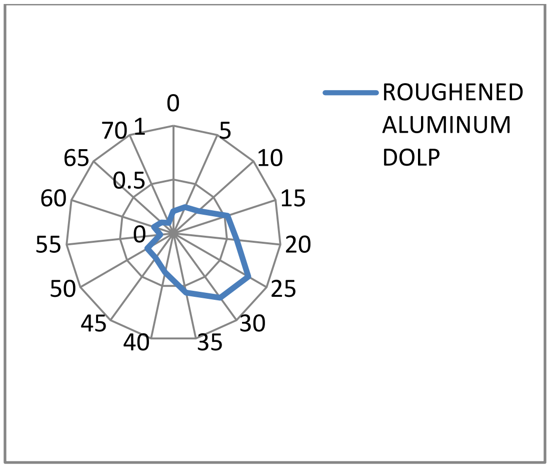

Figure 6.26 Detector at 40 Deg

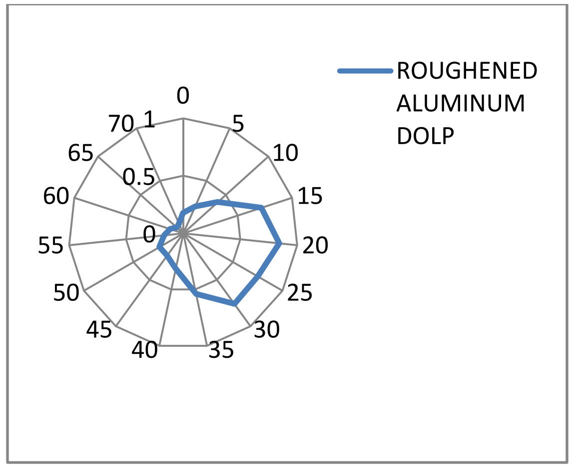

Figure 6.27 Detector at 50 Deg

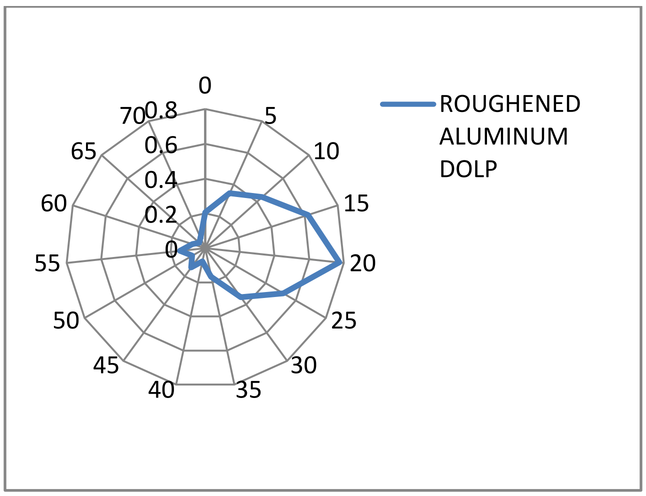

Figure 6.28 Detector at 60 Deg

6.5 Molybdenum

Molybdenum is a high temperature resistant, strong metal used in rigid applications. It is used in spacecrafts in alloy form or as molybdenum disulphide. A piece of molybdenum metal is examined under different orientations. The backscattered intensity curves were found to be broadened curves with high depolarization signatures compared to shiny aluminum foil. Flat DOLP curves can be observed at 0 deg, 10 deg, 20 deg, 30 deg, 40 deg and 50 deg indicates the diffuse nature of surface. The backscattered curve obtained at 60 deg. was found to be sharp due to strong polarization signatures when detector is nearer to laser source. The observed depolarization ratios were in the range of 30%-80%. The DOLP response is shown in polar plots 6.29-6.35 indicates the polarization distributions.

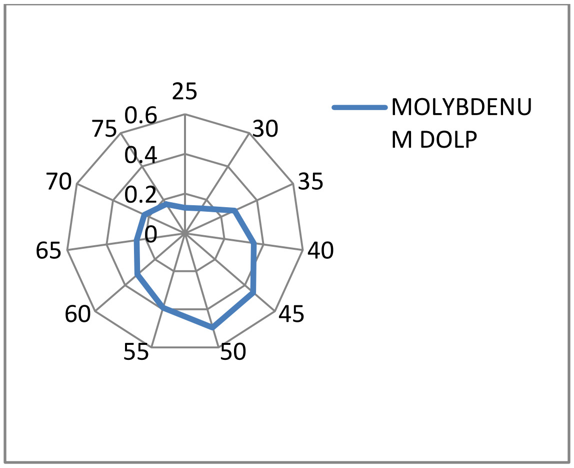

Figure 6.29 Detector at 0 Deg

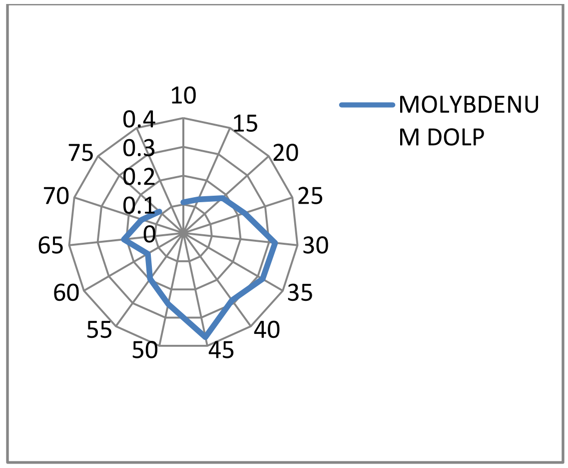

Figure 6.30 Detector at 10 Deg

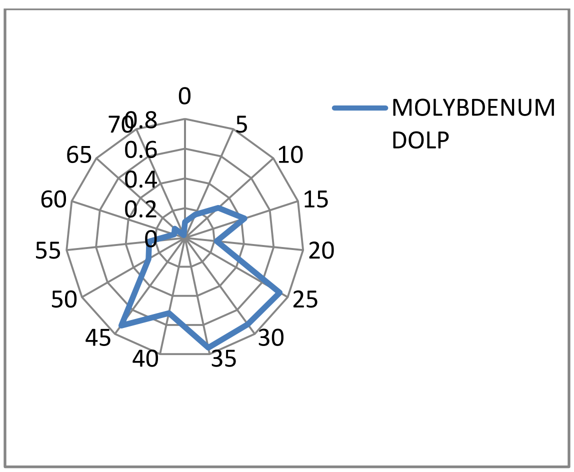

Figure 6.31 Detector at 20 Deg

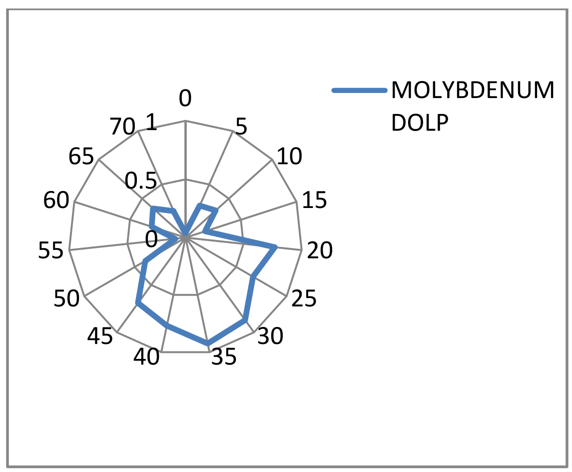

Figure 6.32 Detector at 30 Deg

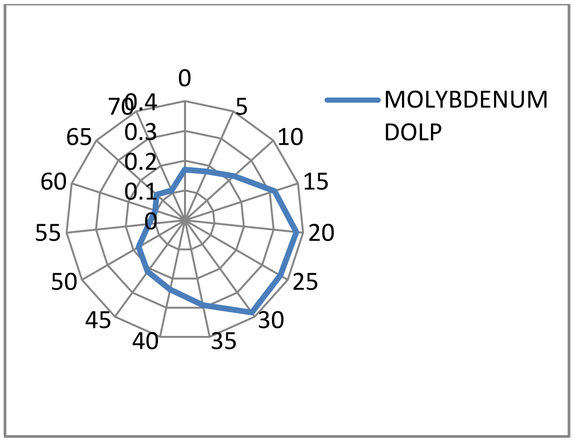

Figure 6.33 Detector at 40 Deg

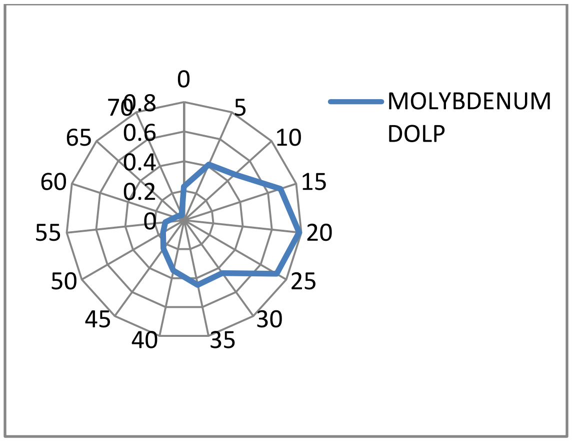

Figure 6.34 Detector at 50 Deg

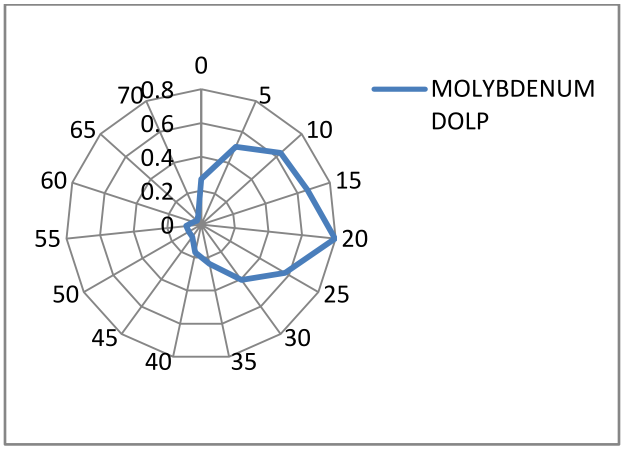

Figure 6.35 Detector at 60 Deg

6.6 White Paint Mixed with Titanium dioxide Particles

A sample of wooden stick painted with white color mixed with Titanium dioxide particles is examined for obtaining polarization characteristics. The high depolarization exhibited by material was caused by strong scattering of light by white color paint. The response obtained was similar to Teflon and therefore can be identified as “Diffusely reflecting” material. The surface defects, subsurface interactions of laser light with Titanium dioxide particles cause strong light depolarization [6]. The obtained DOLP curves representing flat response indicates “Lambertian” nature of the material. The luminance of the surface remained almost same at all angles of detector positions 0 deg through 60 deg. as represented by polar plots 6.36-6.42. The depolarization ratios were in the range of 90%-98%.

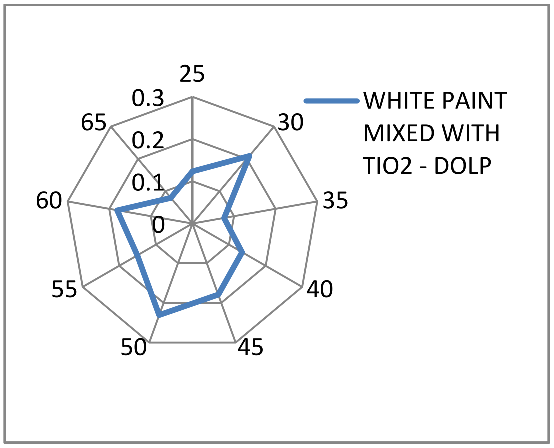

Figure 6.36 Detector at 0 Deg

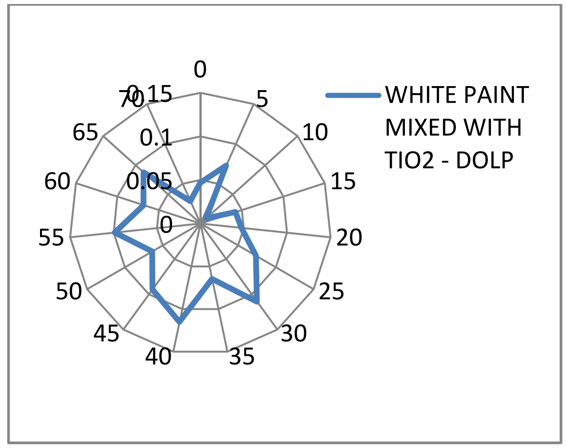

Figure 6.37 Detector at 10 Deg

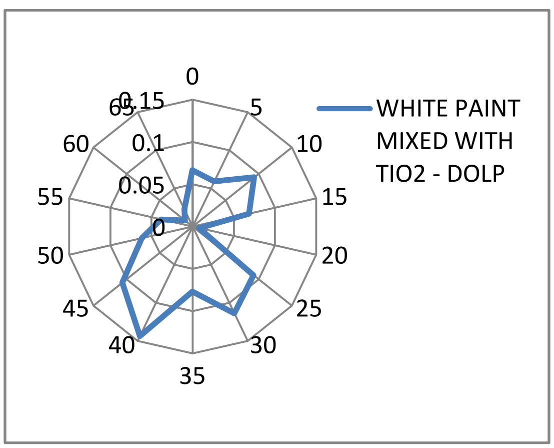

Figure 6.38 Detector at 20 Deg

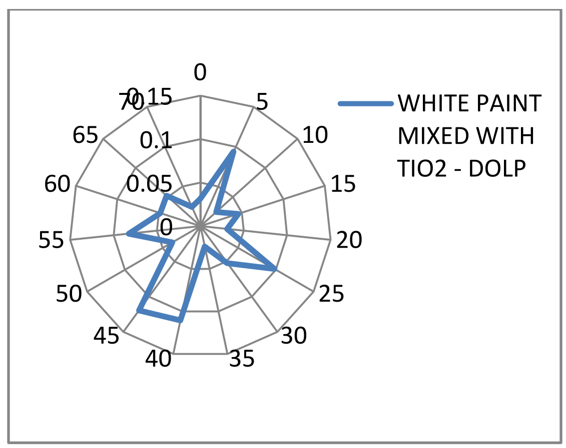

Figure 6.39 Detector at 30 Deg

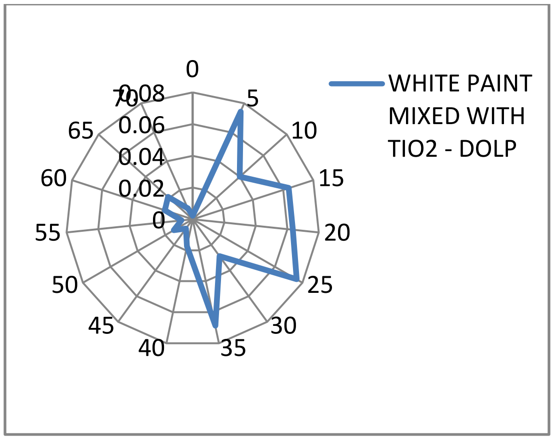

Figure 6.40 Detector at 40 Deg

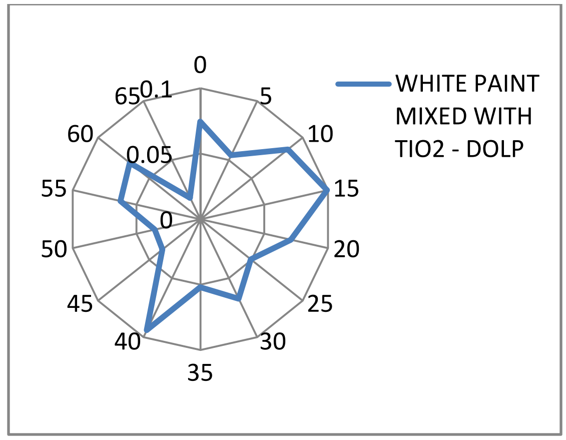

Figure 6.41 Detector at 50 Deg

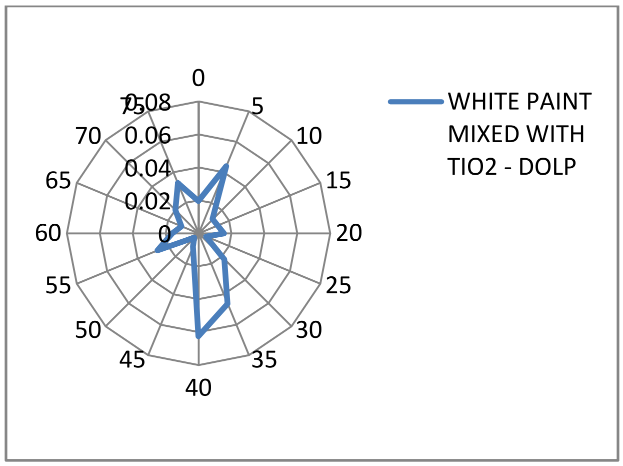

Figure 6.42 Detector at 60 Deg

6.7 Stainless Steel

Stainless steel is a corrosion free metal that has numerous applications in aviation industry and space vehicle design. The DOLP analysis on a sample of stainless steel indicated that backscattered DOLP distributions were of "Specular reflectance" nature and the observed depolarization ratios were around 50%-90%. It can be observed that amount of scattering was less at 40 deg, 50 deg, 60 deg detector positions compared to 0 deg and 10 deg positions. The DOLP curves were found to be sharper at detector positions nearer to the laser source. The polarization response can be observed in polar plots 6.43-6.49.

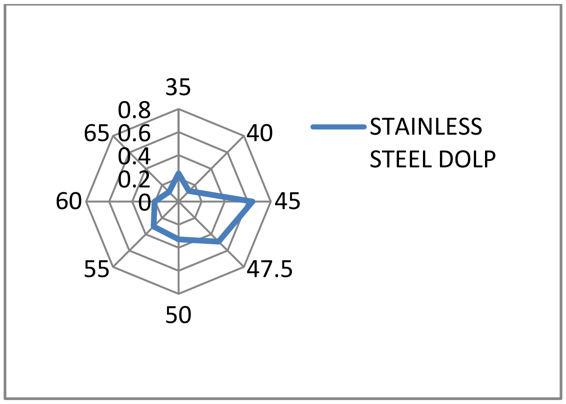

Figure 6.43 Detector at 0 Deg

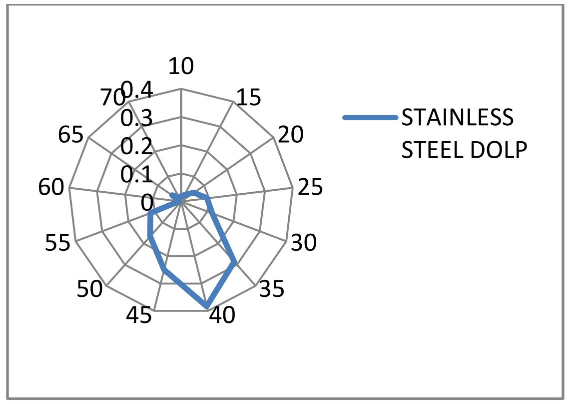

Figure 6.44 Detector at 10 Deg

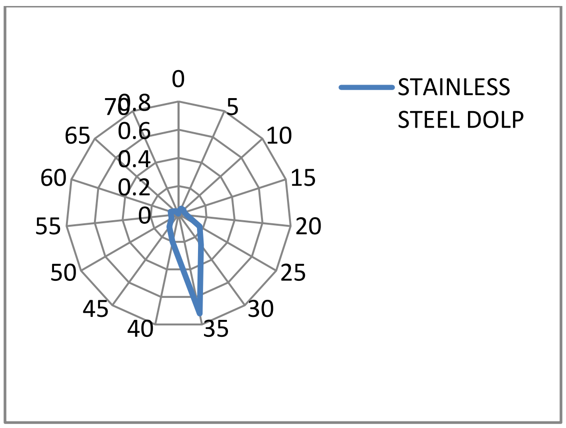

Figure 6.45 Detector at 20 Deg

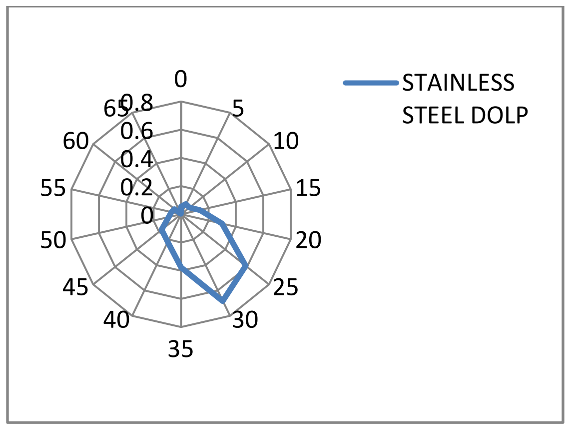

Figure 6.46 Detector at 30 Deg

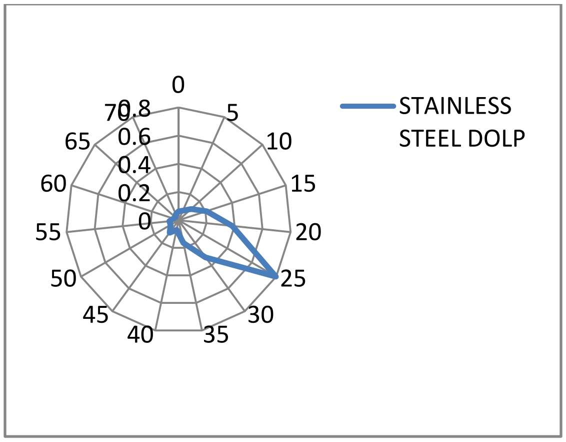

Figure 6.47 Detector at 40 Deg

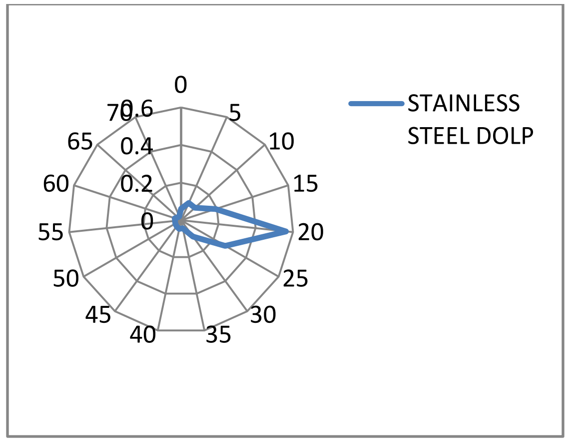

Figure 6.48 Detector at 50 Deg

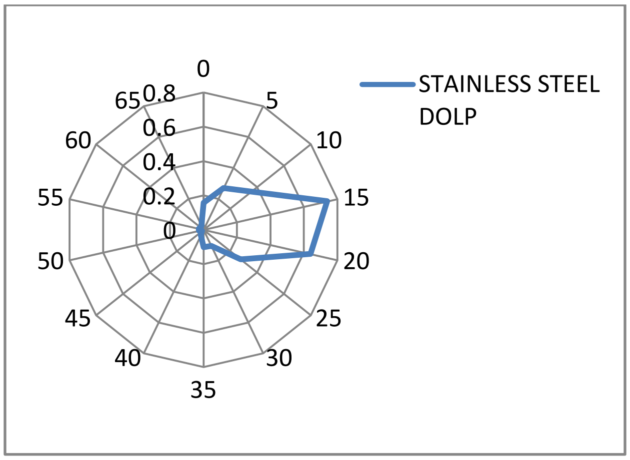

Figure 6.49 Detector at 60 Deg

6.8 Roughened Lithium

Roughly surfaced lithium painted sample was studied to observe depolarization characteristics. The polarization response of wet and roughly surfaced lithium sample was analyzed. The depolarization exhibited by lithium sample can be attributed to roughness and surface wetness of the material [12]. From the polar plots 6.50-6.56, it can be observed that at every detector position from 0 deg. through 60 deg. lithium exhibited a strong polarization signatures at spectral reflectance angle and flat signatures which are highly depolarized at all other orientation angles. The depolarization ratios observed were in the range of 55%-95%.

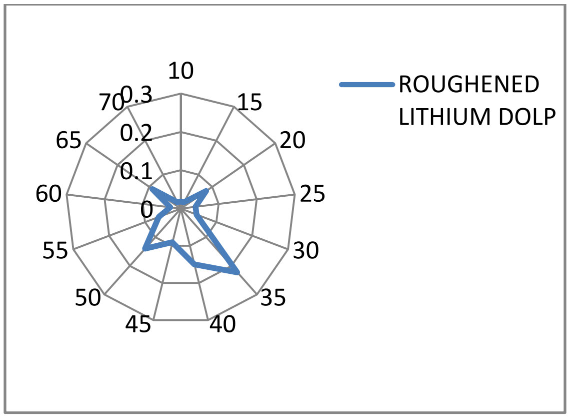

Figure 6.50 Detector at 0 Deg

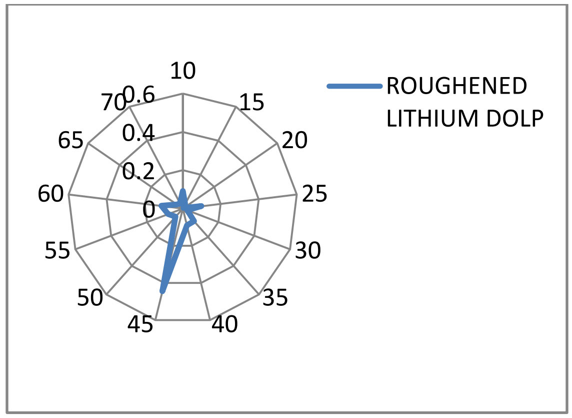

Figure 6.51 Detector at 10 Deg

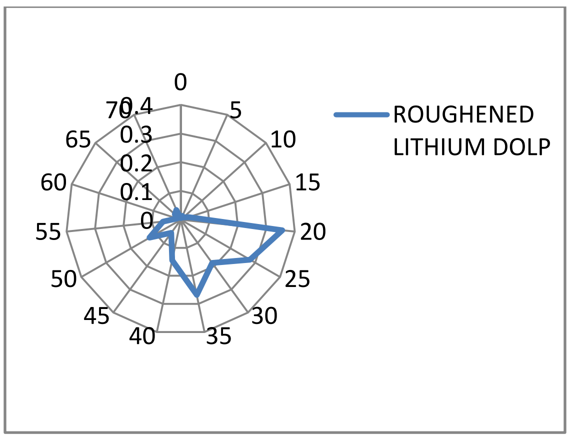

Figure 6.52 Detector at 20 Deg

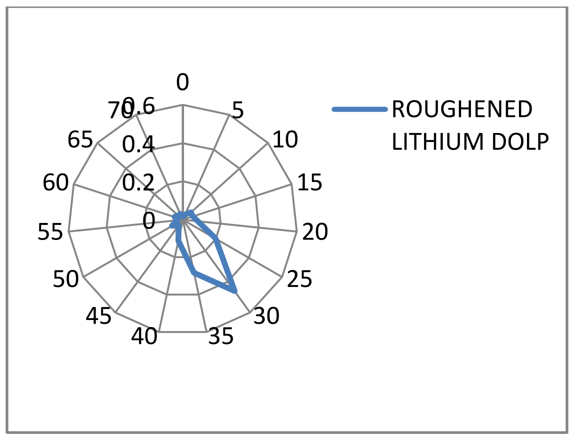

Figure 6.53 Detector at 30 Deg

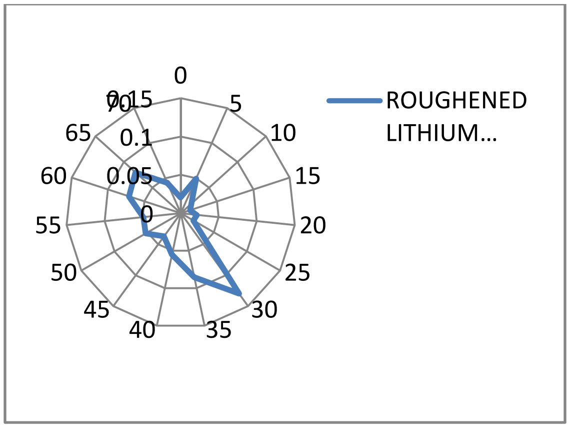

Figure 6.54 Detector at 40 Deg

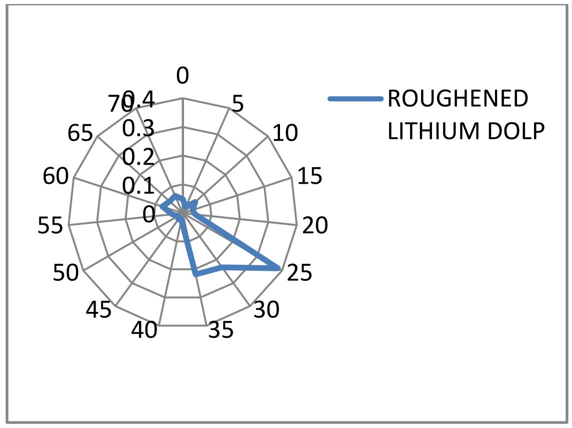

Figure 6.55 Detector at 50 Deg

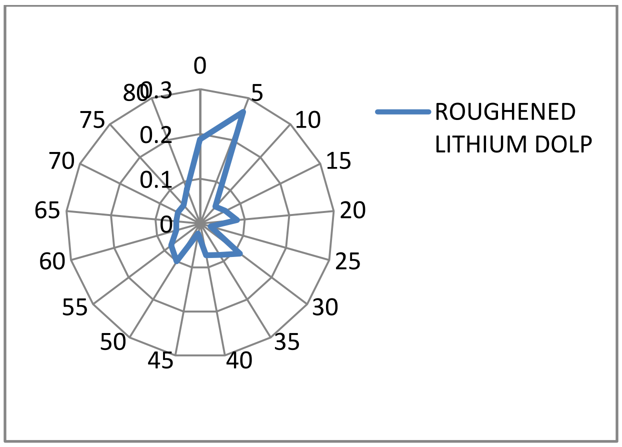

Figure 6.56 Detector at 60 Deg

6.9 Windowless Polysilicon Solar Panel

A sample of polysilicon solar panel without window was interrogated at different detector positions and the DOLP ratio was calculated. The obtained flat DOLP curves indicate "Lambertian nature" of the surface; this response was similar to the response exhibited by Teflon and white paint mixture. It can be observed that there was strong polarization of light at 60 deg. detector position. The flatness of the DOLP curves can be observed in the polar plots 6.60-6.62. The scatter remained almost same at different angles of observations and the depolarization ratios were in the range of 68%-98%. The response can be observed in polar plots 6.57-6.63.

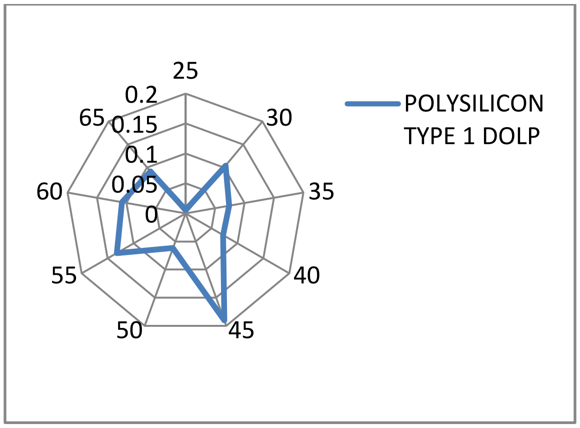

Figure 6.57 Detector at 0 Deg

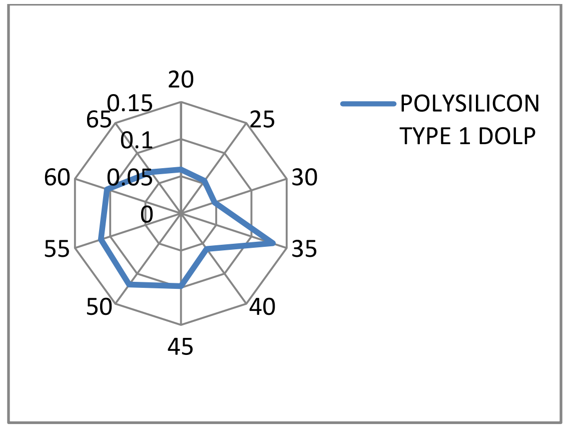

Figure 6.58 Detector at 10 Deg

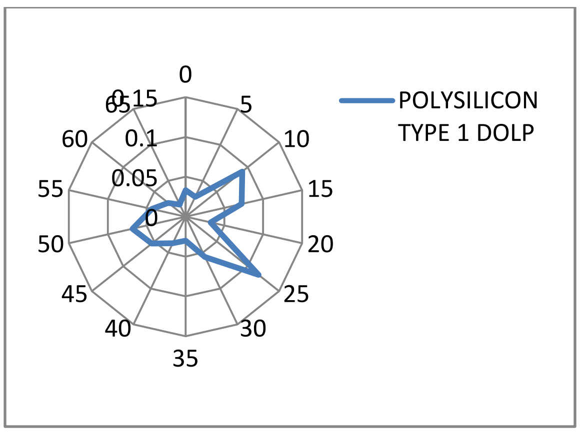

Figure 6.59 Detector at 20 Deg

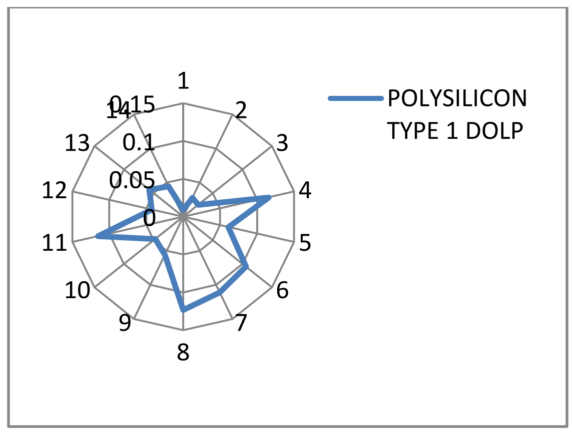

Figure 6.60 Detector at 30 Deg

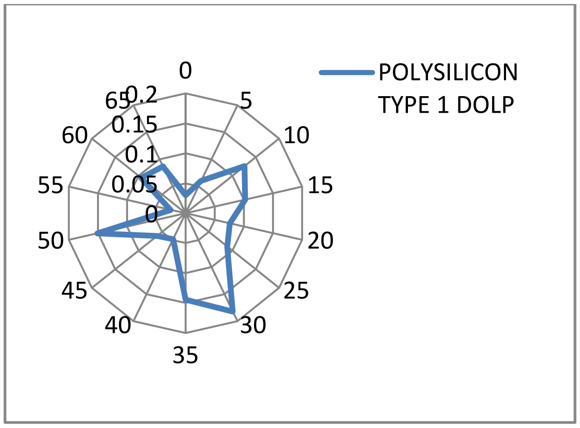

Figure 6.61 Detector at 40 Deg

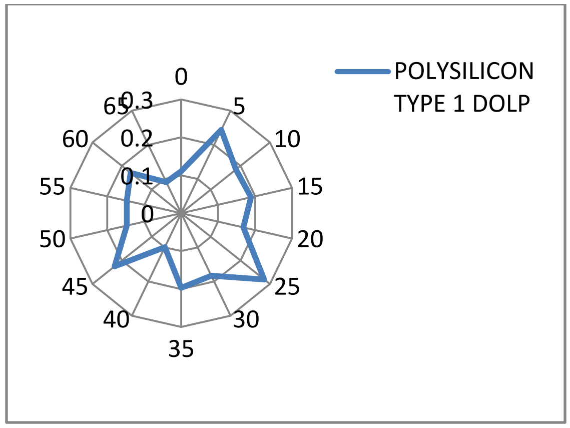

Figure 6.62 Detector at 50 Deg

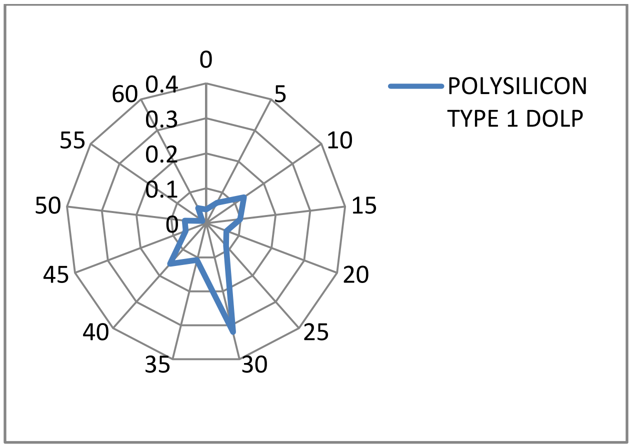

Figure 6.63 Detector at 60 Deg

6.10 Polysilicon Solar Panel with Glass Window

Solar panel made of polysilicon material with glass window was explored to obtain backscattered polarimetric signatures. The observed backscattered distributions as shown in polar plots 6.64-6.60 were found to be sharp indicating specular reflectance nature of the surface. It can be seen that the polarization was 90% at 60 deg. detector position and the backscattered distribution at this position was found to be very sharp. The sharpness of the curve at 60 deg detector position was to due to less scattering of light at position nearer to the source. The effect of windowing and surface roughness on polarization response can be observed by comparing the two types of polysilicon panels which is shown in figures 6.90-6.95. The observed depolarization ratios were in the range of 50%-75%.

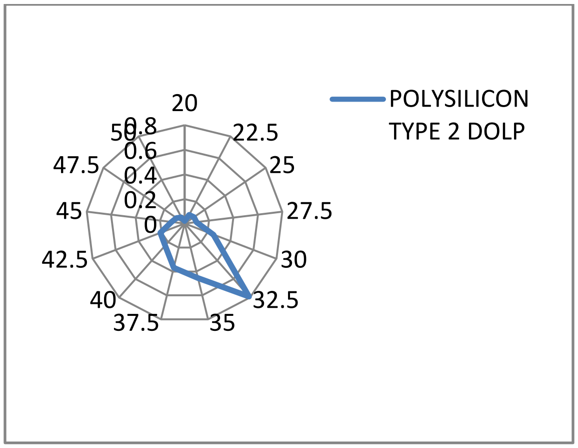

Figure 6.64 Detector at 10 Deg

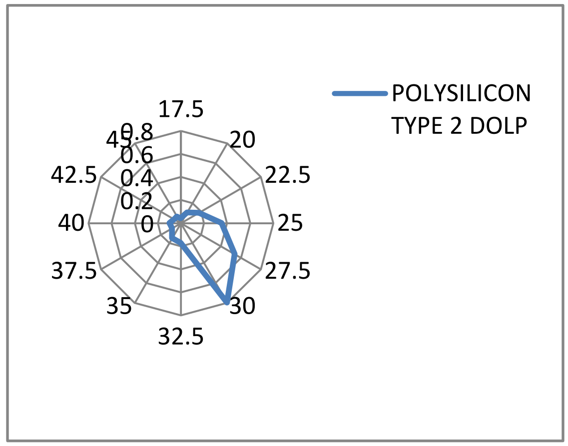

Figure 6.65 Detector at 20 Deg

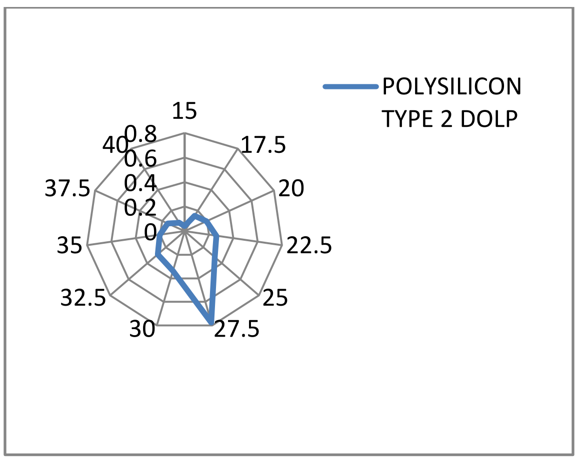

Figure 6.66 Detector at 30 Deg

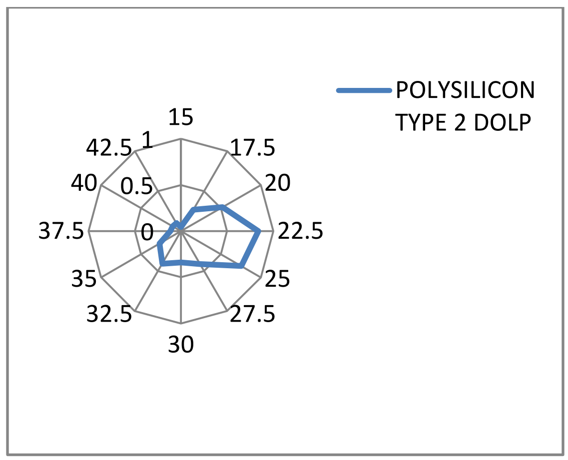

Figure 6.67 Detector at 40 Deg

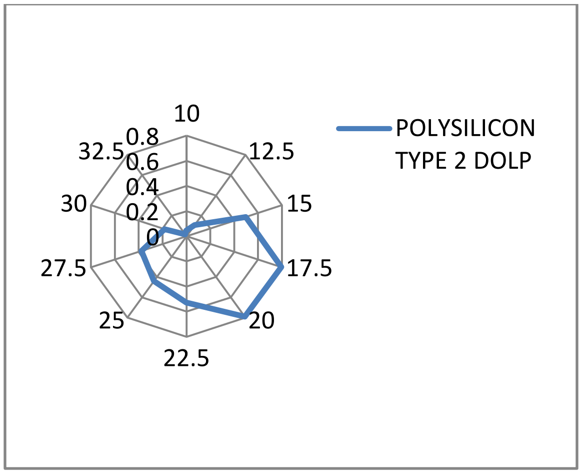

Figure 6.68 Detector at 50 Deg

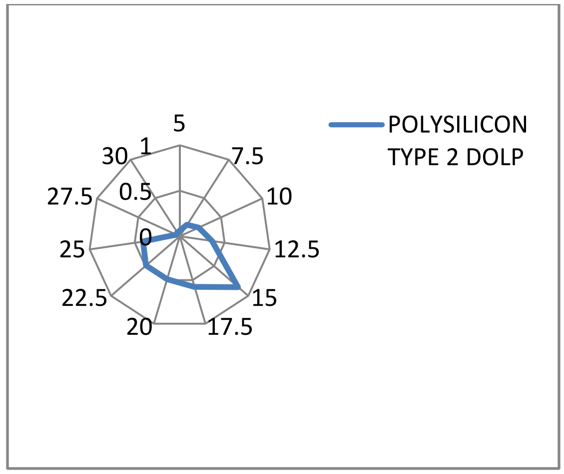

Figure 6.69 Detector at 60 Deg

6.11 Amorphous Silicon Solar Panel with Glass Window

Solar panel made of amorphous silicon with glass window was interrogated to obtain backscattered polarimetric signatures. The obtained DOLP curves were sharp and similar to the windowed polysilicon solar panel but the depolarization exhibited by amorphous silicon solar panel was high compared to polysilicon solar panel with window and depolarization ratios were in the range of 50%-95%. The polarization response can be observed in polar plots 6.70-6.75.

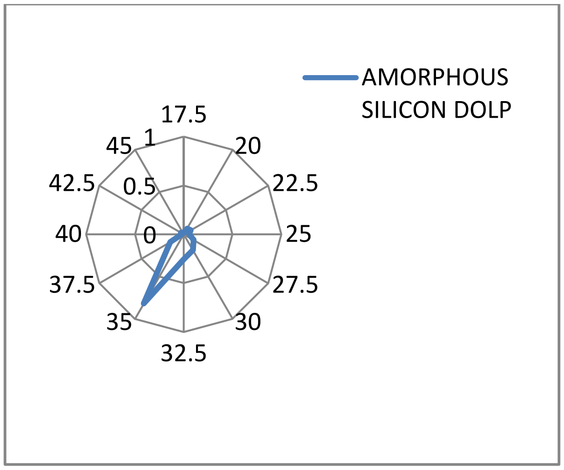

Figure 6.70 Detector at 10 Deg

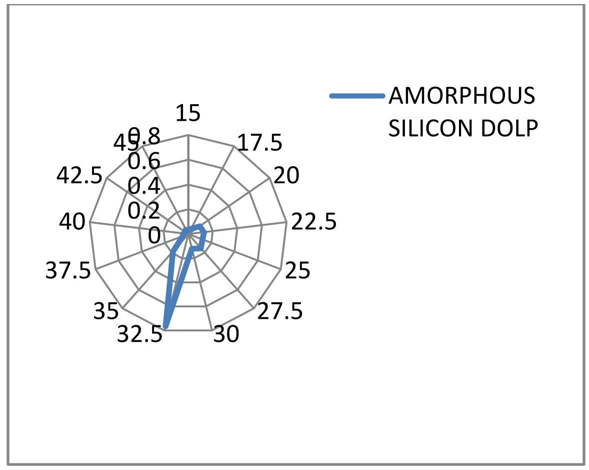

Figure 6.71 Detector at 20 Deg

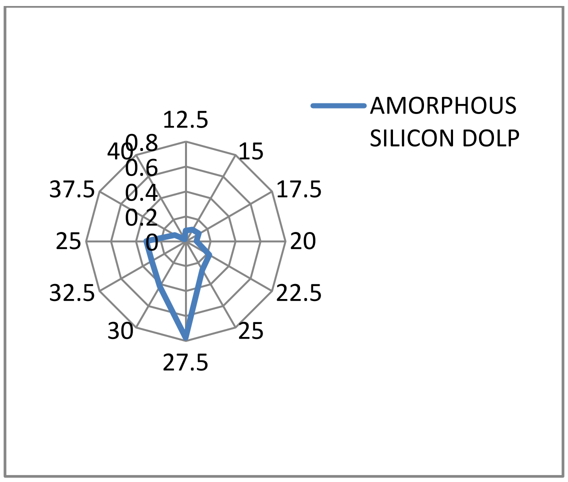

Figure 6.72 Detector at 30 Deg

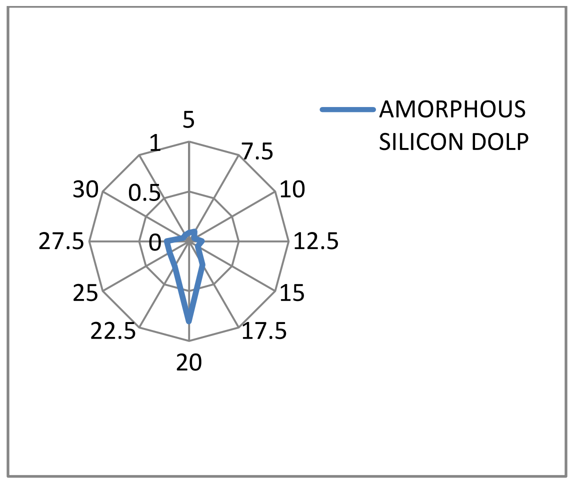

Figure 6.73 Detector at 40 Deg

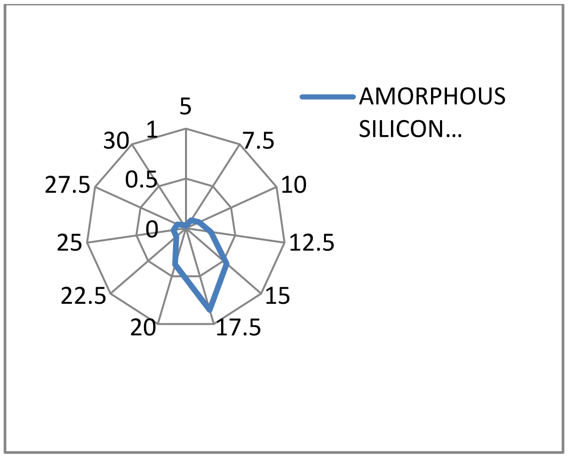

Figure 6.74 Detector at 50 Deg

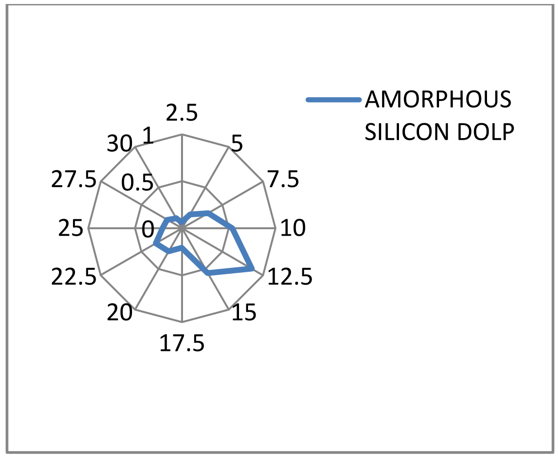

Figure 6.75 Detector at 60 Deg

6.12 Comparison of Different Materials

Different materials are compared based on their degree of linear polarization and presented in the following plots. For ease of comparison, materials are grouped according to their nature.

6.12.1 Comparison of Teflon-Kapton-White paint

The DOLP comparison of Teflon, Kapton and white paint mixture at different detector positions is represented in figures 6.76-6.82.

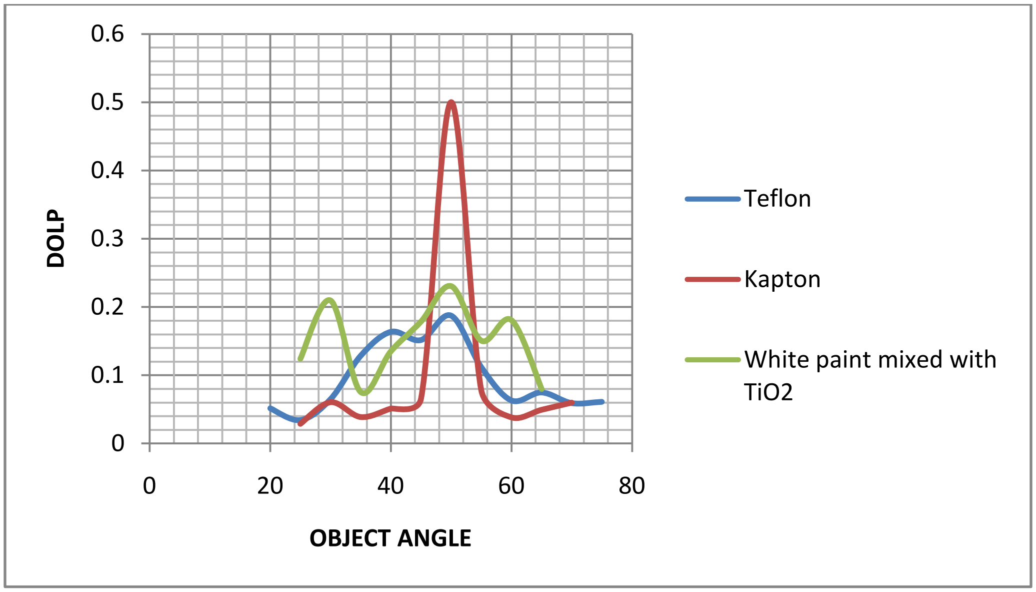

Figure 6.76 Detector at 0 Deg

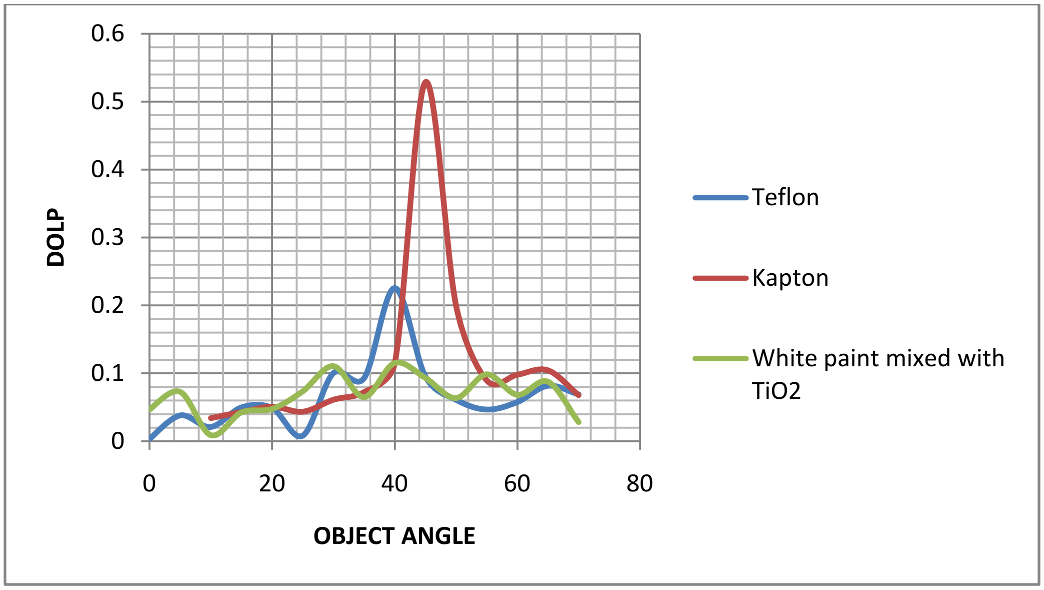

Figure 6.77 Detector at 10 Deg

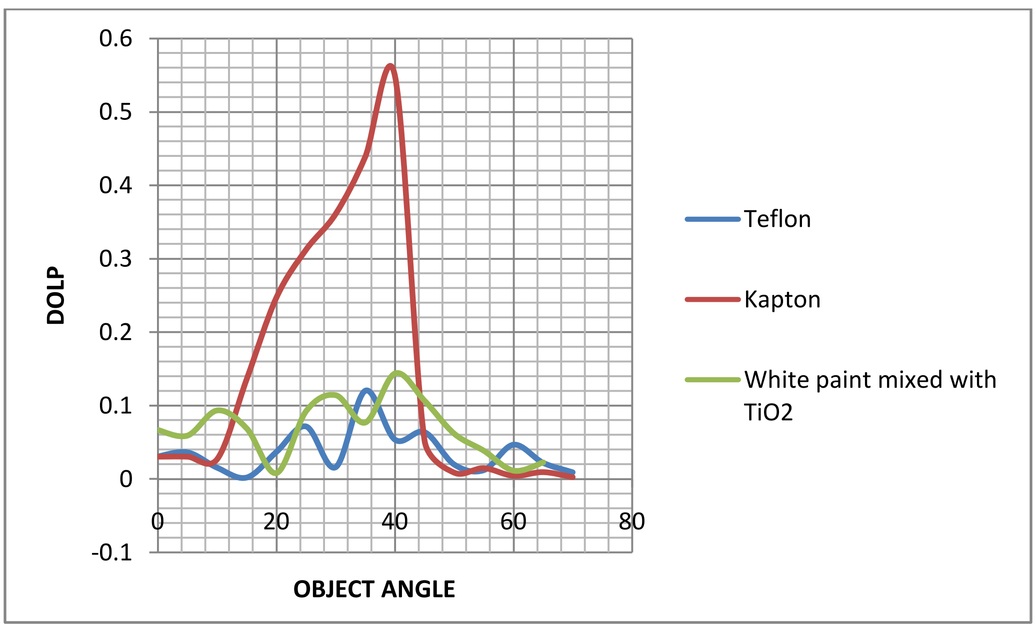

Figure 6.78 Detector at 20 Deg

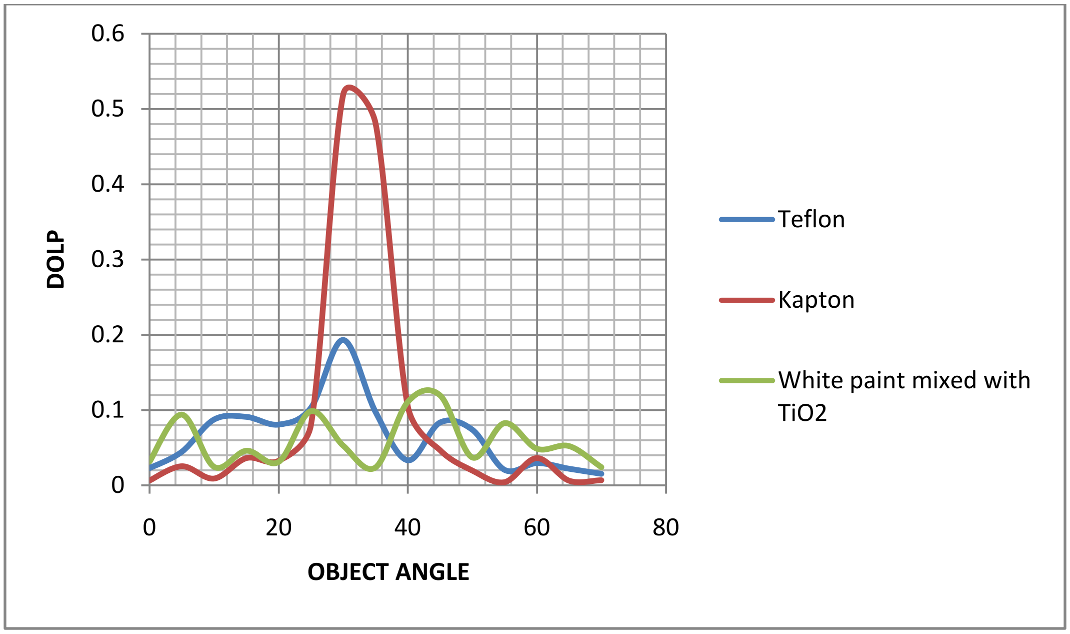

Figure 6.79 Detector at 30 Deg

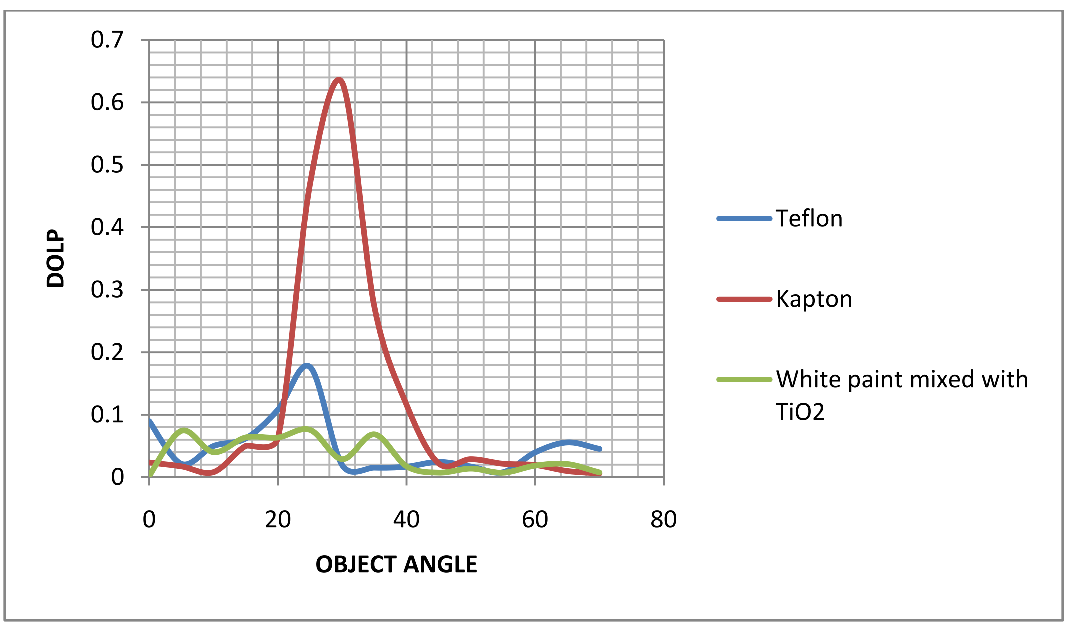

Figure 6.80 Detector at 40 Deg

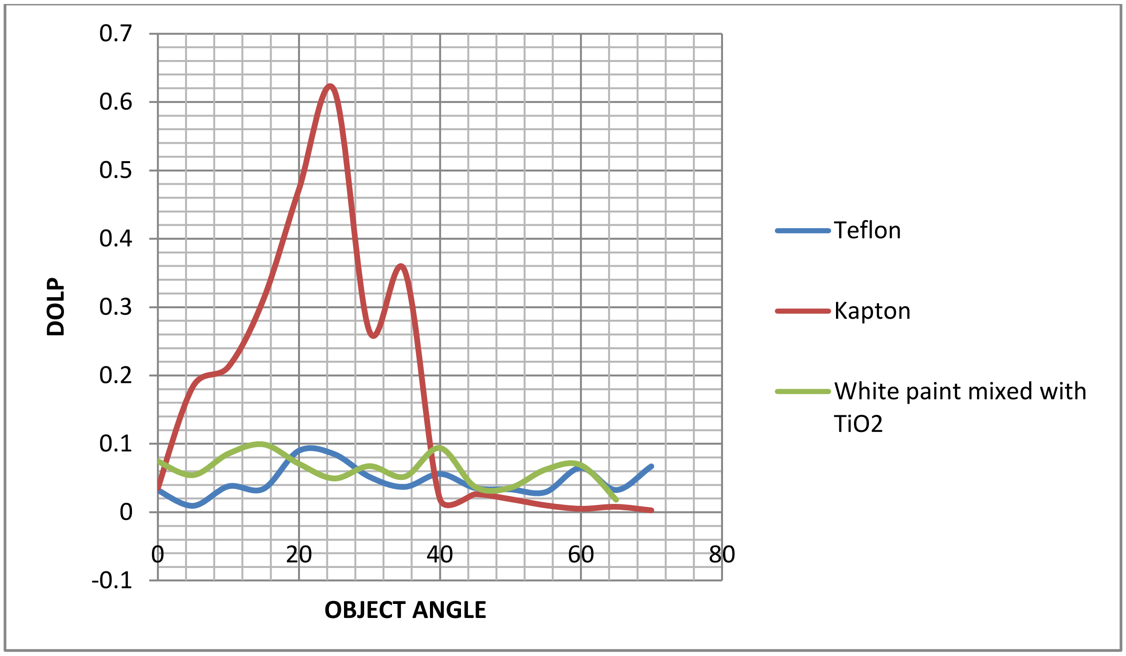

Figure 6.81 Detector at 50 Deg

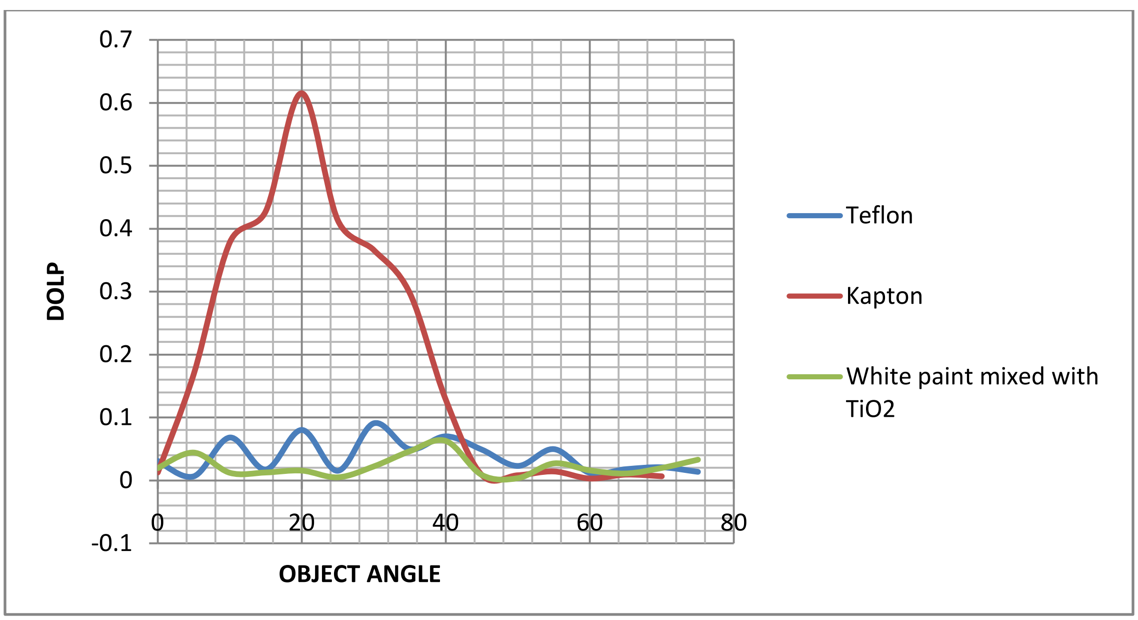

Figure 6.82 Detector at 60 Deg

6.12.2 Comparison of Different Metals

The DOLP comparison of different metallic objects at different detector positions is represented in figures 6.83-6.89.

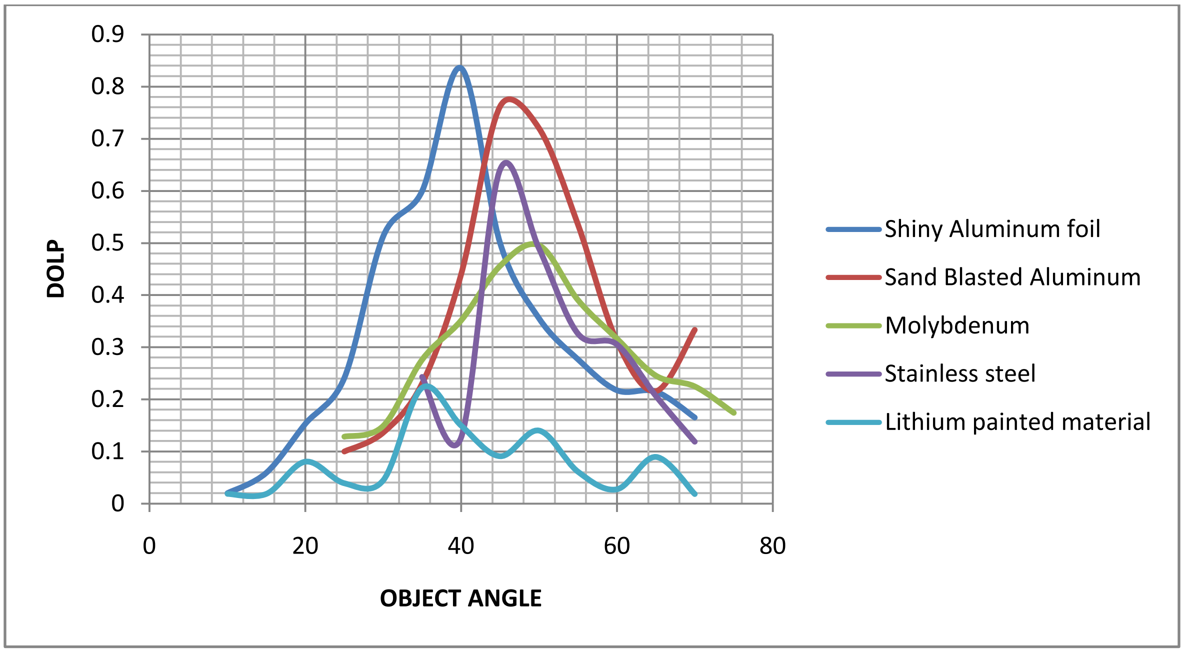

Figure 6.83 Detector at 0 Deg

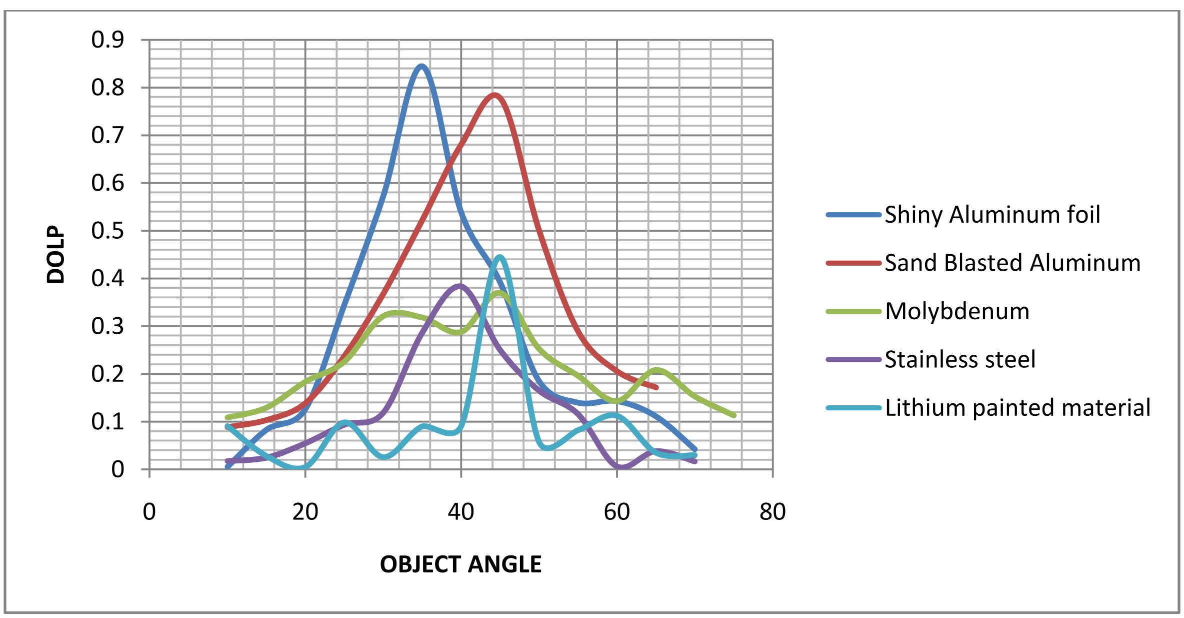

Figure 6.84 Detector at 10 Deg

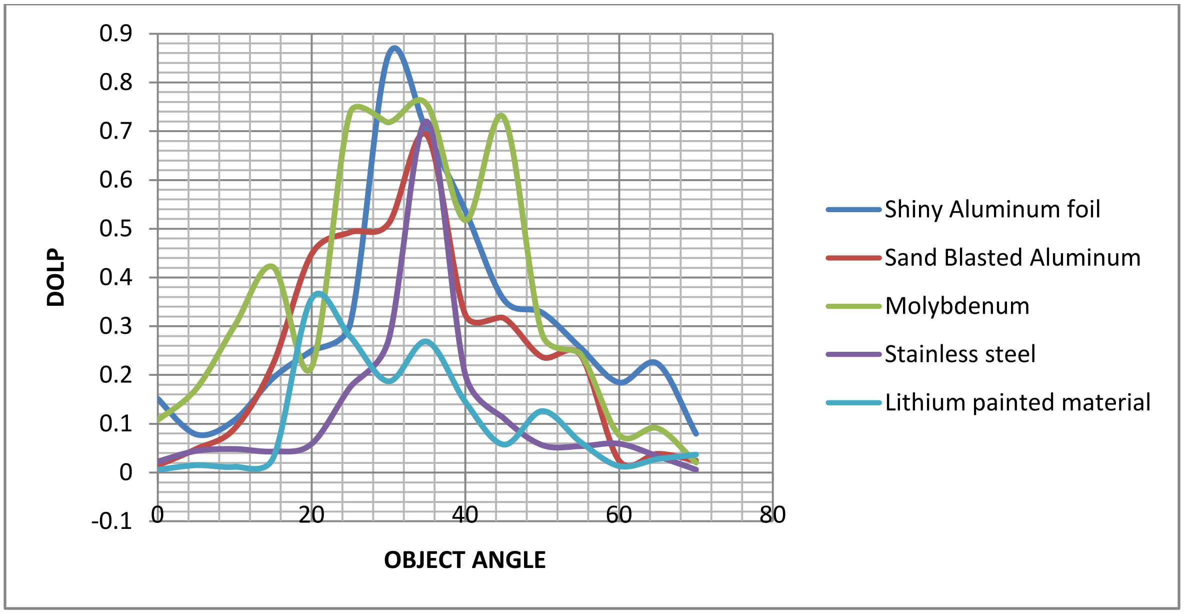

Figure 6.85 Detector at 20 Deg

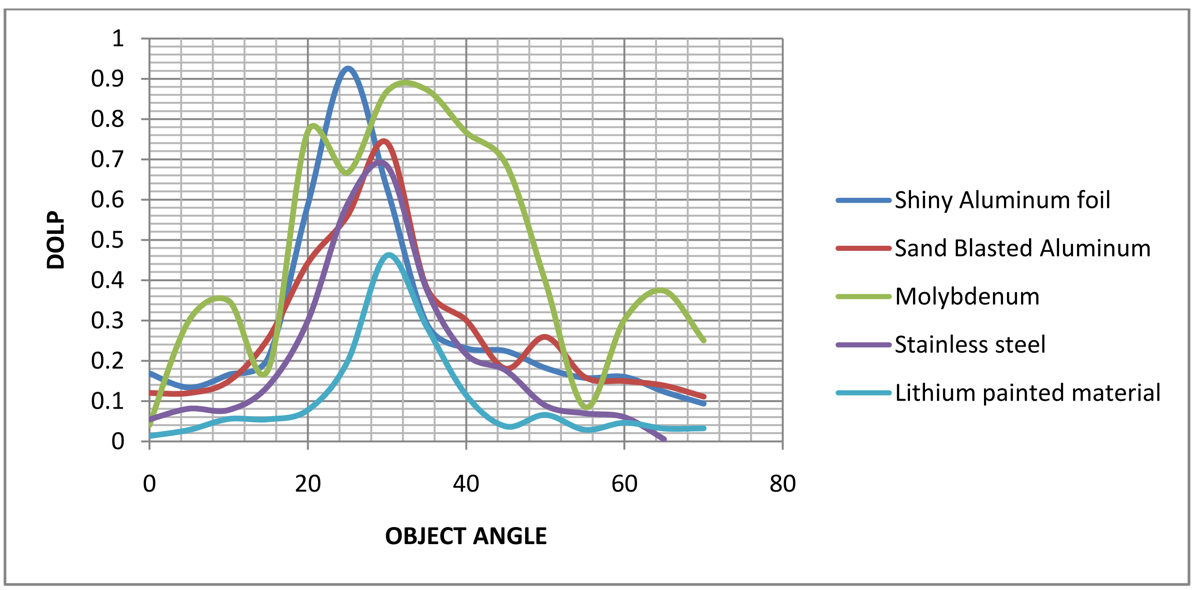

Figure 6.86 Detector at 30 Deg

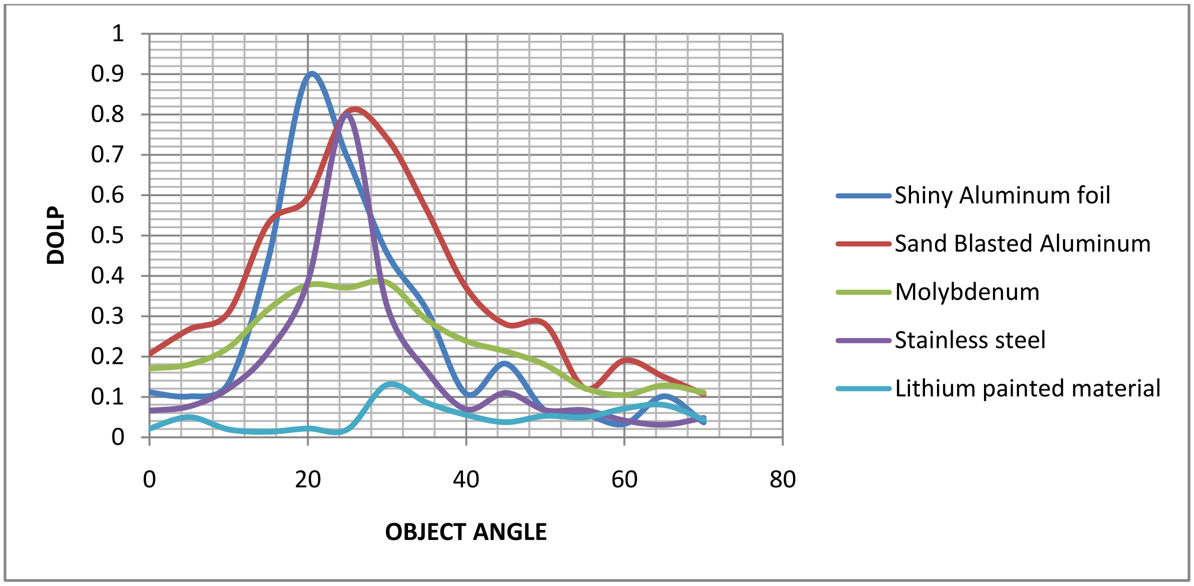

Figure 6.87 Detector at 40 Deg

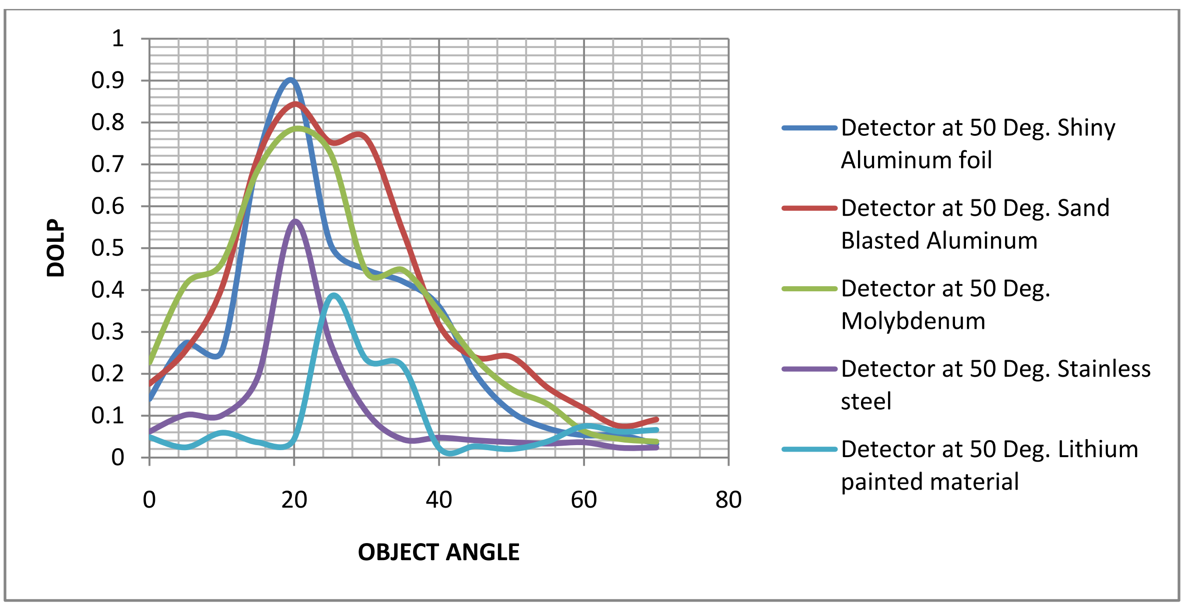

Figure 6.88 Detector at 50 Deg

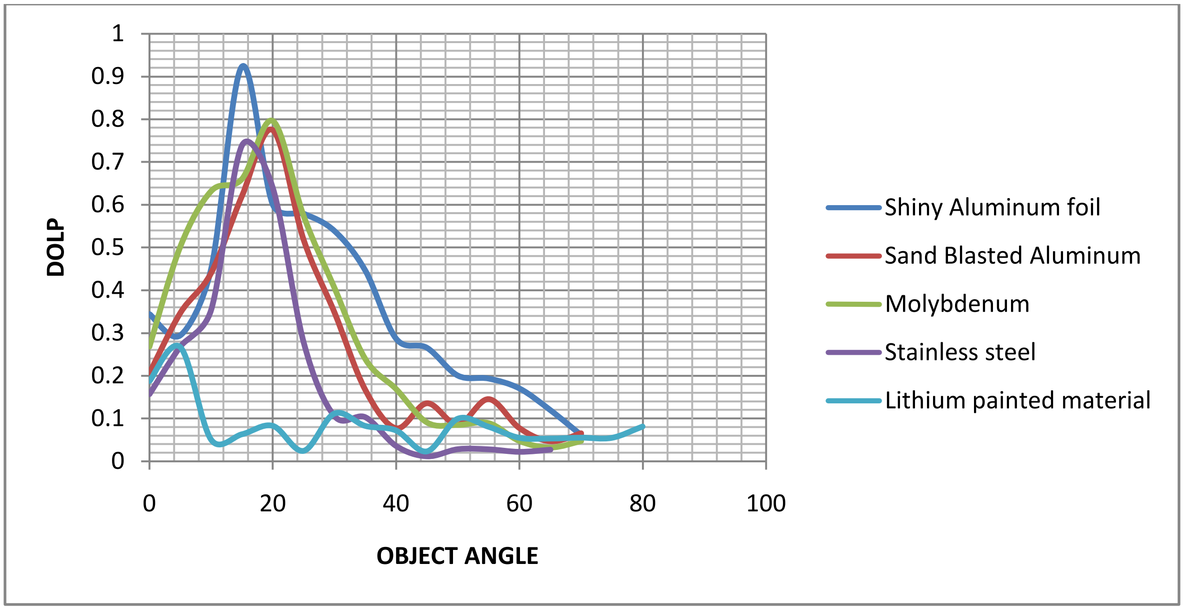

Figure 6.89 Detector at 60 Deg

6.12.3 Comparison of solar panels

The DOLP comparison of different solar panels at different detector positions is presented in figures 6.90-6.95.

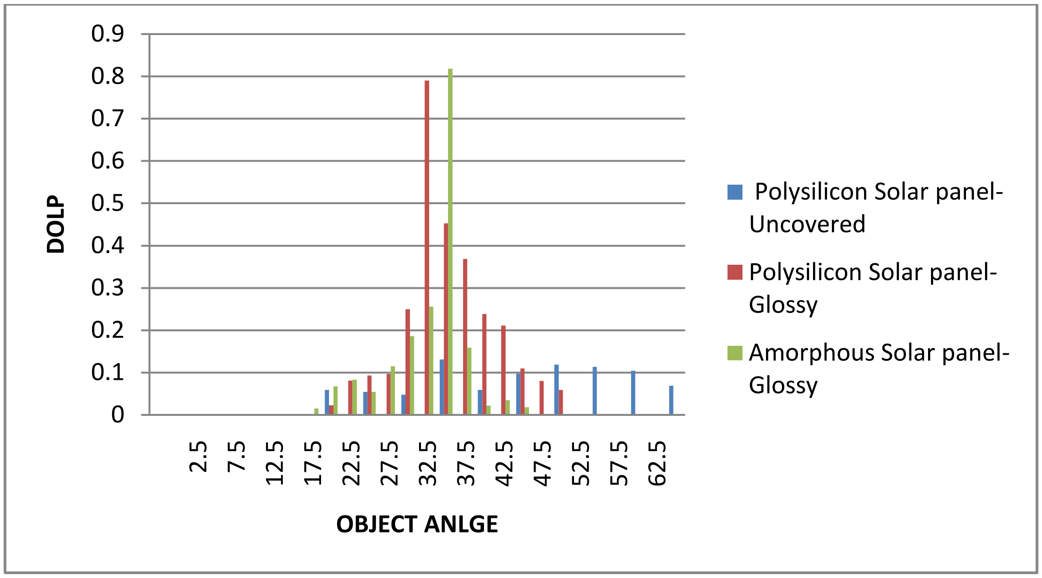

Figure 6.90 Detector at 10 Deg

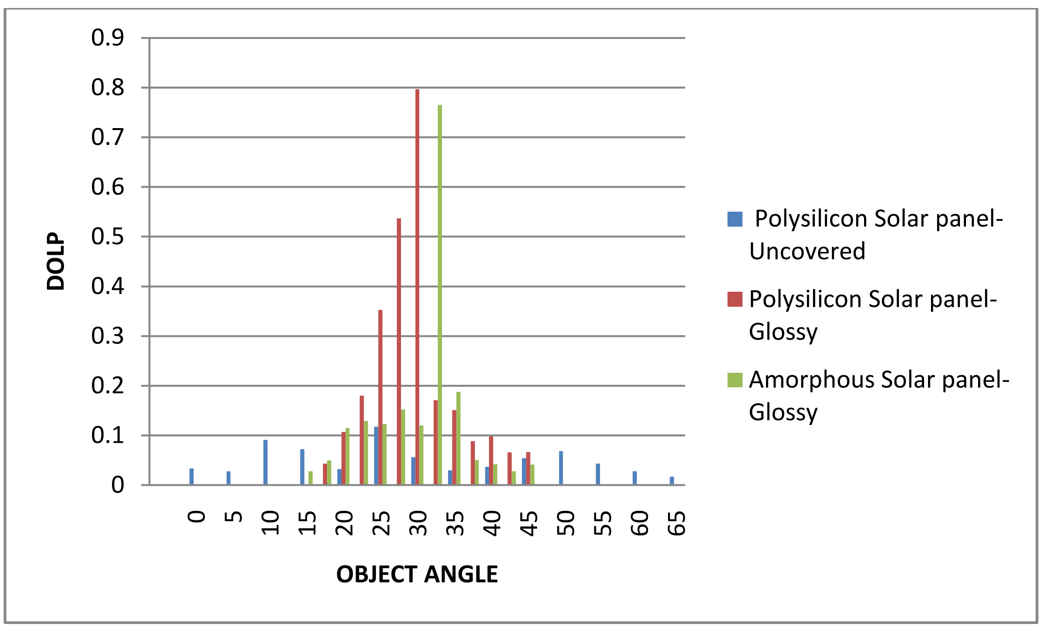

Figure 6.91 Detector at 20 Deg

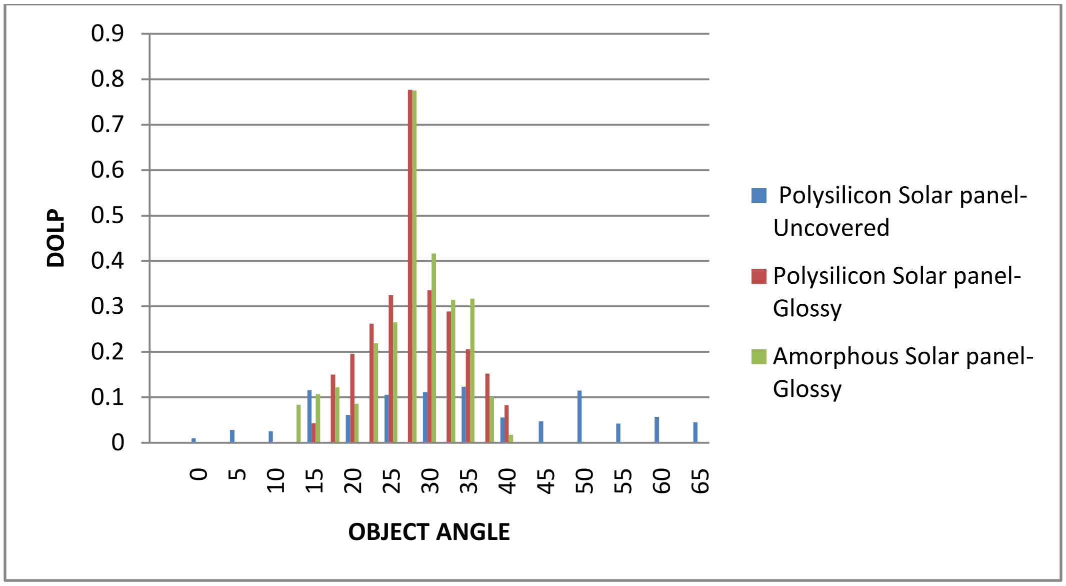

Figure 6.92 Detector at 30 Deg

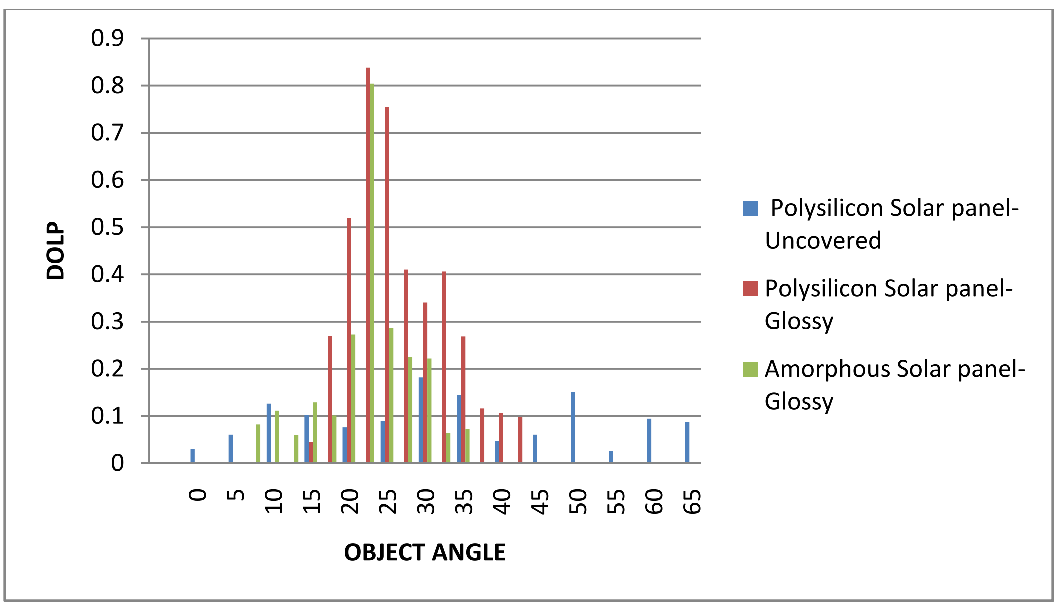

Figure 6.93 Detector at 40 Deg

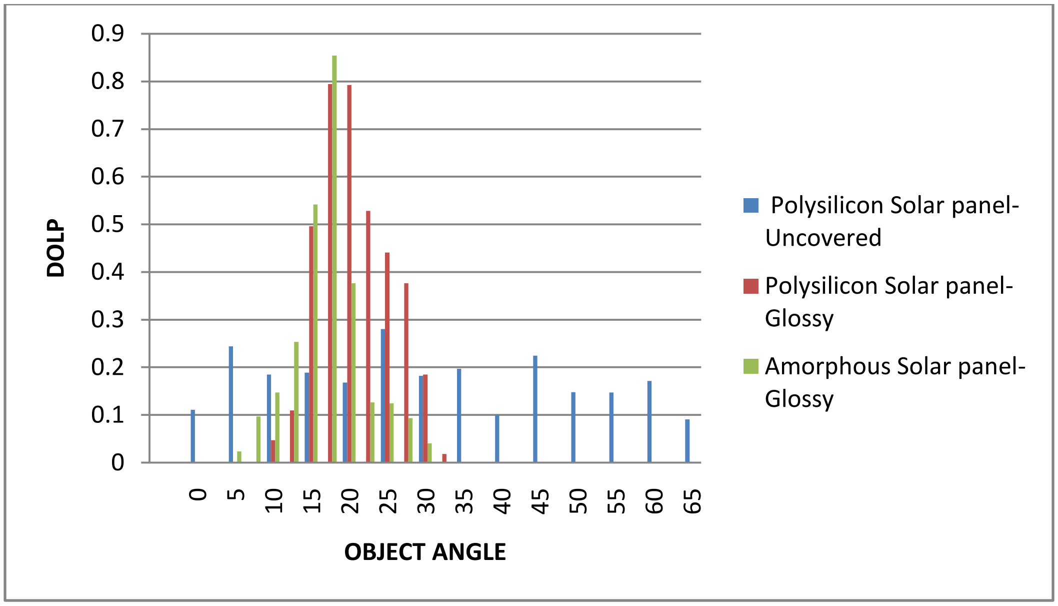

Figure 6.94 Detector at 50 Deg

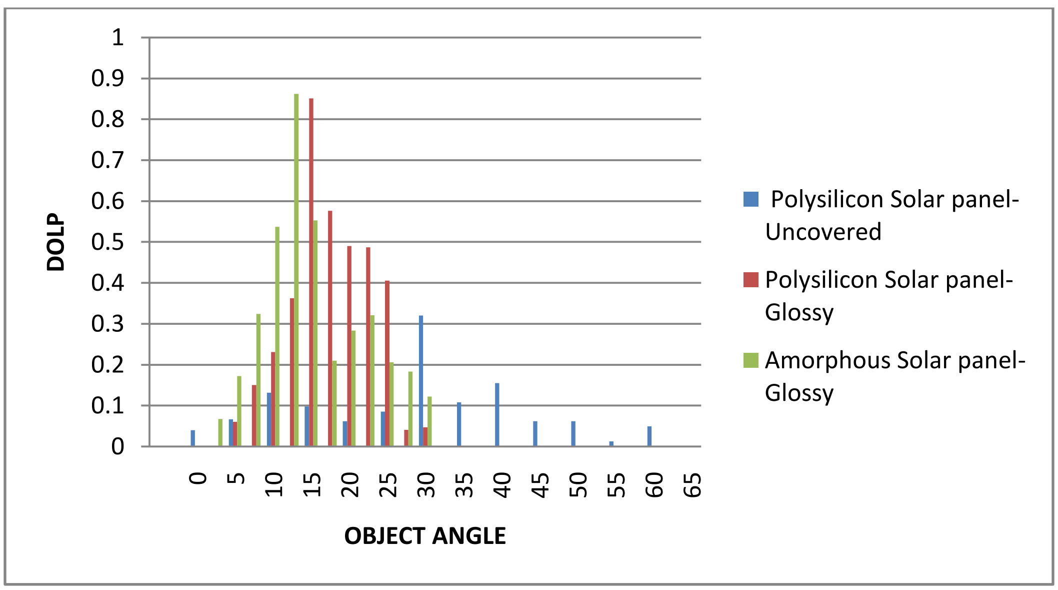

Figure 6.95 Detector at 60 Deg

Table 6.1 shows comparison of polarization response exhibited by different materials based on their degree of depolarization.

Table 6.1 Comparison of different materials

Material	Percentage of Depolarization (%)
Teflon	85-95
Kapton	60-90
Shiny Aluminum foil	10-50
Sand Blasted Aluminum	50-80
Molybdenum	30-80
White paint mixed with TiO_2 particles	90-98
Stainless Steel	50-90
Lithium Painted Material	55-95
Polysilicon Solar Panel-Uncovered	68-98
Polysilicon Solar Panel- Glossy	50-75
Amorphous Silicon Solar Panel- Glossy	50-95

The amount of depolarization exhibited by different materials can be observed from the above table. The depolarization depended on the composition of the material. Object Identification and monitoring can be performed using the obtained optical depolarization signatures and backscattered intensity distributions.

CHAPTER VII

CONCLUSIONS AND FUTURE WORK

A novel experimental study of surface identification of different materials through single pixel analysis of backscattered optical polarimetric signatures has been presented. A highly sensitive single pixel optical imaging system operating under backscattered geometry has been designed. Different materials such as lightweight space materials, metals, rough surfaces and solar panels were interrogated using 830 nm laser beams. The polarimetric signatures obtained from different materials were distinct and polarization response depended on material composition. The experimental results of this study indicated that single pixel polarimetric imaging can effectively detect and discriminate various space materials based on the amount of optical depolarization and backscattered intensity distributions.

As mentioned earlier, the presented single pixel imaging system was developed using single laser wavelength of 830 nm. It can be further tested at different wavelengths to improve multispectral capabilities. Further experiments using different space debris including rock samples from different planets can be performed as future work to increase the polarimetric signature database. Finally, 3-D imaging can be performed to increase imaging and recognition capabilities.

REFERENCES

1) B.B. Das, K.M. Yoo and R.R. Alfano, "Ultrafast time-gated imaging in thick tissues: a step toward optical mammography", Optical Society of America, Optics Letters, Vol.18, No. 13, July 1, 1993.

2) Edward A. Bucher and Robert M. Lerner, "Experiments on light pulse communication and propagation through atmospheric clouds", Applied Optics, Vol. 12, No. 10, October 1973.

3) M.P Rowe, E.N. Pugh, J.S. Tyo and N. Engheta, "Polarization-difference imaging: a biologically inspired technique for observation through scattering media", Optical Society of America, Optics Society of America, Optics Letters, Vol.20, No.6, March 15, 1995.

4) Gareth D. Lewis, David L. Jordan, and P. John Roberts, "Backscattering target detection in a turbid medium by polarization discrimination", Applies Optics, Vol.38, No.18, June 20, 1999.

5) G.C. Giakos, "Multispectral, multifusion, laser polarimetric imaging principles", IEEE IST-2004, International Workshop on Imaging systems and Techniques, Stresa, Italy, 14 May 2004.

6) George.C.Giakos, Richard. H. Picard and Phan D. Dao, "Superresolution multispectral Imaging polarimetric space surveillance LADAR sensor design architectures", Proceedings of the SPIE, Vol. 7107, pp. 71070B-71070B-12, 2008.

7) George C. Giakos, A. Medithe, S. Sumrain, S. Sukumar, L. Fraiwan, and A. Orozco, "Surface defect imaging of semiconductor wafers, microelectronics, and spacecraft structures", IMTC 2005 - Instrumentation and Measurement Technology Conference, Ottawa, Canada, 17 – 19 May 2005.

8) S. Breugnot and P. Clemenceau, "Modeling and performance of polarization active imager at $\lambda = 806$ nm", SPIE, Vol. 3707, April 1999.

9) M. Alouini, A. Grisard, E. Lallier and D. Dolfi, "Target detection and discrimination through active multispectral polarimetric imaging", Computational Optical Sensing and Imaging (COSI), Charlotte, North Carolina, June 6, 2005.

10) M. J. Duggin, W. G. Egan and J. Gregory, "Measurement of polarization of targets of differing albedo and shadow depth", SPIE, Vol. 3699, April 1999.

11) Brian J. DeBoo, Jose M. Sasian, and Russell A. Chipman, "Depolarization of diffusely reflecting man-made objects", Applied Optics, Vol. 44, No. 26, September 10, 2005.

12) W. G. Egan, J. Grusauskas, and H. B. Hallock, "Optical depolarization properties of Surfaces Illuminated by Coherent Light", Applied Optics, Vol. 7, No. 8, August, 1968.

13) Cornell S. L. Chun and Firooz A. Sadjadi, "Polarimetric laser radar target classification", OSA, Optics Letters, Vol. 30, No. 14, July 15, 2005.

14) Daniel A. Lavigne, Mélanie Breton, Mario Pichette, Vincent Larochelle, and Jean-Robert Simard, "Enhanced military target discrimination using active and passive polarimetric imagery", Geoscience and Remote Sensing Symposium, 2008. IGARSS 2008. IEEE International**,** Vol. 5, pp. V - 354-V – 357, 7-11 July 2008.

15) Gareth D. Lewis, David L. Jordan and Eric Jakeman, "Backscatter linear and circular polarization analysis of roughened aluminum", Applied Optics, Vol. 37, No. 25, 1 September 1998

16) G.C. Giakos, "Novel molecular imaging and nanophotonics detection principles", IEEE International Workshop on Imaging Systems and Techniques, Niagara Falls, pp. 103-108, 2005.

17) G.C. Giakos, "Multifusion, multispectral light wave polarimetric detection principles and systems" IEEE transactions on Instrumentation and Measurement, vol. 55, No. 6, pp.1904-1912, December 2006.

18) G.C. Giakos, "Multifusion, multispectral optical polarimetric imaging sensing principles" IEEE transactions on Instrumentation and Measurement, vol. 55, No.5, pp.1628-1633, October 2006.

19) G.C. Giakos, S.A. Paturi, P. Bathini, S. Sukumar, K. Ambadipudi, K. Valluru, D. Wagenar, V. Adya, M. Reddy, "New Pathways for the Enhancement of Image Quality", IEEE Instrumentation and Measurement Technology Conference (IMTC), Poland, May 2007.

20) G.C. Giakos, K. Valluru, S.A. Paturi, V. Adya, K. Ambadipudi, P. Bathini, M. Reddy and S. Sukumar, "Enhanced detection and imaging based on novel molecular nanophotonics principles", IEEE International Workshop on Imaging Systems and Techniques, IST 2007, Krakow, Poland, May 2007.

21) G.C. Giakos, S. Sukumar, P. Bathini, S.A. Paturi, K. Ambadipudi, D. Wagenar. Adya, M. Reddy, S. Sumrain, L. Fraiwan, D.B. Sheffer, "Enhanced Detectability of Targets in Opaque Media" Proc. IEEE IST 2006, International Workshop on Imaging Systems and Techniques, Minori, Italy, April 2006.

22) Article found on web at http://gizmodo.com/5158213/satellite-collision-may-have-endangered-all-future- space.

23) Article found on web at http://www.universetoday.com/2009/03/16/more-debris-on-possible-collision-course.

24) K.K.Sharma, "Optics: Principles and Applications", Academic Press, 2006.

25) Application Notes on "Basic Polarization Techniques and Devices", Meadowlark Optics, Inc.

26) Russell A. Chipman, "Polarimetry", College of Optical Sciences, University of Arizona.

27) Soe-Mie F. Nee., "Polarization Measurement", CRC Press LLC, 1999

28) Edward Collett, "Polarized Light: Fundamentals and Applications", Marcel Dekker, Inc. 1993.

29) Goldstein and Collett, "Polarized Light", CRC Press, 2003

30) G. C. Giakos, L. Fraiwan, N. Patnekar, S. Sumrain, G. B. Mertzios and S. Periyathamby, "A sensitive optical polarimetric imaging technique for surface defects detection of aircraft turbine engines", IEEE Transactions on instrumentation and measurement, Vol. 53, No. 1, Feb 2004.

31) Keerthi Valluru, "Study of biomolecular optical signatures for early disease detection and cell physiology monitoring", Thesis, The University of Akron, 2008.

32) Specification sheet of Optical tabletop, Melles Griot, available on web at http://www.mellesgriot.com/pdf/X_34_3.pdf

33) Iridium 33 and Cosmos 2251 satellite collision video image taken from web at www.agi.com.

APPENDIX

ERROR ANALYSIS

1) Kapton

- S.D refers to Standard deviation and SEM refers to Standard error of mean.
- d1, d2, d3 are 3 sets of DOLP’s obtained from 3 sets of signal measurements.

Table A.1.1 Detector at 0 deg

Kapton		Signal Intensities					DOLP					
Angles	Co-Polarized			Cross-Polarized			d1	d2	d3	Avg.	S.D	SEM
25	310	320	330	300	302	308	0.0164	0.0289	0.0345	0.0266	0.00437	0.00252
30	556	560	564	498	496	490	0.055	0.0606	0.0702	0.0619	0.00362	0.00209
35	390	400	410	360	370	380	0.04	0.039	0.038	0.039	0.00048	0.00028
40	420	410	400	400	370	380	0.0244	0.0513	0.0256	0.0338	0.00715	0.00413
45	560	570	580	490	500	510	0.0667	0.0654	0.0642	0.0654	0.00058	0.00033
50	3.06	3.09	3.25	1.02	1.03	1.01	0.5	0.5	0.5258	0.5086	0.00703	0.00406
55	610	620	640	520	530	540	0.0796	0.0783	0.0847	0.0809	0.00161	0.00093
60	530	540	550	490	500	510	0.0392	0.0385	0.0377	0.0385	0.00035	0.0002
65	540	530	520	500	480	490	0.0385	0.0495	0.0297	0.0392	0.00468	0.0027
70	520	530	540	460	470	480	0.0612	0.06	0.0588	0.06	0.00057	0.00033

Table A.1.2 Detector at 10 deg

Kapton		Signal Intensities						DOLP				
Angles	Co-Polarized			Cross-Polarized			d1	d2	d3	Avg.	S.D	SEM
10	230	227	234	210	212	216	0.04545	0.0342	0.04	0.0399	0.00266	0.001536
15	300	302	298	275	277	280	0.04348	0.0432	0.03114	0.0393	0.00332	0.001915
20	318	319	320	287	288	289	0.05124	0.0511	0.0509	0.0511	7.9E-05	4.58E-05
25	351	359	352	327	329	330	0.0354	0.0436	0.03226	0.0371	0.00276	0.001595
30	420	416	430	372	368	370	0.06061	0.0612	0.075	0.0656	0.00384	0.002215
35	560	562	558	490	486	494	0.06667	0.0725	0.06084	0.0667	0.00275	0.00159
40	688	690	696	544	548	552	0.11688	0.1147	0.11538	0.1157	0.00053	0.000304
45	4.23	4.15	4.16	1.27	1.28	1.29	0.53818	0.5285	0.52661	0.5311	0.00292	0.001687
50	1.12	1.11	1.1	0.73	0.74	0.76	0.21081	0.2	0.1828	0.1979	0.00666	0.003845
55	840	850	860	700	710	720	0.09091	0.0897	0.08861	0.0898	0.00054	0.000313
60	830	840	870	680	690	700	0.09934	0.098	0.10828	0.1019	0.00263	0.001518
65	730	740	720	590	600	610	0.10606	0.1045	0.08271	0.0977	0.00615	0.003552
70	682	676	688	580	590	600	0.08082	0.0679	0.06832	0.0724	0.00346	0.001996

Table A.1.3 Detector at 20 deg

Kapton		Signal Intensities					DOLP				
Angles	Co-Polarized			Cross-Polarized		d1	d2	d3	Avg.	S.D	SEM
0	330	340	350	310	320	330	0.03125	0.0303	0.02941	0.0303	0.00043	0.00025
5	330	340	350	310	320	330	0.03125	0.0303	0.02941	0.0303	0.00043	0.00025
10	370	380	390	350	360	370	0.02778	0.02703	0.02632	0.027	0.00034	0.000199
15	490	500	510	370	380	360	0.13953	0.13636	0.17241	0.1494	0.00941	0.005433
20	529	525	528	316	317	321	0.25207	0.24703	0.24382	0.2476	0.00196	0.001132
25	654	662	661	343	347	348	0.31194	0.31219	0.31021	0.3114	0.00051	0.000294
30	820	822	825	388	386	382	0.35762	0.36093	0.36703	0.3619	0.00225	0.001299
35	1.1	1.2	1.3	0.48	0.47	0.48	0.39594	0.43885	0.4574	0.4307	0.01486	0.00858
40	4.11	4.12	4.15	1.1	1.2	1.3	0.57774	0.54887	0.52294	0.5498	0.01292	0.007461
45	648	644	640	596	580	572	0.0418	0.05229	0.05611	0.0501	0.00349	0.002016
50	580	588	592	576	578	572	0.00346	0.00858	0.01718	0.0097	0.00327	0.001887
55	480	484	488	468	470	472	0.01266	0.01468	0.01667	0.0147	0.00094	0.000545
60	468	470	465	456	466	464	0.01299	0.00427	0.00108	0.0061	0.00291	0.001678
65	440	436	436	424	428	432	0.01852	0.00926	0.00461	0.0108	0.00334	0.001927
70	396	400	404	392	398	400	0.00508	0.00251	0.00498	0.0042	0.00069	0.000396

Table A.1.4 Detector at 30 deg

Kapton		Signal Intensities					DOLP				
Angles	Co-Polarized			Cross-Polarized		d1	d2	d3	Avg.	S.D	SEM
0	308	316	312	304	312	302	0.00654	0.00637	0.01629	0.0097	0.00268	0.00155
5	320	324	332	304	308	312	0.02564	0.02532	0.03106	0.0273	0.00152	0.00088
10	340	336	332	328	330	329	0.01796	0.00901	0.00454	0.0105	0.00322	0.00186
15	340	344	336	332	320	324	0.0119	0.03614	0.01818	0.0221	0.00593	0.00342
20	372	380	384	360	356	352	0.01639	0.03261	0.04348	0.0308	0.00643	0.00371
25	532	540	544	450	460	465	0.0835	0.08	0.0783	0.0806	0.00125	0.00072
30	6.4	6.32	6.34	1.96	2	2.02	0.5311	0.51923	0.51675	0.5224	0.00362	0.00209
35	3.18	3.2	3.22	1.14	1.12	1.1	0.47222	0.48148	0.49074	0.4815	0.00436	0.00252
40	670	630	690	520	510	530	0.12605	0.10526	0.13115	0.1208	0.00646	0.00373
45	540	560	570	500	510	520	0.03846	0.04673	0.04587	0.0437	0.00214	0.00124
50	530	520	510	490	500	508	0.03922	0.01961	0.00196	0.0203	0.00878	0.00507
55	485	480	476	474	476	472	0.01147	0.00418	0.00422	0.0066	0.00198	0.00114
60	340	344	336	332	320	324	0.0119	0.03614	0.01818	0.0221	0.00593	0.00342
65	336	328	316	328	324	310	0.01205	0.00613	0.00958	0.0093	0.0014	0.00081
70	308	300	304	298	296	290	0.0165	0.00671	0.02357	0.0156	0.00399	0.0023

Table A.1.5 Detector at 40 deg

Kapton		Signal Intensities					DOLP				
Angles	Co-Polarized			Cross-Polarized		d1	d2	d3	Avg.	S.D	SEM
0	438	440	433	418	420	424	0.02336	0.02326	0.0105	0.019	0.0035	0.002013
5	478	476	484	458	460	462	0.02137	0.01709	0.0233	0.0206	0.0015	0.000859
10	510	514	516	508	506	510	0.00196	0.00784	0.0058	0.0052	0.0014	0.000814
15	512	506	516	460	458	462	0.0535	0.04979	0.0552	0.0528	0.0013	0.000754
20	644	646	650	562	570	574	0.06799	0.0625	0.0621	0.0642	0.0016	0.000897
25	1.07	1.08	1.1	0.38	0.39	0.37	0.47586	0.46939	0.4966	0.4806	0.0067	0.003869
30	4.98	5	5.12	1.12	1.13	1.14	0.63279	0.63132	0.6358	0.6333	0.0011	0.000619
35	2.2	2.24	2.16	1.3	1.28	1.34	0.25714	0.27273	0.2343	0.2547	0.0091	0.005262
40	1.04	1.06	1.02	0.88	0.84	0.86	0.08333	0.11579	0.0851	0.0947	0.0086	0.004967
45	0.92	0.94	0.96	0.88	0.9	0.89	0.02222	0.02174	0.0378	0.0273	0.0043	0.002493
50	0.88	0.9	0.91	0.84	0.85	0.86	0.02326	0.02857	0.0282	0.0267	0.0014	0.000811
55	0.905	0.96	0.94	0.9	0.92	0.91	0.00277	0.02128	0.0162	0.0134	0.0045	0.002603
60	0.634	0.64	0.64	0.62	0.61	0.61	0.0144	0.01923	0.0256	0.0198	0.0027	0.001535
65	0.574	0.58	0.58	0.57	0.57	0.57	0.00175	0.00959	0.0017	0.0044	0.0021	0.001233
70	0.536	0.53	0.52	0.52	0.52	0.52	0.01132	0.00571	0.001	0.006	0.0024	0.001411

Table A.1.6 Detector at 50 deg

Kapton		Signal Intensities					DOLP				
Angles	Co-Polarized			Cross-Polarized		d1	d2	d3	Avg.	S.D	SEM
0	320	324	328	306	302	308	0.0224	0.0351	0.0314	0.0297	0.0031	0.00179
5	356	360	358	244	248	252	0.1867	0.1842	0.1738	0.1815	0.003228	0.001864
10	380	388	390	248	252	256	0.2102	0.2125	0.2074	0.21	0.001197	0.000691
15	480	488	484	252	256	260	0.3115	0.3118	0.3011	0.3081	0.00288	0.001663
20	828	836	832	296	300	302	0.4733	0.4718	0.4674	0.4708	0.001457	0.000841
25	5.64	5.58	5.52	1.28	1.32	1.24	0.6301	0.6174	0.6331	0.6269	0.003934	0.002271
30	804	812	808	480	472	468	0.2523	0.2648	0.2665	0.2612	0.003638	0.002101
35	440	444	452	208	212	216	0.358	0.3537	0.3533	0.355	0.001241	0.000716
40	420	416	402	396	400	404	0.0294	0.0196	-0.0025	0.0155	0.007701	0.004446
45	428	430	432	404	408	412	0.0288	0.0263	0.0237	0.0263	0.001214	0.000701
50	429	428	416	408	412	404	0.0251	0.019	0.0146	0.0196	0.002474	0.001429
55	400	404	412	398	396	392	0.0025	0.01	0.0249	0.0125	0.005367	0.003099
60	396	400	404	388	396	386	0.0102	0.005	0.0228	0.0127	0.004305	0.002486
65	392	384	388	372	378	380	0.0262	0.0079	0.0104	0.0148	0.004674	0.002699
70	368	370	372	364	368	370	0.0055	0.0027	0.0027	0.0036	0.000752	0.000434

Table A.1.7 Detector at 60 deg

Kapton		Signal Intensities					DOLP				
Angles	Co-Polarized			Cross-Polarized		d1	d2	d3	Avg.	S.D	SEM
0	320	324	322	314	316	318	0.0095	0.0125	0.0063	0.0094	0.00147	0.000851
5	330	332	336	232	236	240	0.1744	0.169	0.1667	0.17	0.00186	0.001076
10	382	390	378	172	176	180	0.3791	0.3781	0.3548	0.3707	0.00646	0.003732
15	520	524	526	204	210	202	0.4365	0.4278	0.4451	0.4364	0.00407	0.002349
20	5.48	5.12	5.4	1.2	1.22	1.24	0.6407	0.6151	0.6265	0.6275	0.00604	0.003488
25	1.04	1.06	1.08	0.42	0.44	0.46	0.4247	0.4133	0.4026	0.4135	0.0052	0.003002
30	778	780	782	360	362	366	0.3673	0.366	0.3624	0.3652	0.00121	0.000698
35	664	665	669	358	360	362	0.2994	0.2976	0.2978	0.2982	0.00048	0.000276
40	452	458	460	356	354	358	0.1188	0.1281	0.1247	0.1239	0.00221	0.001276
45	344	356	358	340	350	349	0.0058	0.0085	0.0127	0.009	0.00164	0.000945
50	370	374	372	366	368	370	0.0054	0.0081	0.0027	0.0054	0.00127	0.000734
55	360	358	354	346	348	350	0.0198	0.0142	0.0057	0.0132	0.00336	0.001938
60	340	342	346	338	340	332	0.0029	0.0029	0.0206	0.0088	0.00482	0.002783
65	329	332	333	325	326	342	0.0061	0.0091	-0.0133	0.0006	0.00575	0.003317
70	310	313	316	308	309	307	0.0032	0.0064	0.0144	0.008	0.00272	0.001572

2) Kapton

Table A.2.1 Detector at 0 deg

Teflon			Signal Intensities					DOLP				
Angles		Co-Polarized			Cross-Polari		d1	d2	d3	Avg.	S.D	SEM
20	590	610	600	530	550	540	0.0536	0.0517	0.053	0.053	0.00044	0.00025
25	740	750	760	690	700	710	0.035	0.0345	0.034	0.034	0.00022	0.00013
30	890	900	880	780	790	800	0.0659	0.0651	0.048	0.06	0.00486	0.00281
35	1.12	1.14	1.13	0.9	0.88	0.87	0.1089	0.1287	0.13	0.123	0.00557	0.00322
40	1.34	1.35	1.38	0.96	0.97	0.98	0.1652	0.1638	0.169	0.166	0.0014	0.00081
45	1.49	1.48	1.5	1.08	1.09	1.1	0.1595	0.1518	0.154	0.155	0.0019	0.0011
50	1.51	1.52	1.53	1.05	1.04	1.02	0.1797	0.1875	0.2	0.189	0.00483	0.00279
55	1.35	1.34	1.32	1.06	1.07	1.08	0.1203	0.112	0.1	0.111	0.00482	0.00278
60	1.25	1.26	1.28	1.1	1.11	1.12	0.0638	0.0633	0.067	0.065	0.00085	0.00049
65	1.28	1.29	1.3	1.1	1.11	1.12	0.0756	0.075	0.074	0.075	0.00029	0.00017
70	1.15	1.16	1.17	1.02	1.03	1.04	0.0599	0.0594	0.059	0.059	0.00026	0.00015
75	1.03	1.04	1.05	0.93	0.92	0.94	0.051	0.0612	0.055	0.056	0.00242	0.00139

Table A.2.2 Detector at 10 deg

Teflon			Siganl Intensities					DOLP				
Angles		Co-Polarized			Cross-Polarize		d1	d2	d3	Avg.	S.D	SEM
0	282	287	290	281	285	287	0.0018	0.0035	0.0052	0.00349	0.000807	0.000466
5	335	340	336	314	315	318	0.0324	0.03817	0.0275	0.03268	0.002513	0.001451
10	430	434	436	412	416	418	0.0214	0.02118	0.0211	0.02121	7.22E-05	4.17E-05
15	560	568	552	520	514	526	0.037	0.04991	0.0241	0.03702	0.006078	0.003509
20	636	640	628	576	580	592	0.0495	0.04918	0.0295	0.04273	0.005399	0.003117
25	730	724	728	706	712	716	0.0167	0.00836	0.0083	0.01113	0.002281	0.001317
30	916	920	924	748	752	740	0.101	0.10048	0.1106	0.10401	0.002685	0.00155
35	0.98	1	0.97	0.828	0.83	0.832	0.0841	0.0929	0.0766	0.08452	0.00385	0.002223
40	1.67	1.63	1.68	1.02	1.03	1.04	0.2416	0.22556	0.2353	0.23416	0.003816	0.002203
45	1.25	1.26	1.27	1.03	1.04	1.05	0.0965	0.09565	0.0948	0.09566	0.000392	0.000226
50	1.29	1.3	1.31	1.14	1.15	1.16	0.0617	0.06122	0.0607	0.06123	0.000236	0.000136
55	1.25	1.23	1.22	1.07	1.12	1.09	0.0776	0.04681	0.0563	0.06022	0.007431	0.00429
60	1.18	1.19	1.21	1.05	1.06	1.04	0.0583	0.05778	0.0756	0.06388	0.00477	0.002754
65	1.2	1.19	1.18	1	1.01	1.02	0.0909	0.08182	0.0727	0.08182	0.004285	0.002474
70	1.15	1.16	1.14	0.98	1.01	0.97	0.0798	0.06912	0.0806	0.0765	0.003017	0.001742

Table A.2.3 Detector at 20 deg

Teflon			Siganl Intensities					DOLP				
Angles		Co-Polarized			Cross-Polariz		d1	d2	d3	Avg.	S.D	SEM
0	392	404	408	376	380	372	0.0208	0.0306	0.046	0.033	0.00602	0.003475
5	428	430	432	396	400	404	0.0388	0.0361	0.033	0.036	0.00126	0.000727
10	452	466	460	448	452	436	0.0044	0.0153	0.027	0.015	0.00527	0.003041
15	520	516	512	510	514	508	0.0097	0.0019	0.004	0.005	0.0019	0.001098
20	566	564	560	522	524	528	0.0404	0.0368	0.029	0.036	0.00265	0.001528
25	632	630	628	550	546	552	0.0694	0.0714	0.064	0.068	0.0017	0.000983
30	630	636	638	610	616	618	0.0161	0.016	0.016	0.016	5E-05	2.91E-05
35	728	830	736	648	652	656	0.0581	0.1201	0.057	0.079	0.01696	0.00979
40	752	748	744	680	672	664	0.0503	0.0535	0.057	0.054	0.00154	0.00089
45	764	768	772	680	676	682	0.0582	0.0637	0.062	0.061	0.00133	0.000769
50	720	728	724	696	700	704	0.0169	0.0196	0.014	0.017	0.00132	0.000763
55	680	676	672	652	660	662	0.021	0.012	0.007	0.013	0.00325	0.001875
60	768	764	760	692	696	690	0.0521	0.0466	0.048	0.049	0.00132	0.000763
65	696	698	680	660	668	670	0.0265	0.022	0.007	0.019	0.00471	0.00272
70	684	672	676	658	660	652	0.0194	0.009	0.018	0.015	0.00266	0.001537

Table A.2.4 Detector at 30 deg

Teflon			Siganl Intensities					DOLP				
Angles		Co-Polarized			Cross-Polariz		d1	d2	d3	Avg.	S.D	SEM
0	445	450	460	420	430	440	0.0289	0.02273	0.0222	0.0246	0.00175	0.001012
5	460	470	480	440	430	420	0.0222	0.04444	0.0667	0.0444	0.01048	0.006048
10	550	560	570	460	470	480	0.0891	0.08738	0.0857	0.0874	0.0008	0.000462
15	580	600	620	470	500	510	0.1048	0.09091	0.0973	0.0977	0.00327	0.001887
20	650	670	660	560	570	580	0.0744	0.08065	0.0645	0.0732	0.00383	0.002213
25	770	750	760	620	610	600	0.1079	0.10294	0.1176	0.1095	0.00353	0.002036
30	1.09	1.05	0.96	0.7	0.71	0.72	0.2179	0.19318	0.1429	0.1846	0.01802	0.010406
35	910	900	920	730	740	750	0.1098	0.09756	0.1018	0.103	0.00292	0.001685
40	790	780	770	720	730	740	0.0464	0.03311	0.0199	0.0331	0.00624	0.003605
45	770	780	790	670	660	650	0.0694	0.08333	0.0972	0.0833	0.00655	0.00378
50	790	800	810	680	690	700	0.0748	0.07383	0.0728	0.0738	0.00047	0.00027
55	740	750	760	710	720	700	0.0207	0.02041	0.0411	0.0274	0.00559	0.003229
60	710	700	690	650	660	670	0.0441	0.02941	0.0147	0.0294	0.00693	0.004002
65	690	700	682	660	670	680	0.0222	0.0219	0.0015	0.0152	0.0056	0.003236
70	660	670	680	650	650	640	0.0076	0.01515	0.0303	0.0177	0.00544	0.003143

Table A.2.5 Detector at 40 deg

Teflon			Siganl Intensities					DOLP				
Angles		Co-Polarized			Cross-Polariz		d1	d2	d3	Avg.	S.D	SEM
0	952	956	958	800	799	804	0.09	0.08946	0.0874	0.087872	0.000665	0.000384
5	964	960	956	916	920	924	0.03	0.02128	0.01702	0.021277	0.002006	0.001158
10	1.01	0.99	0.97	0.9	0.896	0.9	0.06	0.04984	0.03522	0.04755	0.005356	0.003092
15	1.19	1.2	1.21	1.07	1.06	1.05	0.05	0.06195	0.0708	0.061947	0.004172	0.002409
20	1.45	1.44	1.4	1.18	1.16	1.17	0.1	0.10769	0.08949	0.099949	0.00443	0.002558
25	1.62	1.87	1.75	1.3	1.31	1.32	0.11	0.1761	0.14007	0.141918	0.015695	0.009062
30	1.33	1.32	1.25	1.25	1.27	1.24	0.03	0.01931	0.00402	0.01811	0.006381	0.003684
35	1.31	1.33	1.35	1.28	1.29	1.27	0.01	0.01527	0.03053	0.019128	0.004737	0.002735
40	1.2	1.21	1.23	1.19	1.17	1.16	0	0.01681	0.02929	0.01676	0.005917	0.003416
45	1.25	1.26	1.27	1.21	1.2	1.19	0.02	0.02439	0.03252	0.02439	0.003833	0.002213
50	1.18	1.19	1.16	1.14	1.15	1.14	0.02	0.01709	0.00738	0.013906	0.002664	0.001538
55	1.26	1.27	1.28	1.24	1.25	1.23	0.01	0.00794	0.01992	0.011952	0.003253	0.001878
60	1.14	1.18	1.19	1.08	1.09	1.1	0.03	0.03965	0.0393	0.035325	0.003389	0.001956
65	1.13	1.14	1.15	1.06	1.02	1.01	0.03	0.05556	0.06481	0.050778	0.007985	0.00461
70	1.06	1.04	1.05	0.94	0.95	0.96	0.06	0.04523	0.04478	0.050001	0.004084	0.002358

Table A.2.6 Detector at 50 deg

Teflon			Siganl Intensities					DOLP				
Angles		Co-Polarized			Cross-Polarize		d1	d2	d3	Avg.	S.D	SEM
0	636	640	632	596	600	604	0.032	0.0323	0.0227	0.029126	0.002643	0.001526
5	652	648	650	642	636	640	0.008	0.0093	0.0078	0.008275	0.000437	0.000252
10	700	712	702	656	660	662	0.032	0.0379	0.0293	0.033225	0.002046	0.001181
15	720	724	728	680	676	672	0.029	0.0343	0.04	0.034286	0.002694	0.001555
20	840	848	844	704	708	712	0.088	0.09	0.0848	0.08763	0.001226	0.000708
25	896	892	900	748	752	756	0.09	0.0852	0.087	0.08738	0.00116	0.00067
30	856	852	858	772	768	764	0.052	0.0519	0.058	0.053801	0.001696	0.000979
35	856	840	848	776	780	768	0.049	0.037	0.0495	0.045187	0.003329	0.001922
40	824	828	830	744	740	736	0.051	0.0561	0.06	0.055723	0.002129	0.001229
45	764	760	752	704	708	712	0.041	0.0354	0.0273	0.034539	0.003214	0.001856
50	732	742	736	692	694	700	0.028	0.0334	0.0251	0.028862	0.001995	0.001152
55	704	700	696	664	660	652	0.029	0.0294	0.0326	0.030431	0.000903	0.000521
60	684	688	680	608	604	612	0.059	0.065	0.0526	0.058824	0.002919	0.001685
65	632	636	630	588	596	590	0.036	0.0325	0.0328	0.033773	0.000939	0.000542
70	640	636	632	560	556	552	0.067	0.0671	0.0676	0.067116	0.000212	0.000123

Table A.2.7 Detector at 60 deg

Teflon			Siganl Intensities				DOLP				
Angles		Co-Polarized		Cross-Polariz		d1	d2	d3	Avg.	S.D	SEM
0	301	302	305	278	284	276	0.0397	0.03072	0.0499	0.0401	0.0045	0.002614
5	316	318	322	312	314	308	0.0064	0.00633	0.0222	0.0116	0.0043	0.002494
10	348	346	352	300	302	304	0.0741	0.0679	0.0732	0.0717	0.0016	0.000907
15	410	414	416	398	400	402	0.0149	0.0172	0.0171	0.0164	0.0006	0.000362
20	496	500	504	424	426	428	0.0783	0.07991	0.0815	0.0799	0.0008	0.000447
25	462	470	464	450	456	454	0.0132	0.01512	0.0109	0.0131	0.001	0.000576
30	488	494	496	402	412	406	0.0966	0.09051	0.0998	0.0956	0.0022	0.001283
35	442	446	450	410	404	412	0.0376	0.04941	0.0441	0.0437	0.0028	0.001616
40	422	414	418	358	360	362	0.0821	0.06977	0.0718	0.0745	0.0031	0.001792
45	384	388	372	344	352	356	0.0549	0.04865	0.022	0.0419	0.0083	0.004763
50	398	404	402	382	386	398	0.0205	0.02278	0.005	0.0161	0.0046	0.002634
55	420	424	428	382	384	388	0.0474	0.0495	0.049	0.0486	0.0005	0.000303
60	352	346	344	336	338	340	0.0233	0.0117	0.0058	0.0136	0.0042	0.002411
65	344	346	348	338	334	340	0.0088	0.01765	0.0116	0.0127	0.0021	0.00123
70	344	346	342	328	332	334	0.0238	0.02065	0.0118	0.0188	0.0029	0.001689
75	300	302	304	296	294	298	0.0067	0.01342	0.01	0.01	0.0016	0.000913

3) Shiny Aluminum foil

Table A.3.1 Detector at 0 deg

Shiny AL			Signal Intensities				DOLP				
Angles		Co-Polarized			Cross-Polarize	d1	d2	d3	Avg.	S.D	SEM
10	101	102	104	95	98	99	0.0306	0.02	0.02463	0.02508	0.002508	0.001448
15	132	134	126	114	119	121	0.0732	0.05929	0.02024	0.0509	0.012937	0.007469
20	126	128	131	98	94	101	0.125	0.15315	0.12931	0.13582	0.007148	0.004127
25	126	121	123	75	74	77	0.2537	0.24103	0.23	0.24159	0.005598	0.003232
30	200	202	207	57	65	60	0.5564	0.51311	0.55056	0.54003	0.011077	0.006395
35	411	416	412	102	104	106	0.6023	0.6	0.59073	0.59769	0.002893	0.00167
40	2.7	2.9	2.6	0.24	0.26	0.28	0.8367	0.83544	0.80556	0.82591	0.008316	0.004801
45	13	13.2	13.3	4.8	4.4	4.1	0.4607	0.5	0.52874	0.49647	0.016107	0.009299
50	1.7	1.6	1.5	0.8	0.761	0.78	0.36	0.35536	0.31579	0.34372	0.011453	0.006613
55	168	173	160	92	98	94	0.2923	0.27675	0.25984	0.2763	0.007654	0.004419
60	139	140	141	86	90	93	0.2356	0.21739	0.20513	0.21936	0.007217	0.004167
65	128	130	132	82	84	86	0.219	0.21495	0.21101	0.215	0.001895	0.001094
70	55	60	62	48	43	45	0.068	0.16505	0.15888	0.13063	0.025626	0.014795

Table A.3.2 Detector at 10 deg

Shiny AL			Signal Intensities				DOLP				
Angles		Co-Polarized			Cross-Polarize	d1	d2	d3	Avg.	S.D	SEM
10	190	193	197	188	191	187	0.0053	0.00521	0.02604	0.01218	0.00566	0.003267
15	184	183	186	154	155	156	0.0888	0.08284	0.08772	0.08644	0.00149	0.00086
20	182	174	183	127	135	133	0.178	0.12621	0.15823	0.15414	0.01232	0.007112
25	164	158	165	75	77	74	0.3724	0.34468	0.38075	0.36594	0.0089	0.005139
30	476	500	512	124	136	130	0.5867	0.57233	0.59502	0.58467	0.00541	0.003123
35	14.3	14.2	14.4	1.1	1.2	1.3	0.8571	0.84416	0.83439	0.84523	0.00538	0.003106
40	890	900	910	260	270	280	0.5478	0.53846	0.52941	0.53857	0.00434	0.002506
45	812	824	852	350	360	370	0.3976	0.39189	0.39444	0.39464	0.00135	0.000777
50	120	125	127	88	86	92	0.1538	0.18483	0.15982	0.16617	0.00775	0.004475
55	91	98	97	70	74	72	0.1304	0.13953	0.14793	0.1393	0.00412	0.002381
60	82	84	86	60	63	62	0.1549	0.14286	0.16216	0.15332	0.0046	0.002654
65	78	80	85	61	64	66	0.1223	0.11111	0.12583	0.11975	0.00362	0.002091
70	60	62	65	54	57	53	0.0526	0.04202	0.10169	0.06545	0.01501	0.008665

Table A.3.3 Detector at 20 deg

Shiny AL			Signal Intensities					DOLP				
Angles		Co-Polarized			Cross-Polarize		d1	d2	d3	Avg.	S.D	SEM
0	144	152	148	110	112	116	0.1339	0.1515	0.12121	0.1355	0.00717	0.004142
5	324	330	326	280	282	286	0.0728	0.0784	0.06536	0.0722	0.00309	0.001785
10	150	154	152	122	124	126	0.1029	0.1079	0.09353	0.1015	0.00344	0.001989
15	158	160	162	112	108	116	0.1704	0.194	0.16547	0.1766	0.0072	0.004157
20	196	200	198	116	120	118	0.2564	0.25	0.25316	0.2532	0.00151	0.000872
25	698	700	702	370	374	378	0.3071	0.3035	0.3	0.3036	0.00168	0.000968
30	7.8	7.7	7.2	0.65	0.6	0.64	0.8462	0.8554	0.83673	0.8461	0.0044	0.002543
35	10	9.9	9.92	1.72	1.76	1.8	0.7065	0.6981	0.69283	0.6991	0.00325	0.001874
40	1.12	1.16	1.2	0.34	0.35	0.366	0.5342	0.5364	0.53257	0.5344	0.00091	0.000526
45	278	275	270	130	131	132	0.3627	0.3547	0.34328	0.3536	0.00461	0.002661
50	238	241	240	117	122	126	0.3408	0.3278	0.31148	0.3267	0.00694	0.004005
55	225	226	227	130	134	137	0.2676	0.2556	0.24725	0.2568	0.00482	0.002785
60	210	218	212	146	150	152	0.1798	0.1848	0.16484	0.1765	0.00489	0.002824
65	204	208	212	135	132	140	0.2035	0.2235	0.20455	0.2105	0.00531	0.003065
70	180	176	172	145	150	162	0.1077	0.0798	0.02994	0.0725	0.01857	0.010719

Table A.3.4 Detector at 30 deg

Shiny AL			Signal Intensities					DOLP				
Angles		Co-Polarized			Cross-Polariz		d1	d2	d3	Avg.	S.D	SEM
0	210	215	209	149	153	154	0.16992	0.1685	0.1515	0.1633	0.004824	0.002785
5	177	183	182	143	140	145	0.10625	0.1331	0.1131	0.1175	0.00658	0.003799
10	174	180	183	134	129	128	0.12987	0.165	0.1768	0.1573	0.011521	0.006652
15	207	201	202	134	132	133	0.21408	0.2072	0.206	0.2091	0.002059	0.001189
20	458	460	454	122	120	124	0.57931	0.5862	0.5709	0.5788	0.003605	0.002082
25	7.4	8	8.2	0.39	0.311	0.34	0.89987	0.9252	0.9199	0.915	0.006292	0.003633
30	2.32	2.8	2.4	0.68	0.64	0.72	0.54667	0.6279	0.5385	0.571	0.023308	0.013457
35	880	840	920	420	460	440	0.35385	0.2923	0.3529	0.333	0.016627	0.0096
40	235	240	237	144	150	148	0.24011	0.2308	0.2312	0.234	0.002488	0.001437
45	230	235	240	144	149	157	0.22995	0.224	0.2091	0.221	0.005068	0.002926
50	225	221	219	150	153	157	0.2	0.1818	0.1649	0.1822	0.008276	0.004778
55	231	232	230	164	169	162	0.16962	0.1571	0.1735	0.1667	0.004033	0.002328
60	208	207	210	152	150	147	0.15556	0.1597	0.1765	0.1639	0.005224	0.003016
65	191	192	195	148	150	151	0.12684	0.1228	0.1272	0.1256	0.001145	0.000661
70	180	182	177	156	151	152	0.07143	0.0931	0.076	0.0802	0.005384	0.003109

Table A.3.5 Detector at 40 Deg

Shiny AL			Signal Intensities					DOLP				
Angles		Co-Polarized			Cross-Polar		d1	d2	d3	Avg.	S.D	SEM
0	297	300	301	238	240	241	0.1103	0.111111	0.1107	0.1107	0.0002	0.000113
5	255	257	253	211	210	208	0.0944	0.100642	0.0976	0.0976	0.0015	0.000847
10	213	216	219	164	165	160	0.13	0.133858	0.1557	0.1398	0.0065	0.00377
15	177	180	176	67	70	71	0.4508	0.44	0.4251	0.4386	0.0061	0.003514
20	1.58	1.61	1.6	0.09	0.09	0.1	0.8909	0.894118	0.8801	0.8884	0.0034	0.00199
25	870	880	890	150	160	170	0.7059	0.692308	0.6792	0.6925	0.0063	0.003625
30	336	332	340	90	124	126	0.5775	0.45614	0.4592	0.4976	0.0326	0.018826
35	144	150	160	74	78	82	0.3211	0.315789	0.3223	0.3197	0.0016	0.000944
40	134	124	130	96	100	102	0.1652	0.107143	0.1207	0.131	0.0143	0.008269
45	128	130	112	86	90	95	0.1963	0.181818	0.0821	0.1534	0.0293	0.016915
50	112	114	110	96	100	98	0.0769	0.065421	0.0577	0.0667	0.0046	0.002634
55	108	104	102	90	93	96	0.0909	0.055838	0.0303	0.059	0.0143	0.008281
60	102	96	108	86	90	78	0.0851	0.032258	0.1613	0.0929	0.0306	0.017655
65	90	98	102	82	80	86	0.0465	0.101124	0.0851	0.0776	0.0132	0.007641
70	84	86	87	76	80	84	0.05	0.036145	0.0175	0.0346	0.0077	0.004432

Table A.3.6 Detector at 50 Deg

Shiny AL			Signal Intensities					DOLP				
Angles		Co-Polarized			Cross-Polar		d1	d2	d3	Avg.	S.D	SEM
0	96	98	102	70	74	68	0.1566	0.1395	0.2	0.1654	0.01469	0.008483
5	108	112	116	60	64	56	0.2857	0.2727	0.3488	0.3024	0.01919	0.011081
10	92	94	102	60	56	54	0.2105	0.2533	0.3077	0.2572	0.02296	0.013254
15	662	674	656	104	112	108	0.7285	0.715	0.7173	0.7202	0.00339	0.001959
20	1.95	1.84	1.86	0.1	0.1	0.99	0.9024	0.8959	0.3053	0.7012	0.16165	0.09333
25	390	400	410	120	130	150	0.5294	0.5094	0.4643	0.501	0.01573	0.00908
30	310	315	320	110	120	130	0.4762	0.4483	0.4222	0.4489	0.01272	0.007346
35	210	230	240	92	94	96	0.3907	0.4198	0.4286	0.413	0.00933	0.005389
40	160	170	180	82	80	81	0.3223	0.36	0.3793	0.3539	0.01366	0.007889
45	112	108	110	80	72	76	0.1667	0.2	0.1828	0.1832	0.00786	0.004537
50	104	102	112	88	82	86	0.0833	0.1087	0.1313	0.1078	0.01132	0.006533
55	110	108	112	96	94	92	0.068	0.0693	0.098	0.0784	0.00801	0.004624
60	97	100	102	88	90	92	0.0486	0.0526	0.0515	0.0509	0.00097	0.00056
65	94	100	102	86	90	92	0.0444	0.0526	0.0515	0.0495	0.0021	0.00121
70	90	96	94	88	90	86	0.0112	0.0323	0.0444	0.0293	0.00792	0.004572

Table A.3.7 Detector at 60 Deg

Shiny AL			Signal Intensities					DOLP				
Angles		Co-Polarized			Cross-Polariz		d1	d2	d3	Avg.	S.D	SEM
0	252	254	256	130	124	128	0.3194	0.3439	0.33333	0.332207	0.005803	0.003351
5	262	264	260	142	144	152	0.297	0.2941	0.26214	0.284428	0.009126	0.005269
10	520	522	516	188	198	186	0.4689	0.45	0.47009	0.463004	0.005316	0.003069
15	2.14	2.28	2.02	0.09	0.091	0.09	0.9184	0.9232	0.91378	0.918479	0.002227	0.001286
20	430	440	460	120	110	130	0.5636	0.6	0.55932	0.574319	0.010533	0.006081
25	380	390	370	108	104	102	0.5574	0.5789	0.5678	0.56804	0.005085	0.002936
30	320	340	350	106	102	104	0.5023	0.5385	0.54185	0.527553	0.010321	0.005959
35	230	240	210	90	92	94	0.4375	0.4458	0.38158	0.421621	0.016463	0.009505
40	152	155	160	82	86	84	0.2991	0.2863	0.31148	0.298976	0.005933	0.003425
45	146	148	144	81	86	90	0.2863	0.265	0.23077	0.26069	0.013214	0.007629
50	136	138	142	90	92	94	0.2035	0.2	0.20339	0.20231	0.000944	0.000545
55	132	136	138	90	92	87	0.1892	0.193	0.22667	0.202946	0.009725	0.005615
60	122	124	120	92	88	89	0.1402	0.1698	0.14833	0.152775	0.007215	0.004166
65	110	108	104	87	85	89	0.1168	0.1192	0.07772	0.104547	0.010967	0.006332
70	98	96	94	83	85	89	0.0829	0.0608	0.02732	0.05699	0.013184	0.007612

4) Roughened Aluminum

Table A.4.1 Detector at 0 Deg

Rough Al			Signal Intensites				DOLP				
Angles		Co-Polarized			Cross-Polari	d1	d2	d3	Avg.	S.D	SEM
25	840	880	960	680	720	760	0.1053	0.1	0.1163	0.1072	0.003916	0.002261
30	1.04	1	1.12	0.72	0.76	0.8	0.1818	0.13636	0.1667	0.1616	0.01091	0.006299
35	1.24	1.28	1.36	0.76	0.8	0.84	0.24	0.23077	0.2364	0.2357	0.002192	0.001266
40	2.12	2.16	2.2	0.8	0.84	0.88	0.4521	0.44	0.4286	0.4402	0.005536	0.003196
45	7.52	7.4	7.36	0.96	1	1.04	0.7736	0.7619	0.7524	0.7626	0.005006	0.00289
50	6.08	6.88	6.84	1.04	1.12	1.2	0.7079	0.72	0.7015	0.7098	0.004432	0.002559
55	2.96	3.04	3.12	0.88	0.92	0.96	0.5417	0.53535	0.5294	0.5355	0.002889	0.001668
60	1.52	1.6	1.64	0.8	0.84	0.88	0.3103	0.31148	0.3016	0.3078	0.002551	0.001473
65	1.16	1.24	1.2	0.76	0.8	0.84	0.2083	0.21569	0.1765	0.2002	0.009827	0.005673
70	1.56	1.6	1.68	0.76	0.8	0.84	0.3448	0.33333	0.3333	0.3372	0.003128	0.001806

Table A.4.2 Detector at 10 Deg

Rough Al			Signal Intensites				DOLP				
Angles		Co-Polarized			Cross-Polar	d1	d2	d3	Avg.	S.D	SEM
10	318	320	322	276	268	274	0.0707	0.0884	0.0805	0.07989	0.004187	0.002417
15	332	342	322	276	278	274	0.0921	0.1032	0.0805	0.09196	0.005348	0.003088
20	372	378	380	272	286	278	0.1553	0.1386	0.155	0.14962	0.004517	0.002608
25	460	464	466	282	286	288	0.2399	0.2373	0.2361	0.23777	0.000917	0.000529
30	660	658	654	310	304	308	0.3608	0.368	0.3597	0.36283	0.002123	0.001226
35	1.08	1.09	1.05	0.34	0.3	0.34	0.5233	0.5223	0.5152	0.52026	0.002096	0.00121
40	3.6	3.58	3.54	0.7	0.7	0.72	0.6744	0.6808	0.662	0.67238	0.004504	0.0026
45	7.08	7.2	7.18	0.86	0.9	0.92	0.7834	0.7778	0.7728	0.778	0.002485	0.001435
50	1.88	1.92	1.84	0.62	0.6	0.68	0.504	0.5	0.4603	0.48811	0.011384	0.006572
55	1.12	1.16	1.14	0.62	0.6	0.6	0.2874	0.2889	0.3103	0.29553	0.006059	0.003498
60	0.92	0.88	0.9	0.54	0.6	0.6	0.2603	0.2055	0.2	0.22192	0.015712	0.009071
65	0.84	0.82	0.88	0.56	0.6	0.6	0.2	0.1714	0.1892	0.18687	0.0068	0.003926

Table A.4.3 Detector at 20 deg

Rough Al			Signal Intensites					DOLP				
Angles		Co-Polarized			Cross-Polar		d1	d2	d3	Avg.	S.D	SEM
0	274	276	280	262	268	270	0.0224	0.01471	0.01818	0.01843	0.001813	0.001047
5	258	260	254	232	236	238	0.0531	0.04839	0.03252	0.04466	0.005075	0.00293
10	246	259	252	214	216	218	0.0696	0.09053	0.07234	0.07748	0.005367	0.003099
15	240	236	232	148	150	152	0.2371	0.2228	0.20833	0.22275	0.006784	0.003916
20	188	194	190	72	74	78	0.4462	0.44776	0.41791	0.43728	0.007915	0.00457
25	196	200	204	63	68	70	0.5135	0.49254	0.48905	0.49837	0.006238	0.003601
30	1.1	1.11	1.12	0.34	0.36	0.35	0.5278	0.5102	0.52381	0.5206	0.004345	0.002508
35	3.56	3.57	3.52	0.6	0.65	0.63	0.7115	0.69194	0.69639	0.69996	0.004843	0.002796
40	3.65	3.6	3.62	1.93	1.84	1.85	0.3082	0.32353	0.32358	0.31845	0.004168	0.002406
45	1.08	1.11	1.12	0.59	0.58	0.57	0.2934	0.31673	0.32388	0.31134	0.00751	0.004336
50	380	376	372	230	232	234	0.2459	0.23684	0.22772	0.23682	0.004285	0.002474
55	200	196	192	112	120	124	0.2821	0.24051	0.21519	0.24592	0.015913	0.009188
60	118	126	130	116	120	128	0.0085	0.02439	0.00775	0.01356	0.004424	0.002554
65	104	108	112	96	100	102	0.04	0.03846	0.04673	0.04173	0.002073	0.001197
70	78	84	78	74	80	76	0.0263	0.02439	0.01299	0.02123	0.003396	0.001961

Table A.4.4 Detector at 30 deg

Rough Al			Signal Intensites					DOLP				
Angles		Co-Polarized			Cross-Polar		d1	d2	d3	Avg.	S.D	SEM
0	268	270	272	204	212	210	0.1356	0.12033	0.1286	0.12819	0.003602	0.002079
5	276	280	286	218	220	222	0.1174	0.12	0.126	0.12113	0.002073	0.001197
10	310	308	312	224	228	226	0.161	0.14925	0.1599	0.15672	0.00306	0.001767
15	390	388	392	228	230	232	0.2621	0.25566	0.2564	0.25807	0.001669	0.000964
20	596	600	602	230	232	234	0.4431	0.44231	0.4402	0.44187	0.000709	0.000409
25	1.01	1.02	1.04	0.28	0.29	0.28	0.5659	0.55963	0.5805	0.56869	0.00506	0.002922
30	6.46	6.32	6.52	0.92	0.94	0.96	0.7507	0.74105	0.7433	0.74501	0.002373	0.00137
35	3.01	3.04	3.05	1.34	1.36	1.37	0.3839	0.38182	0.3801	0.38194	0.000901	0.00052
40	1.21	1.19	1.22	0.62	0.64	0.66	0.3224	0.30055	0.2979	0.30694	0.006344	0.003663
45	680	670	660	450	465	440	0.2035	0.18062	0.2	0.19472	0.005817	0.003359
50	500	510	520	290	300	310	0.2658	0.25926	0.253	0.25936	0.00302	0.001743
55	390	400	410	280	290	300	0.1642	0.15942	0.1549	0.15951	0.00218	0.001259
60	324	330	328	240	244	236	0.1489	0.14983	0.1631	0.15396	0.003745	0.002162
65	308	312	304	240	236	248	0.1241	0.13869	0.1014	0.12141	0.008845	0.005107
70	284	290	282	244	232	236	0.0758	0.11111	0.0888	0.09189	0.008428	0.004866

Table A.4.5 Detector at 40 deg

Rough Al			Signal Intensites					DOLP				
Angles		Co-Polarized			Cross-Polari		d1	d2	d3	Avg.	S.D	SEM
0	360	362	356	248	238	236	0.1842	0.20667	0.2027	0.19786	0.00565	0.003262
5	430	422	426	246	244	248	0.2722	0.26727	0.2641	0.26785	0.00192	0.00111
10	490	482	488	258	254	260	0.3102	0.30978	0.3048	0.30825	0.00141	0.000812
15	930	924	916	286	284	290	0.5296	0.5298	0.5191	0.52616	0.00289	0.001671
20	1.56	1.57	1.59	0.39	0.4	0.41	0.6	0.59391	0.59	0.59464	0.00238	0.001372
25	4.9	4.94	4.72	0.52	0.53	0.54	0.8081	0.80622	0.7947	0.803	0.00343	0.00198
30	4.92	4.98	4.9	0.64	0.74	0.7	0.7698	0.74126	0.75	0.75368	0.00689	0.003978
35	2.12	2.08	2.1	0.56	0.58	0.6	0.5821	0.56391	0.5556	0.56718	0.0064	0.003692
40	1.2	1.22	1.21	0.58	0.56	0.57	0.3483	0.37079	0.3596	0.35955	0.0053	0.003058
45	920	960	900	580	540	520	0.2267	0.28	0.2676	0.25809	0.01316	0.007596
50	940	960	980	520	540	560	0.2877	0.28	0.2727	0.28013	0.00352	0.002034
55	700	740	760	500	580	560	0.1667	0.12121	0.1515	0.14646	0.01091	0.006299
60	416	412	420	292	280	300	0.1751	0.19075	0.1667	0.17752	0.00576	0.003325
65	396	400	408	300	296	292	0.1379	0.14943	0.1657	0.15102	0.00658	0.0038
70	368	372	364	296	300	304	0.1084	0.10714	0.0898	0.1018	0.0049	0.002829

Table A.4.6 Detector at 50 deg

Rough Al			Signal Intensites					DOLP				
Angles		Co-Polarized			Cross-Polar		d1	d2	d3	Avg.	S.D	SEM
0	133	137	134	92	96	95	0.1822	0.17597	0.1703	0.176165	0.00281	0.001622
5	164	167	169	97	99	106	0.2567	0.25564	0.2291	0.247145	0.007375	0.004258
10	255	260	266	108	110	112	0.405	0.40541	0.4074	0.405924	0.000615	0.000355
15	604	608	612	96	100	104	0.7257	0.71751	0.7095	0.717575	0.003822	0.002207
20	6.16	6.12	6.15	0.6	0.52	0.56	0.8225	0.84337	0.8331	0.832981	0.004924	0.002843
25	3.56	3.54	3.52	0.48	0.5	0.56	0.7624	0.75248	0.7255	0.746781	0.009	0.005196
30	596	588	580	76	80	84	0.7738	0.76048	0.747	0.760426	0.006322	0.00365
35	300	308	304	90	92	96	0.5385	0.54	0.52	0.532821	0.005246	0.003029
40	204	208	212	104	108	110	0.3247	0.31646	0.3168	0.3193	0.002196	0.001268
45	172	176	180	106	108	110	0.2374	0.23944	0.2414	0.239409	0.000936	0.00054
50	120	124	128	72	76	78	0.25	0.24	0.2427	0.244239	0.002437	0.001407
55	104	112	108	72	80	84	0.1818	0.16667	0.125	0.157828	0.01387	0.008008
60	72	76	70	56	60	64	0.125	0.11765	0.0448	0.095808	0.020906	0.01207
65	68	72	74	56	62	60	0.0968	0.07463	0.1045	0.09196	0.007305	0.004218

Table A.4.7 Detector at 60 deg

Rough Al			Signal Intensites				DOLP				
Angles		Co-Polarized			Cross-Polariz	d1	d2	d3	Avg.	S.D	SEM
0	321	325	331	210	214	217	0.209	0.2059	0.20803	0.2077	0.00075	0.000431
5	480	474	488	232	230	236	0.3483	0.3466	0.34807	0.3477	0.00044	0.000254
10	626	638	630	244	248	250	0.4391	0.4402	0.43182	0.437	0.00214	0.001237
15	2.6	2.56	2.64	0.58	0.6	0.649	0.6352	0.6203	0.60535	0.6203	0.00704	0.004065
20	2.84	2.83	2.87	0.35	0.36	0.37	0.7806	0.7743	0.7716	0.7755	0.00217	0.001251
25	1.05	1.07	1.04	0.33	0.34	0.32	0.5217	0.5177	0.52941	0.523	0.0028	0.001615
30	600	620	630	310	300	330	0.3187	0.3478	0.3125	0.3263	0.00889	0.005135
35	410	420	430	290	300	310	0.1714	0.1667	0.16216	0.1668	0.00218	0.001261
40	370	350	360	290	300	310	0.1212	0.0769	0.07463	0.0909	0.01238	0.007147
45	283	285	289	215	217	221	0.1365	0.1355	0.13333	0.1351	0.00077	0.000445
50	252	254	257	212	214	216	0.0862	0.0855	0.08668	0.0861	0.00029	0.000166
55	287	288	280	211	215	217	0.1526	0.1451	0.12676	0.1415	0.00627	0.00362
60	240	244	236	206	209	213	0.0762	0.0773	0.05122	0.0682	0.00695	0.004013
65	232	236	240	211	215	213	0.0474	0.0466	0.0596	0.0512	0.00344	0.001986
70	248	245	250	212	215	217	0.0783	0.0652	0.07066	0.0714	0.00309	0.001783

5) Molybdenum

Table A.5.1 Detector at 0 deg

Molybdenum			Signal Intensities					DOLP				
Angles		Co-Polarized			Cross-Polari:		d1	d2	d3	Avg.	S.D	SEM
25	840	880	920	640	680	720	0.13514	0.128205	0.12195	0.1284	0.00538	0.003109
30	1.12	1.08	1.04	0.76	0.8	0.84	0.19149	0.148936	0.10638	0.1489	0.03474	0.02006
35	1.32	1.34	1.26	0.72	0.76	0.8	0.29412	0.27619	0.2233	0.2645	0.01736	0.010021
40	1.96	2	2.04	0.92	0.96	0.98	0.36111	0.351351	0.35099	0.3545	0.00271	0.001562
45	3.84	3.96	3.56	1.44	1.48	1.52	0.45455	0.455882	0.40157	0.4373	0.0146	0.008431
50	6.32	6.28	6.34	1.96	2.12	2.04	0.52657	0.495238	0.51313	0.5116	0.00741	0.004278
55	2.24	2.28	2.16	0.96	1	1.04	0.4	0.390244	0.35	0.3801	0.01249	0.007213
60	1.52	1.54	1.58	0.76	0.8	0.84	0.33333	0.316239	0.30579	0.3185	0.00656	0.003785
65	1.36	1.32	1.28	0.76	0.8	0.84	0.28302	0.245283	0.20755	0.2453	0.01779	0.01027
70	1.16	1.2	1.24	0.72	0.76	0.8	0.23404	0.22449	0.21569	0.2247	0.00433	0.002499
75	1.04	1.08	1.12	0.72	0.76	0.8	0.18182	0.173913	0.16667	0.1741	0.00357	0.002063

Table A.5.2 Detector at 10 deg

Molybdenum			Signal Intensities					DOLP				
Angles		Co-Polarized			Cross-Polarize		d1	d2	d3	Avg.	S.D	SEM
10	324	332	335	271	267	275	0.0891	0.1085	0.0984	0.0987	0.00458	0.002646
15	366	363	374	277	280	281	0.1384	0.1291	0.142	0.1365	0.00314	0.001813
20	450	452	444	318	312	320	0.1719	0.1832	0.1623	0.1725	0.00494	0.002853
25	590	582	584	370	368	364	0.2292	0.2253	0.2321	0.2288	0.00161	0.000929
30	1.04	1.05	1.08	0.536	0.54	0.528	0.3198	0.3208	0.3433	0.3279	0.00627	0.003618
35	1.2	1.19	1.21	0.612	0.616	0.62	0.3245	0.3178	0.3224	0.3216	0.00161	0.000929
40	2.8	2.82	2.7	1.54	1.56	1.48	0.2903	0.2877	0.2919	0.29	0.001	0.000577
45	2.7	2.78	2.68	1.24	1.28	1.32	0.3706	0.3695	0.34	0.36	0.00817	0.004718
50	1.4	1.44	1.36	0.84	0.86	0.82	0.25	0.2522	0.2477	0.25	0.00105	0.000608
55	1.14	1.16	1.19	0.76	0.78	0.7	0.2	0.1959	0.2593	0.2184	0.01672	0.009652
60	900	880	910	680	660	640	0.1392	0.1429	0.1742	0.1521	0.00906	0.005231
65	550	552	544	384	362	378	0.1777	0.2079	0.18	0.1886	0.00791	0.004566
70	480	476	450	360	350	354	0.1429	0.1525	0.1194	0.1383	0.00803	0.004638
75	430	434	424	340	346	338	0.1169	0.1128	0.1129	0.1142	0.0011	0.000635

Table A.5.3 Detector at 20 deg

Molybdenum			Signal Intensities				DOLP				
Angles		Co-Polarized			Cross-Polariz	d1	d2	d3	Avg.	S.D	SEM
0	151	149	124	118	120	123	0.12268	0.10781	0.00405	0.07818	0.03047	0.017589
5	139	140	143	98	99	97	0.173	0.17155	0.19167	0.17874	0.00529	0.003054
10	130	134	133	71	72	77	0.29353	0.30097	0.26667	0.28706	0.00851	0.004911
15	110	113	108	54	46	51	0.34146	0.42138	0.35849	0.37378	0.01984	0.011457
20	149	152	147	99	98	101	0.20161	0.216	0.18548	0.20103	0.0072	0.004155
25	532	528	524	78	80	84	0.74426	0.73684	0.72368	0.73493	0.00491	0.002836
30	2.12	2.13	2.14	0.34	0.35	0.36	0.72358	0.71774	0.712	0.71777	0.00273	0.001575
35	4.96	5	4.92	0.64	0.7	0.72	0.77143	0.75439	0.74468	0.75683	0.00638	0.003685
40	1.72	1.76	1.8	0.54	0.56	0.6	0.52212	0.51724	0.5	0.51312	0.00548	0.003163
45	512	508	504	84	80	72	0.71812	0.72789	0.75	0.732	0.0077	0.004445
50	276	272	270	156	152	160	0.27778	0.28302	0.25581	0.2722	0.0068	0.003928
55	172	164	168	104	100	96	0.24638	0.24242	0.27273	0.25384	0.00777	0.004483
60	108	112	120	100	96	94	0.03846	0.07692	0.1215	0.07896	0.01959	0.01131
65	104	96	100	76	80	84	0.15556	0.09091	0.08696	0.11114	0.01816	0.010483
70	96	100	104	84	96	92	0.06667	0.02041	0.06122	0.04943	0.01192	0.006881

Table A.5.4 Detector at 30 deg

Molybdenum			Signal Intensities				DOLP				
Angles		Co-Polarized			Cross-Polariz	d1	d2	d3	Avg.	S.D	SEM
0	76	78	80	70	72	68	0.0411	0.04	0.08108	0.054059	0.011035	0.006371
5	134	130	122	68	70	72	0.32673	0.3	0.25773	0.294822	0.0164	0.009469
10	182	174	178	86	84	90	0.35821	0.348837	0.32836	0.345135	0.007196	0.004155
15	260	264	268	176	184	186	0.19266	0.178571	0.18062	0.18395	0.003589	0.002072
20	1.06	1.04	1.05	0.13	0.14	0.13	0.78451	0.768707	0.77365	0.775623	0.003811	0.0022
25	3.16	3.2	3.24	0.68	0.64	0.66	0.64583	0.666667	0.66154	0.658013	0.005117	0.002954
30	7.8	7.68	7.6	0.52	0.54	0.56	0.875	0.868613	0.86275	0.868786	0.002889	0.001668
35	3.21	3.25	3.24	0.12	0.13	0.14	0.92793	0.923077	0.91716	0.922722	0.002542	0.001468
40	1.28	1.29	1.3	0.16	0.17	0.18	0.77778	0.767123	0.75676	0.767219	0.004955	0.002861
45	612	608	604	108	112	106	0.7	0.688889	0.70141	0.696766	0.003233	0.001866
50	200	296	204	130	128	132	0.21212	0.396226	0.21429	0.274211	0.049815	0.028761
55	124	128	130	104	108	112	0.08772	0.084746	0.07438	0.082282	0.003301	0.001906
60	108	112	116	58	60	64	0.3012	0.302326	0.28889	0.297473	0.003514	0.002029
65	110	114	112	48	52	58	0.39241	0.373494	0.31765	0.361182	0.018323	0.010579
70	94	100	102	56	60	62	0.25333	0.25	0.2439	0.249079	0.002254	0.001302

Table A.5.5 Detector at 40 deg

Molybdenum			Signal Intensities					DOLP				
Angles		Co-Polarized			Cross-Polari:		d1	d2	d3	Avg.	S.D	SEM
0	414	412	416	302	292	288	0.1564	0.1705	0.1818	0.16957	0.006	0.003462
5	468	472	484	330	328	324	0.1729	0.18	0.198	0.18365	0.0061	0.003521
10	562	556	566	350	354	358	0.2325	0.222	0.2251	0.22651	0.00254	0.001464
15	936	948	952	500	492	488	0.3036	0.3167	0.3222	0.31417	0.0045	0.002599
20	2.02	2.01	2.03	0.9	0.91	0.89	0.3836	0.3767	0.3904	0.38356	0.00323	0.001864
25	4.17	4.16	4.1	1.92	1.91	1.9	0.3695	0.3707	0.3667	0.36893	0.00097	0.000559
30	2.34	2.31	2.28	1.04	1.03	1.05	0.3846	0.3832	0.3694	0.37907	0.00397	0.002295
35	1.14	1.13	1.17	0.6	0.62	0.64	0.3103	0.2914	0.2928	0.2982	0.00497	0.002869
40	770	780	760	490	480	510	0.2222	0.2381	0.1969	0.21906	0.00981	0.005662
45	540	536	524	350	348	356	0.2135	0.2127	0.1909	0.20569	0.00604	0.003485
50	452	454	456	312	316	304	0.1832	0.1792	0.2	0.18749	0.00519	0.002999
55	472	480	474	374	376	380	0.1158	0.1215	0.1101	0.1158	0.00269	0.001555
60	350	348	356	278	282	286	0.1146	0.1048	0.109	0.10948	0.00234	0.00135
65	330	334	326	260	258	254	0.1186	0.1284	0.1241	0.12372	0.0023	0.001328
70	330	332	324	260	266	258	0.1186	0.1104	0.1134	0.11414	0.00197	0.00114

Table A.5.6 Detector at 50 deg

Molybdenum			Signal Intensities					DOLP				
Angles		Co-Polarized			Cross-Polari		d1	d2	d3	Avg.	S.D	SEM
0	412	416	418	264	262	260	0.21893	0.22714	0.23304	0.22637	0.00334	0.001928
5	636	640	642	274	266	268	0.3978	0.4128	0.41099	0.4072	0.00386	0.002228
10	780	786	788	284	288	280	0.46617	0.46369	0.47566	0.4685	0.00298	0.001719
15	1.88	1.89	1.9	0.34	0.35	0.36	0.69369	0.6875	0.68142	0.68754	0.00289	0.001671
20	6.04	6.12	6.18	0.72	0.74	0.76	0.78698	0.78426	0.78098	0.78407	0.00142	0.000818
25	5.12	5.04	5.08	0.76	0.8	0.82	0.7415	0.72603	0.72203	0.72985	0.00485	0.002798
30	1.84	1.86	1.82	0.68	0.72	0.74	0.46032	0.44186	0.42188	0.44135	0.00906	0.005233
35	756	760	764	288	290	292	0.44828	0.44762	0.44697	0.44762	0.00031	0.000178
40	592	596	600	284	288	276	0.3516	0.34842	0.36986	0.35663	0.00546	0.00315
45	456	460	448	280	284	288	0.23913	0.23656	0.21739	0.23103	0.0056	0.003233
50	380	384	388	280	276	282	0.15152	0.16364	0.15821	0.15779	0.00286	0.001652
55	352	354	348	280	274	272	0.11392	0.12739	0.12258	0.1213	0.00322	0.001857
60	324	320	316	276	282	280	0.08	0.06312	0.0604	0.06784	0.005	0.00289
65	312	308	304	280	282	292	0.05405	0.04407	0.02013	0.03942	0.00822	0.004744
70	296	300	306	268	278	280	0.04965	0.03806	0.04437	0.04403	0.00273	0.001578

Table A.5.7 Detector at 60 deg

Molybdenum			Signal Intensities					DOLP				
Angles		Co-Polarized			Cross-Polar		d1	d2	d3	Avg.	S.D	SEM
0	510	520	530	280	300	290	0.29114	0.26829	0.29268	0.28404	0.006438	0.003717
5	680	676	682	230	224	228	0.49451	0.50222	0.4989	0.49854	0.001825	0.001054
10	1.01	1.02	1.03	0.23	0.23	0.2	0.62641	0.632	0.62975	0.62939	0.001326	0.000766
15	2.52	2.64	2.58	0.48	0.54	0.5	0.68	0.66038	0.66452	0.6683	0.004876	0.002815
20	2.72	2.73	2.7	0.32	0.31	0.3	0.78947	0.79605	0.78218	0.78923	0.003272	0.001889
25	924	916	908	252	248	250	0.57143	0.57388	0.56822	0.57118	0.001338	0.000773
30	604	596	608	248	252	256	0.41784	0.40566	0.40741	0.4103	0.003105	0.001792
35	400	404	408	244	248	252	0.24224	0.23926	0.23636	0.23929	0.001384	0.000799
40	340	332	344	240	236	232	0.17241	0.16901	0.19444	0.17862	0.006508	0.003757
45	290	288	292	244	240	236	0.08614	0.09091	0.10606	0.09437	0.004903	0.002831
50	276	280	284	240	236	248	0.06977	0.08527	0.06767	0.07424	0.004532	0.002617
55	272	268	270	232	224	240	0.07937	0.08943	0.05882	0.07587	0.007354	0.004246
60	256	264	252	236	240	242	0.04065	0.04762	0.02024	0.03617	0.006707	0.003872
65	248	256	260	232	240	244	0.03333	0.03226	0.03175	0.03245	0.000382	0.00022
70	260	264	268	236	240	232	0.04839	0.04762	0.072	0.056	0.006534	0.003772

6) White paint mixed with TiO_2 particles

Table A.6.1 Detector at 0 deg

white paint			Signal Intensities				DOLP				
Angles		Co-Polarized			Cross-Polariz	d1	d2	d3	Avg.	S.D	SEM
25	396	380	394	292	296	300	0.1512	0.12426	0.13545	0.13696	0.00637	0.003678
30	468	462	458	296	302	298	0.2251	0.20942	0.21164	0.2154	0.00401	0.002314
35	524	526	518	456	452	450	0.0694	0.07566	0.07025	0.07177	0.0016	0.000926
40	670	664	656	498	506	508	0.1473	0.13504	0.12715	0.13648	0.00478	0.002758
45	1	1.01	1.02	0.698	0.704	0.712	0.1779	0.17853	0.17783	0.17807	0.00019	0.000108
50	1.08	1.1	1.13	0.692	0.688	0.696	0.219	0.23043	0.23768	0.22902	0.00445	0.002568
55	0.99	0.97	1	0.724	0.716	0.712	0.1552	0.15065	0.16822	0.15802	0.0043	0.002483
60	0.99	1	1.01	0.7	0.694	0.704	0.1716	0.18064	0.17853	0.17692	0.00223	0.001287
65	0.86	0.85	0.876	0.716	0.724	0.73	0.0914	0.08005	0.09091	0.08744	0.00302	0.001744

Table A.6.2 Detector at 10 deg

white paint			Signal Intensities				DOLP				
Angles		Co-Polarized			Cross-Polariz	d1	d2	d3	Avg.	S.D	SEM
0	197	190	202	170	173	177	0.0736	0.0468	0.066	0.0621	0.00649	0.003749
5	274	280	276	240	242	249	0.0661	0.0728	0.0514	0.0635	0.00515	0.002976
10	344	336	336	326	330	334	0.0269	0.009	0.003	0.013	0.00585	0.00338
15	462	466	458	430	428	436	0.0359	0.0425	0.0246	0.0343	0.00427	0.002463
20	590	594	588	544	540	554	0.0406	0.0476	0.0298	0.0393	0.00424	0.002446
25	684	686	676	590	592	600	0.0738	0.0736	0.0596	0.069	0.00384	0.002217
30	860	864	856	688	692	694	0.1111	0.1105	0.1045	0.1087	0.00172	0.000994
35	856	852	864	744	748	750	0.07	0.065	0.0706	0.0685	0.00145	0.00084
40	912	968	904	764	768	776	0.0883	0.1152	0.0762	0.0932	0.00941	0.005435
45	1.1	1.09	1.12	0.9	0.904	0.9	0.1	0.0933	0.11	0.1011	0.00397	0.002291
50	1.16	1.17	1.18	1.02	1.03	0.99	0.0642	0.0636	0.0876	0.0718	0.00643	0.003714
55	1.19	1.17	1.18	0.95	0.96	0.94	0.1121	0.0986	0.1132	0.108	0.00384	0.002218
60	1.12	1.11	1.1	0.972	0.968	0.99	0.0707	0.0683	0.0516	0.0636	0.00491	0.002834
65	1.25	1.24	1.23	1.03	1.04	1.06	0.0965	0.0877	0.0742	0.0861	0.00528	0.003051
70	1.08	1.09	1.1	1.02	1.03	1.04	0.0286	0.0283	0.028	0.0283	0.00013	7.27E-05

Table A.6.3 Detector at 20 deg

white paint			Signal Intensities				DOLP				
Angles		CO-polarised			Cross-Polar	d1	d2	d3	Avg.	S.D	SEM
0	316	320	324	278	280	282	0.06397	0.0667	0.0693	0.0666	0.00126	0.000726
5	372	376	378	330	334	332	0.05983	0.0592	0.0648	0.0613	0.00145	0.000837
10	416	410	422	336	340	342	0.10638	0.0933	0.1047	0.1015	0.00335	0.001933
15	426	436	438	383	380	386	0.05315	0.0686	0.0631	0.0616	0.0037	0.002135
20	498	500	504	490	492	496	0.0081	0.0081	0.008	0.0081	2.3E-05	1.35E-05
25	530	532	524	440	442	444	0.09278	0.0924	0.0826	0.0893	0.00271	0.001564
30	592	586	584	462	466	468	0.12334	0.1141	0.1103	0.1159	0.00317	0.00183
35	636	630	626	536	540	544	0.08532	0.0769	0.0701	0.0774	0.0036	0.002077
40	754	748	750	558	560	562	0.14939	0.1437	0.1433	0.1455	0.0016	0.000926
45	720	728	736	592	588	596	0.09756	0.1064	0.1051	0.103	0.00225	0.001298
50	716	724	720	632	640	652	0.06231	0.0616	0.0496	0.0578	0.00338	0.001949
55	700	704	708	648	652	660	0.03858	0.0383	0.0351	0.0373	0.00092	0.000531
60	708	712	716	692	696	700	0.01143	0.0114	0.0113	0.0114	3E-05	1.76E-05
65	672	680	676	648	650	652	0.01818	0.0226	0.0181	0.0196	0.00121	0.000696

Table A.6.4 Detector at 30 deg

white paint			Signal Intensities				DOLP				
Angles		CO-polarised			Cross-Polar	d1	d2	d3	Avg.	S.D	SEM
0	520	524	522	490	492	498	0.0297	0.0315	0.0235	0.0282	0.00197	0.001137
5	546	548	544	450	454	458	0.0964	0.0938	0.0858	0.092	0.0026	0.001498
10	582	584	578	554	556	558	0.0246	0.0246	0.0176	0.0223	0.0019	0.0011
15	662	660	656	600	602	606	0.0491	0.046	0.0396	0.0449	0.00228	0.001318
20	700	696	702	652	654	660	0.0355	0.0311	0.0308	0.0325	0.00123	0.000713
25	808	804	802	650	660	664	0.1084	0.0984	0.0941	0.1003	0.00345	0.00199
30	836	840	844	752	756	764	0.0529	0.0526	0.0498	0.0518	0.00082	0.000475
35	792	776	784	732	740	730	0.0394	0.0237	0.0357	0.0329	0.00385	0.002222
40	912	924	920	736	740	732	0.1068	0.1106	0.1138	0.1104	0.00165	0.000954
45	896	900	912	712	708	720	0.1144	0.1194	0.1176	0.1172	0.00119	0.000687
50	892	896	900	820	832	830	0.0421	0.037	0.0405	0.0399	0.00121	0.000698
55	884	892	886	760	756	780	0.0754	0.0825	0.0636	0.0739	0.0045	0.002598
60	816	820	824	740	744	742	0.0488	0.0486	0.0524	0.0499	0.00099	0.000574
65	844	848	852	768	764	782	0.0471	0.0521	0.0428	0.0474	0.00219	0.001262
70	852	848	850	804	808	812	0.029	0.0242	0.0229	0.0253	0.00152	0.000878

Table A.6.5 Detector at 40 deg

white paint			Signal Intensities					DOLP				
Angles		CO-polarised			Cross-Polarise		d1	d2	d3	Avg.	S.D	SEM
0	1	0.96	0.97	0.99	0.956	0.96	0.005	0.0021	0.0062	0.0044	0.001	0.000578
5	1.07	1.1	1.08	0.94	0.948	0.95	0.0647	0.0742	0.064	0.0676	0.0027	0.001552
10	1.16	1.17	1.18	1.1	1.08	1.09	0.0265	0.04	0.0396	0.0354	0.0036	0.002087
15	1.13	1.17	1.19	1.02	1.03	1.04	0.0512	0.0636	0.0673	0.0607	0.004	0.002299
20	1.33	1.34	1.35	1.17	1.18	1.19	0.064	0.0635	0.063	0.0635	0.0002	0.000137
25	1.45	1.42	1.43	1.21	1.22	1.23	0.0902	0.0758	0.0752	0.0804	0.004	0.002319
30	1.42	1.43	1.44	1.34	1.35	1.36	0.029	0.0288	0.0286	0.0288	1E-04	5.63E-05
35	1.47	1.48	1.45	1.28	1.29	1.3	0.0691	0.0686	0.0545	0.0641	0.0039	0.002247
40	1.47	1.46	1.45	1.43	1.41	1.42	0.0138	0.0174	0.0105	0.0139	0.0016	0.000949
45	1.38	1.39	1.4	1.36	1.37	1.35	0.0073	0.0072	0.0182	0.0109	0.003	0.001714
50	1.47	1.48	1.49	1.43	1.44	1.45	0.0138	0.0137	0.0136	0.0137	4E-05	2.55E-05
55	1.44	1.42	1.45	1.39	1.4	1.41	0.0177	0.0071	0.014	0.0129	0.0025	0.001461
60	1.37	1.38	1.39	1.32	1.33	1.34	0.0186	0.0185	0.0183	0.0185	6E-05	3.71E-05
65	1.45	1.46	1.47	1.39	1.4	1.41	0.0211	0.021	0.0208	0.021	7E-05	3.99E-05
70	1.34	1.35	1.39	1.32	1.33	1.34	0.0075	0.0075	0.0183	0.0111	0.0029	0.001701

Table A.6.6 Detector at 50 deg

white paint			Signal Intensities					DOLP				
Angles		CO-polarised			Cross-Polari		d1	d2	d3	Avg.	S.D	SEM
0	700	720	710	630	620	640	0.0526	0.07463	0.0519	0.0597	0.0061	0.003519
5	690	680	670	620	610	630	0.0534	0.05426	0.0308	0.04616	0.00628	0.003628
10	770	760	790	620	640	630	0.1079	0.08571	0.1127	0.1021	0.00678	0.003916
15	820	830	840	670	680	690	0.1007	0.09934	0.098	0.09935	0.00062	0.000358
20	810	830	840	710	720	730	0.0658	0.07097	0.0701	0.06894	0.0013	0.000753
25	840	850	860	750	770	760	0.0566	0.04938	0.0617	0.0559	0.00292	0.001688
30	850	870	880	750	760	740	0.0625	0.06748	0.0864	0.07213	0.00595	0.003435
35	800	810	820	720	730	740	0.0526	0.05195	0.0513	0.05195	0.00032	0.000184
40	910	930	940	760	770	780	0.0898	0.09412	0.093	0.09232	0.00105	0.000608
45	830	840	850	770	780	790	0.0375	0.03704	0.0366	0.03704	0.00022	0.000124
50	860	870	880	800	810	820	0.0361	0.03571	0.0353	0.03572	0.0002	0.000116
55	840	850	860	740	750	760	0.0633	0.0625	0.0617	0.06251	0.00037	0.000213
60	920	930	940	800	810	820	0.0698	0.06897	0.0682	0.06897	0.00037	0.000216
65	830	840	820	800	810	815	0.0184	0.01818	0.0031	0.01321	0.00415	0.002394

Table A.6.7 Detector at 60 deg

white paint			Signal Intensities				DOLP				
Angles		CO-polarised			Cross-Polari	d1	d2	d3	Avg.	S.D	SEM
0	518	520	522	498	500	502	0.0197	0.01961	0.0195	0.0196	3.6E-05	2.09E-05
5	566	568	572	516	520	524	0.0462	0.04412	0.0438	0.0447	0.00062	0.000357
10	580	582	584	566	568	570	0.0122	0.01217	0.0121	0.0122	2E-05	1.15E-05
15	554	558	546	542	544	538	0.0109	0.0127	0.0074	0.0103	0.00128	0.000738
20	582	584	588	568	566	570	0.0122	0.01565	0.0155	0.0145	0.00093	0.000538
25	590	592	588	582	586	584	0.0068	0.00509	0.0034	0.0051	0.0008	0.000464
30	606	596	588	566	570	562	0.0341	0.0223	0.0226	0.0263	0.00318	0.001835
35	598	610	602	554	556	558	0.0382	0.04631	0.0379	0.0408	0.00225	0.001297
40	602	612	614	538	540	536	0.0561	0.0625	0.0678	0.0622	0.00276	0.001592
45	574	576	580	568	566	560	0.0053	0.00876	0.0175	0.0105	0.00298	0.001723
50	536	540	542	528	536	524	0.0075	0.00372	0.0169	0.0094	0.00319	0.001845
55	576	570	574	536	540	542	0.036	0.02703	0.0287	0.0306	0.00224	0.001296
60	576	572	564	552	554	558	0.0213	0.01599	0.0053	0.0142	0.00382	0.002208
65	548	544	552	530	532	524	0.0167	0.01115	0.026	0.018	0.00354	0.002045
70	556	564	558	540	542	548	0.0146	0.01989	0.009	0.0145	0.00256	0.001477
75	536	534	540	494	500	506	0.0408	0.03288	0.0325	0.0354	0.0022	0.001271

7) Stainless Steel

Table A.7.1 Detector at 0 deg

S.Steel			Signal Intensities					DOLP				
Angles		CO-polarised			Cross-Polaris		d1	d2	d3	Avg.	S.D	SEM
35	220	230	240	130	140	150	0.25714	0.24324	0.2308	0.24372	0.00622	0.003591
40	840	800	760	600	620	640	0.16667	0.12676	0.0857	0.12638	0.01908	0.011017
45	4.16	4.2	4.24	0.88	0.92	0.96	0.65079	0.64063	0.6308	0.64073	0.00472	0.002725
47.5	14	13.9	13.7	4.72	4.76	4.8	0.49573	0.48982	0.4811	0.48888	0.00347	0.002005
50	1.2	1.24	1.16	0.64	0.63	0.72	0.30435	0.3262	0.234	0.2882	0.0227	0.013106
55	460	470	480	230	250	260	0.33333	0.30556	0.2973	0.31206	0.0089	0.005138
60	330	350	360	220	230	240	0.2	0.2069	0.2	0.2023	0.00188	0.001084
65	195	193	191	150	152	156	0.13043	0.11884	0.1009	0.11671	0.00702	0.004055

Table A.7.2 Detector at 10 deg

S.Steel			Signal Intensities					DOLP				
Angles		CO-polarised			Cross-Polaris		d1	d2	d3	Avg.	S.D	SEM
10	231	235	230	226	227	224	0.01094	0.01732	0.01322	0.01382	0.00152	0.000879
15	266	252	259	237	240	249	0.05765	0.02439	0.01969	0.03391	0.00976	0.005633
20	285	290	292	258	260	262	0.04972	0.05455	0.05415	0.05281	0.00126	0.000729
25	350	357	360	295	296	290	0.08527	0.09342	0.10769	0.09546	0.00535	0.003089
30	439	434	436	337	342	333	0.13144	0.11856	0.13394	0.12798	0.00389	0.002247
35	1.02	1.03	1.01	0.57	0.572	0.57	0.2798	0.28589	0.2801	0.28193	0.00162	0.000935
40	6.44	6.32	6.52	2.76	2.82	2.72	0.4	0.38293	0.41126	0.39806	0.00672	0.003881
45	1.48	1.5	1.44	0.94	0.9	0.92	0.22314	0.25	0.22034	0.23116	0.00772	0.004457
50	540	544	548	400	390	410	0.14894	0.16488	0.14405	0.15262	0.00514	0.002965
55	420	424	432	340	336	328	0.10526	0.11579	0.13684	0.1193	0.00758	0.004376
60	372	328	385	316	324	328	0.0814	0.00613	0.07994	0.05582	0.02029	0.011714
65	336	328	332	300	304	296	0.0566	0.03797	0.05732	0.05063	0.00517	0.002986
70	304	308	312	288	298	292	0.02703	0.0165	0.03311	0.02555	0.00396	0.002287

Table A.7.3 Detector at 20 deg

S.Steel			Signal Intensities				DOLP				
Angles		CO-polarised		Cross-Polarise		d1	d2	d3	Avg.	S.D	SEM
0	272	276	280	260	264	258	0.02256	0.02222	0.04089	0.02856	0.005036	0.002908
5	280	284	282	272	260	268	0.01449	0.04412	0.02545	0.02802	0.007061	0.004077
10	288	284	280	272	258	260	0.02857	0.04797	0.03704	0.03786	0.004585	0.002647
15	288	292	296	276	268	264	0.02128	0.04286	0.05714	0.04043	0.008512	0.004914
20	304	308	300	268	274	280	0.06294	0.05842	0.03448	0.05195	0.007209	0.004162
25	400	404	412	292	284	288	0.15607	0.17442	0.17714	0.16921	0.005403	0.003119
30	576	572	574	324	328	332	0.28	0.27111	0.26711	0.27274	0.003111	0.001796
35	12.9	13	12.8	2.1	2.12	2.08	0.72	0.71958	0.72043	0.72	0.000201	0.000116
40	1.9	2.1	2.12	1.3	1.4	1.5	0.1875	0.2	0.17127	0.18626	0.006791	0.003921
45	1.4	1.5	1.6	1.3	1.2	1.25	0.03704	0.11111	0.12281	0.09032	0.021926	0.012659
50	330	340	350	292	304	290	0.06109	0.0559	0.09375	0.07025	0.009672	0.005584
55	296	294	298	262	264	258	0.06093	0.05376	0.07194	0.06221	0.004317	0.002492
60	278	288	290	260	256	280	0.03346	0.05882	0.01754	0.03661	0.009814	0.005666
65	282	280	278	258	262	274	0.04444	0.03321	0.00725	0.0283	0.008994	0.005193
70	268	269	272	265	266	270	0.00563	0.00561	0.00369	0.00498	0.000525	0.000303

Table A.7.4 Detector at 30 Deg

S.Steel			Signal Intensities				DOLP				
Angles		CO-polarised		Cross-Polaris		d1	d2	d3	Avg.	S.D	SEM
0	157	165	167	150	148	151	0.0228	0.05431	0.0503	0.04248	0.00809	0.004669
5	184	180	182	154	153	155	0.08876	0.08108	0.0801	0.08332	0.00223	0.001289
10	192	194	196	159	166	162	0.09402	0.07778	0.095	0.08892	0.00456	0.00263
15	211	215	216	165	163	169	0.12234	0.13757	0.1221	0.12733	0.00418	0.002413
20	330	328	329	173	177	179	0.31213	0.29901	0.2953	0.30214	0.00417	0.002409
25	928	924	930	238	240	232	0.59177	0.58763	0.6007	0.59336	0.00315	0.001816
30	1.8	1.81	1.82	0.33	0.34	0.35	0.69014	0.68372	0.6774	0.68376	0.003	0.001731
35	610	620	600	260	280	270	0.4023	0.37778	0.3793	0.38646	0.00648	0.003739
40	300	298	296	188	192	184	0.22951	0.21633	0.2333	0.22639	0.00421	0.002428
45	250	254	248	180	178	182	0.16279	0.17593	0.1535	0.16407	0.00531	0.003068
50	212	208	214	172	174	180	0.10417	0.08901	0.0863	0.09316	0.00454	0.002621
55	196	200	198	176	174	180	0.05376	0.06952	0.0476	0.05697	0.00532	0.003074
60	210	212	214	172	188	180	0.09948	0.06	0.0863	0.08192	0.00947	0.00547
65	196	188	200	188	186	182	0.02083	0.00535	0.0471	0.02443	0.00996	0.005748

Table A.7.5 Detector at 40 deg

S.Steel			Signal Intensities					DOLP				
Angles		CO-polarised			Cross-Polaris		d1	d2	d3	Avg.	S.D	SEM
0	332	324	330	280	284	276	0.08497	0.0658	0.0891	0.07996	0.00586	0.003386
5	336	340	344	280	292	284	0.09091	0.0759	0.0955	0.08747	0.00483	0.002787
10	368	372	370	284	292	296	0.12883	0.1205	0.1111	0.12014	0.00418	0.002413
15	428	436	440	288	284	292	0.19553	0.2111	0.2022	0.20294	0.00369	0.002128
20	692	694	696	312	308	304	0.37849	0.3852	0.392	0.38524	0.00319	0.001839
25	4.66	4.4	4.44	0.49	0.49	0.486	0.81041	0.7989	0.8027	0.80398	0.00278	0.001602
30	1.06	1.1	1.09	0.62	0.56	0.6	0.2619	0.3253	0.2899	0.29238	0.01498	0.008646
35	820	780	800	540	560	520	0.20588	0.1642	0.2121	0.19406	0.01229	0.007094
40	640	620	680	520	540	580	0.10345	0.069	0.0794	0.08393	0.00834	0.004814
45	332	334	228	266	268	270	0.11037	0.1096	-0.0843	0.04522	0.05289	0.030538
50	310	304	302	264	266	256	0.08014	0.0667	0.0824	0.07641	0.00402	0.002319
55	292	288	290	254	252	258	0.0696	0.0667	0.0584	0.06489	0.00274	0.001581
60	272	278	274	258	256	254	0.02642	0.0412	0.0379	0.03516	0.00366	0.002111
65	274	268	270	248	252	254	0.04981	0.0308	0.0305	0.03704	0.00521	0.00301
70	280	286	284	256	260	264	0.04478	0.0476	0.0365	0.04296	0.00272	0.001573

Table A.7.6 Detector at 50 deg

S.Steel			Signal Intensities					DOLP				
Angles		CO-polarised			Cross-Polari		d1	d2	d3	Avg.	S.D	SEM
0	316	312	308	280	276	284	0.0604	0.06122	0.04054	0.05406	0.00552	0.003188
5	344	348	350	276	284	280	0.10968	0.10127	0.11111	0.10735	0.00251	0.001448
10	348	352	360	280	288	284	0.10828	0.1	0.11801	0.10876	0.00425	0.002454
15	448	444	440	296	300	304	0.2043	0.19355	0.1828	0.19355	0.00507	0.002927
20	2.32	2.36	2.34	0.64	0.66	0.68	0.56757	0.56291	0.54967	0.56005	0.00438	0.002528
25	940	980	960	580	560	600	0.23684	0.27273	0.23077	0.24678	0.01069	0.006172
30	660	720	700	560	580	540	0.08197	0.10769	0.12903	0.10623	0.01111	0.006414
35	600	610	620	520	560	580	0.07143	0.04274	0.03333	0.04917	0.00936	0.005401
40	324	312	316	280	284	286	0.07285	0.04698	0.04983	0.05655	0.00669	0.00386
45	312	308	304	280	284	288	0.05405	0.04054	0.02703	0.04054	0.00637	0.003678
50	292	288	284	272	268	270	0.03546	0.03597	0.02527	0.03223	0.00285	0.001643
55	280	284	288	272	266	264	0.01449	0.03273	0.04348	0.03023	0.00691	0.003988
60	284	290	292	268	270	266	0.02899	0.03571	0.04659	0.0371	0.00419	0.002418
65	267	269	274	255	257	259	0.02299	0.02281	0.02814	0.02465	0.00143	0.000824
70	270	264	265	251	252	256	0.03647	0.02326	0.01727	0.02567	0.00463	0.002673

Table A.7.7 Detector at 60 deg

S.Steel			Signal Intensities					DOLP				
Angles		CO-polarised			Cross-Polaris		d1	d2	d3	Avg.	S.D	SEM
0	207	214	211	151	156	160	0.15642	0.15676	0.13747	0.15022	0.00521	0.003005
5	274	272	270	153	157	155	0.28337	0.26807	0.27059	0.27401	0.00387	0.002234
10	352	350	344	164	167	160	0.36434	0.35397	0.36508	0.36113	0.00293	0.001691
15	2.14	2.13	2.16	0.33	0.32	0.34	0.73279	0.73878	0.728	0.73319	0.00254	0.001469
20	904	908	916	194	200	198	0.64663	0.63899	0.64452	0.64338	0.00186	0.001074
25	364	368	372	204	208	212	0.28169	0.27778	0.27397	0.27781	0.00182	0.00105
30	248	252	244	200	204	198	0.10714	0.10526	0.10407	0.10549	0.00073	0.000421
35	232	236	228	196	192	204	0.08411	0.1028	0.05556	0.08082	0.01122	0.006476
40	187	190	181	174	177	179	0.03601	0.03542	0.00556	0.02566	0.00821	0.00474
45	180	178	183	171	174	175	0.02564	0.01136	0.02235	0.01978	0.00352	0.002035
50	181	183	186	177	173	180	0.01117	0.02809	0.01639	0.01855	0.00408	0.002358
55	179	185	186	169	175	176	0.02874	0.02778	0.02762	0.02805	0.00028	0.000164
60	181	187	189	177	179	181	0.01117	0.02186	0.02162	0.01822	0.00288	0.001661
65	188	191	195	179	181	185	0.02452	0.02688	0.02632	0.02591	0.00058	0.000335

8) Lithium painted material

Table A.8.1 Detector at 0 deg

Lithium			Signal Intensities					DOLP				
Angles		CO-polarised			Cross-Polarise		d1	d2	d3	Avg	S.D	SEM
10	440	436	444	416	420	424	0.028	0.01869	0.023	0.02326	0.0022	0.001273
15	636	652	648	624	628	630	0.0095	0.01875	0.0141	0.01412	0.00217	0.001256
20	716	712	708	608	606	604	0.0816	0.08042	0.0793	0.08042	0.00054	0.000313
25	688	692	698	636	640	632	0.0393	0.03904	0.0496	0.04265	0.00285	0.001645
30	836	840	844	772	768	776	0.0398	0.04478	0.042	0.04218	0.00118	0.000679
35	1.75	1.745	1.73	1.1	1.11	1.12	0.2281	0.22242	0.214	0.22151	0.00333	0.001922
40	1.68	1.69	1.7	1.24	1.25	1.26	0.1507	0.14966	0.1486	0.14966	0.00048	0.000277
45	1.43	1.44	1.45	1.19	1.2	1.21	0.0916	0.09091	0.0902	0.09091	0.00032	0.000187
50	1.74	1.75	1.7	1.31	1.32	1.31	0.141	0.14007	0.1296	0.13687	0.00299	0.001726
55	1.31	1.3	1.34	1.12	1.15	1.17	0.0782	0.06122	0.0677	0.06905	0.00403	0.002329
60	1.32	1.31	1.29	1.22	1.24	1.25	0.0394	0.02745	0.0157	0.02752	0.00557	0.003215
65	1.53	1.52	1.5	1.31	1.27	1.3	0.0775	0.08961	0.0714	0.0795	0.00436	0.00252
70	1.38	1.39	1.4	1.32	1.34	1.36	0.0222	0.01832	0.0145	0.01834	0.00182	0.001052

Table A.8.2 Detector at 10 deg

Lithium			Signal Intensities					DOLP				
Angles		CO-polarised			Cross-Polaris		d1	d2	d3	Avg	S.D	SEM
10	237	241	233	195	201	202	0.0972	0.0905	0.0713	0.08633	0.00635	0.003667
15	422	425	426	399	402	406	0.028	0.02781	0.024	0.02662	0.00106	0.000609
20	329	312	319	314	309	306	0.0233	0.00483	0.0208	0.01632	0.00473	0.00273
25	376	380	384	310	312	316	0.0962	0.09827	0.0971	0.09721	0.00049	0.00028
30	476	484	490	456	460	462	0.0215	0.02542	0.0294	0.02543	0.00187	0.001082
35	736	740	752	620	618	622	0.0855	0.08984	0.0946	0.09	0.00214	0.001235
40	890	916	886	760	764	768	0.0788	0.09048	0.0713	0.0802	0.00455	0.002625
45	2.01	2.02	2.03	0.78	0.78	0.786	0.4409	0.44492	0.4418	0.44251	0.00101	0.00058
50	1	1.01	1.02	0.89	0.9	0.91	0.0582	0.05759	0.057	0.0576	0.00028	0.000164
55	0.97	0.99	1	0.85	0.84	0.86	0.0659	0.08197	0.0753	0.07439	0.0038	0.002192
60	1.08	1.09	1.12	0.85	0.87	0.88	0.1192	0.11224	0.12	0.11714	0.00201	0.001159
65	880	890	870	820	830	840	0.0353	0.03488	0.0175	0.02924	0.00478	0.002758
70	860	870	880	810	820	840	0.0299	0.02959	0.0233	0.02759	0.00177	0.001024

Table A.8.3 Detector at 20 deg

Lithium			Signal Intensities				DOLP				
Angles		CO-polarised			Cross-Polaris	d1	d2	d3	Avg	S.D	SEM
0	364	368	370	360	364	368	0.00552	0.00546	0.00271	0.00457	0.00076	0.000438
5	408	412	406	396	400	404	0.01493	0.01478	0.00247	0.01072	0.00337	0.001946
10	476	480	484	456	469	448	0.02146	0.01159	0.03863	0.02389	0.00645	0.003723
15	452	456	460	428	430	432	0.02727	0.02935	0.03139	0.02934	0.00097	0.00056
20	1.38	1.39	1.4	0.65	0.66	0.67	0.35961	0.3561	0.35266	0.35612	0.00164	0.000946
25	1.2	1.17	1.19	0.65	0.66	0.67	0.2973	0.27869	0.27957	0.28519	0.00495	0.002857
30	1.07	1.08	1.09	0.73	0.74	0.76	0.18889	0.18681	0.17838	0.18469	0.00262	0.001515
35	1.31	1.3	1.31	0.76	0.75	0.78	0.2657	0.26829	0.25359	0.26253	0.0037	0.002136
40	970	950	960	700	710	720	0.16168	0.14458	0.14286	0.1497	0.0049	0.002832
45	730	740	750	650	660	670	0.05797	0.05714	0.05634	0.05715	0.00038	0.000222
50	810	850	820	650	660	670	0.10959	0.12583	0.10067	0.11203	0.00601	0.003471
55	760	770	750	690	680	700	0.04828	0.06207	0.03448	0.04828	0.0065	0.003754
60	770	780	790	750	760	770	0.01316	0.01299	0.01282	0.01299	8E-05	4.59E-05
65	740	750	722	700	710	720	0.02778	0.0274	0.00139	0.01885	0.00713	0.004117
70	700	710	720	650	660	670	0.03704	0.0365	0.03597	0.0365	0.00025	0.000145

Table A.8.4 Detector at 30 deg

Lithium			Signal Intensities				DOLP				
Angles		CO-polarised			Cross-Polari	d1	d2	d3	Avg	S.D	SEM
0	302	306	308	296	298	294	0.01003	0.01325	0.02326	0.01551	0.00325	0.001877
5	396	400	402	376	378	382	0.02591	0.02828	0.02551	0.02656	0.00071	0.000407
10	376	380	384	336	340	342	0.05618	0.05556	0.05785	0.05653	0.00056	0.000323
15	330	328	332	290	294	296	0.06452	0.05466	0.05732	0.05883	0.0024	0.001387
20	428	430	434	374	368	380	0.06733	0.07769	0.06634	0.07045	0.00296	0.001712
25	930	940	950	610	630	640	0.20779	0.19745	0.19497	0.20007	0.00321	0.001851
30	1.77	1.71	1.7	0.61	0.63	0.64	0.48739	0.46154	0.45299	0.46731	0.00844	0.004875
35	1.23	1.24	1.25	0.67	0.69	0.68	0.29474	0.28497	0.29534	0.29168	0.00274	0.001583
40	720	730	750	570	580	590	0.11628	0.1145	0.1194	0.11673	0.00117	0.000675
45	690	700	710	640	650	660	0.03759	0.03704	0.0365	0.03704	0.00026	0.000149
50	720	730	750	630	640	650	0.06667	0.06569	0.07143	0.06793	0.00145	0.000835
55	710	720	730	670	680	690	0.02899	0.02857	0.02817	0.02858	0.00019	0.000111
60	670	680	690	610	620	630	0.04688	0.04615	0.04545	0.04616	0.00033	0.000193
65	660	650	640	600	610	620	0.04762	0.03175	0.01587	0.03175	0.00748	0.00432
70	630	640	650	590	600	610	0.03279	0.03226	0.03175	0.03226	0.00025	0.000142

Table A.8.5 Detector at 40 deg

Lithium			Signal Intensities			d1	DOLP				
Angles		CO-polarised		Cross-Polarise		d1	d2	d3	Avg	S.D	SEM
0	0.99	0.98	1	0.93	0.94	0.92	0.031	0.0208	0.0417	0.03125	0.0049	0.002835
5	1.05	1.06	1.04	0.93	0.96	0.94	0.061	0.0495	0.0505	0.05354	0.0029	0.001671
10	1.07	1.08	1.09	1.03	1.04	1.05	0.019	0.0189	0.0187	0.01887	8E-05	4.85E-05
15	1.17	1.16	1.15	1.11	1.13	1.14	0.026	0.0131	0.0044	0.01459	0.0052	0.003008
20	1.19	1.2	1.18	1.14	1.15	1.16	0.021	0.0213	0.0085	0.01709	0.0035	0.002015
25	1.36	1.34	1.39	1.28	1.29	1.31	0.03	0.019	0.0296	0.02631	0.003	0.001724
30	1.72	1.74	1.67	1.32	1.34	1.35	0.132	0.1299	0.106	0.12247	0.0068	0.003898
35	1.5	1.52	1.51	1.29	1.28	1.3	0.075	0.0857	0.0747	0.07857	0.0029	0.001685
40	1.43	1.44	1.45	1.28	1.29	1.3	0.055	0.0549	0.0545	0.05495	0.0002	0.00011
45	1.39	1.4	1.36	1.29	1.3	1.31	0.037	0.037	0.0187	0.03103	0.005	0.002899
50	1.39	1.4	1.41	1.24	1.26	1.28	0.057	0.0526	0.0483	0.05266	0.0021	0.001185
55	1.38	1.39	1.4	1.27	1.26	1.24	0.042	0.0491	0.0606	0.05039	0.0045	0.002618
60	1.49	1.51	1.52	1.29	1.31	1.32	0.072	0.0709	0.0704	0.0711	0.0004	0.000211
65	1.48	1.49	1.5	1.26	1.27	1.28	0.08	0.0797	0.0791	0.07971	0.0003	0.000157
70	1.31	1.32	1.3	1.2	1.21	1.22	0.044	0.0435	0.0317	0.03968	0.0032	0.001871

Table A.8.6 Detector at 50 deg

Lithium			Signal Intensities				DOLP				
Angles		CO-polarised			Cross-Polaris		d1	d2	d3	Avg	S.D	SEM
0	640	650	660	570	590	600	0.0579	0.0484	0.048	0.0513	0.0027	0.001551
5	630	640	650	620	610	630	0.008	0.024	0.016	0.0159	0.0038	0.002178
10	710	720	730	620	640	650	0.0677	0.0588	0.058	0.0615	0.0025	0.001462
15	740	750	730	680	698	700	0.0423	0.0359	0.021	0.033	0.0051	0.002973
20	810	820	830	740	750	720	0.0452	0.0446	0.071	0.0536	0.0071	0.004101
25	1.51	1.48	1.49	0.67	0.66	0.65	0.3853	0.3832	0.393	0.387	0.0023	0.001332
30	970	980	990	600	610	620	0.2357	0.2327	0.23	0.2327	0.0014	0.000797
35	910	950	920	600	610	620	0.2053	0.2179	0.195	0.206	0.0055	0.003154
40	700	690	710	650	660	670	0.037	0.0222	0.029	0.0294	0.0035	0.002019
45	750	770	780	700	730	690	0.0345	0.0267	0.061	0.0408	0.0085	0.004932
50	750	770	780	730	740	750	0.0135	0.0199	0.02	0.0177	0.0017	0.000979
55	700	680	690	620	630	640	0.0606	0.0382	0.038	0.0455	0.0062	0.003572
60	710	720	730	610	620	630	0.0758	0.0746	0.074	0.0746	0.0005	0.000303
65	680	690	700	600	610	620	0.0625	0.0615	0.061	0.0615	0.0004	0.000258
70	710	730	740	630	640	650	0.0597	0.0657	0.065	0.0634	0.0015	0.000877

Table A.8.7 Detector at 60 deg

Lithium			Signal Intensities					DOLP				
Angles		CO-polarised			Cross-Polaris		d1	d2	d3	Avg	S.D	SEM
0	388	386	390	268	264	270	0.1829	0.1877	0.1818	0.1841	0.0015	0.000849
5	556	560	564	322	324	320	0.2665	0.267	0.276	0.2698	0.0025	0.001459
10	330	332	336	298	300	304	0.051	0.0506	0.05	0.0505	0.0002	0.000132
15	400	404	398	350	356	348	0.0667	0.0632	0.067	0.0656	0.001	0.000581
20	394	392	390	334	332	328	0.0824	0.0829	0.0864	0.0839	0.001	0.000586
25	374	378	372	354	360	352	0.0275	0.0244	0.0276	0.0265	0.0009	0.000497
30	430	438	434	354	350	358	0.0969	0.1117	0.096	0.1015	0.0042	0.002396
35	454	458	450	390	388	392	0.0758	0.0827	0.0689	0.0758	0.0033	0.001886
40	452	446	436	390	386	394	0.0736	0.0721	0.0506	0.0655	0.0061	0.003506
45	400	398	404	376	380	384	0.0309	0.0231	0.0254	0.0265	0.0019	0.001092
50	416	420	412	340	344	334	0.1005	0.0995	0.1046	0.1015	0.0013	0.00073
55	390	388	392	328	330	334	0.0864	0.0808	0.0799	0.0823	0.0017	0.000953
60	408	404	412	360	362	364	0.0625	0.0548	0.0619	0.0597	0.002	0.001158
65	420	416	424	372	374	378	0.0606	0.0532	0.0574	0.057	0.0018	0.001015
70	380	382	384	340	342	336	0.0556	0.0552	0.0667	0.0592	0.0031	0.001771
75	310	308	312	274	276	272	0.0616	0.0548	0.0685	0.0616	0.0032	0.001864

9) Windowless polysilicon solar panel

Table A.9.1 Detector at 0 deg

Poly-1			Signal Intensities					DOLP				
Angles		CO-polarised			Cross-Polarise		d1	d2	d3	Avg.	S.D	SEM
25	262	258	253	247	255	252	0.0295	0.0058	0.002	0.01243	0.00701	0.00405
30	331	329	334	256	267	255	0.1278	0.104	0.1341	0.12197	0.00748	0.004318
35	307	319	316	272	275	274	0.0604	0.0741	0.0712	0.06857	0.00338	0.001954
40	291	295	292	252	255	254	0.0718	0.0727	0.0696	0.07138	0.00076	0.000438
45	420	426	428	284	290	275	0.1932	0.1899	0.2176	0.20025	0.00714	0.004121
50	304	310	306	272	274	276	0.0556	0.0616	0.0515	0.05625	0.0024	0.001384
55	438	444	432	338	340	330	0.1289	0.1327	0.1339	0.13179	0.00123	0.000709
60	356	360	364	286	290	294	0.109	0.1077	0.1064	0.1077	0.00062	0.000361
65	340	346	348	290	288	292	0.0794	0.0915	0.0875	0.08612	0.00291	0.001681

Table A.9.2 Detector at 10 deg

Poly-1			Signal Intensities					DOLP				
Angles		CO-polarised			Cross-Polarise		d1	d2	d3	Avg.	S.D	SEM
20	257	260	264	228	231	237	0.0598	0.05906	0.05389	0.05758	0.001517	0.000876
25	278	272	271	242	244	247	0.0692	0.05426	0.04633	0.05661	0.005482	0.003165
30	265	263	270	236	239	241	0.0579	0.04781	0.05675	0.05415	0.002602	0.001502
35	301	303	307	232	233	228	0.1295	0.1306	0.14766	0.13591	0.004808	0.002776
40	255	260	263	229	231	233	0.0537	0.05906	0.06048	0.05776	0.001682	0.000971
45	295	297	303	241	244	246	0.1007	0.09797	0.10383	0.10085	0.001381	0.000798
50	404	396	398	310	312	316	0.1317	0.11864	0.11485	0.12171	0.004155	0.002399
55	330	324	332	252	258	254	0.134	0.1134	0.13311	0.12684	0.005491	0.00317
60	310	306	308	244	248	250	0.1191	0.10469	0.10394	0.10926	0.004036	0.00233
65	276	280	282	240	244	248	0.0698	0.0687	0.06415	0.06754	0.001406	0.000812

Table A.9.3 Detector at 20 deg

Poly-1			Signal Intensities				DOLP				
Angles		CO-polarised			Cross-Polaris	d1	d2	d3	Avg.	S.D	SEM
0	66	62	64	56	58	60	0.08197	0.03333	0.0323	0.04919	0.01339	0.007728
5	70	74	78	62	70	68	0.06061	0.02778	0.0685	0.05229	0.01018	0.005877
10	92	96	90	78	80	88	0.08235	0.09091	0.0112	0.0615	0.02062	0.011904
15	100	104	106	88	90	92	0.06383	0.07216	0.0707	0.0689	0.0021	0.001212
20	164	160	168	148	150	154	0.05128	0.03226	0.0435	0.04234	0.00451	0.002603
25	214	210	216	156	166	162	0.15676	0.11702	0.1429	0.13888	0.00951	0.005488
30	182	188	190	162	168	166	0.05814	0.05618	0.0674	0.06058	0.00283	0.001634
35	168	172	166	158	162	164	0.03067	0.02994	0.0061	0.02223	0.0066	0.003811
40	192	196	198	178	182	184	0.03784	0.03704	0.0366	0.03717	0.00029	0.000165
45	174	176	172	152	158	162	0.06748	0.05389	0.0299	0.05044	0.00896	0.005174
50	202	204	208	176	178	174	0.06878	0.06806	0.089	0.07528	0.0056	0.003236
55	190	192	188	174	176	178	0.04396	0.04348	0.0273	0.03825	0.00446	0.002577
60	186	184	182	178	174	172	0.02198	0.02793	0.0282	0.02605	0.00167	0.000961
65	178	180	182	176	174	170	0.00565	0.01695	0.0341	0.0189	0.00675	0.003897

Table A.9.4 Detector at 30 deg

Poly-1			Signal Intensities				DOLP				
Angles		CO-polarised			Cross-Polar	d1	d2	d3	Avg.	S.D	SEM
0	100	104	106	98	102	104	0.0101	0.00971	0.00952	0.00978	0.00014	8.02E-05
5	112	110	114	100	104	108	0.0566	0.02804	0.02703	0.03722	0.00792	0.00457
10	118	122	124	114	116	118	0.01724	0.02521	0.02479	0.02241	0.00211	0.001221
15	162	164	168	128	130	132	0.11724	0.11565	0.12	0.11763	0.00104	0.000599
20	170	174	178	152	154	156	0.0559	0.06098	0.06587	0.06091	0.00235	0.001356
25	180	178	174	142	144	152	0.11801	0.10559	0.06748	0.09703	0.01241	0.007166
30	228	230	236	182	184	188	0.1122	0.11111	0.11321	0.11217	0.00049	0.000285
35	226	228	230	176	178	182	0.12438	0.12315	0.1165	0.12135	0.002	0.001153
40	210	208	214	182	186	180	0.07143	0.05584	0.08629	0.07119	0.00718	0.004145
45	202	200	198	180	182	186	0.05759	0.04712	0.03125	0.04532	0.00625	0.00361
50	244	242	246	190	192	196	0.12442	0.11521	0.11312	0.11758	0.00284	0.001637
55	194	196	190	170	180	184	0.06593	0.04255	0.01604	0.04151	0.01177	0.006794
60	208	204	202	180	182	186	0.07216	0.05699	0.04124	0.0568	0.00729	0.004209
65	212	210	208	190	192	198	0.05473	0.04478	0.02463	0.04138	0.00723	0.004173

Table A.9.5 Detector at 40 deg

Poly-1			Signal Intensities				DOLP				
Angles		CO-polarised			Cross-Polaris	d1	d2	d3	Avg.	S.D	SEM
0	252	257	253	245	242	247	0.0141	0.03006	0.012	0.01871	0.00466	0.002689
5	274	273	275	241	242	237	0.0641	0.06019	0.07422	0.06616	0.00341	0.001971
10	314	317	315	242	246	250	0.1295	0.12611	0.11504	0.12355	0.00356	0.002057
15	310	307	308	246	250	251	0.1151	0.10233	0.10197	0.10647	0.00353	0.002037
20	291	283	287	244	243	245	0.0879	0.07605	0.07895	0.08095	0.0029	0.001674
25	295	292	293	243	244	248	0.0967	0.08955	0.08318	0.0898	0.00318	0.001835
30	354	367	365	255	254	253	0.1626	0.18196	0.18123	0.17525	0.00518	0.002993
35	333	337	339	249	252	247	0.1443	0.14431	0.157	0.14855	0.00345	0.001992
40	275	263	274	241	239	244	0.0659	0.04781	0.05792	0.05721	0.00427	0.002466
45	271	272	278	243	241	245	0.0545	0.06043	0.0631	0.05933	0.00208	0.001201
50	331	335	337	253	247	249	0.1336	0.1512	0.15017	0.14498	0.00467	0.002695
55	271	262	277	251	249	252	0.0383	0.02544	0.04726	0.037	0.00517	0.002985
60	306	307	305	252	254	248	0.0968	0.09447	0.10307	0.09811	0.0021	0.001212
65	303	300	297	247	252	254	0.1018	0.08696	0.07804	0.08894	0.00566	0.003269

Table A.9.6 Detector at 50 deg

Poly-1			Signal Intensities				DOLP				
Angles		CO-polarised			Cross-Polarise	d1	d2	d3	Avg.	S.D	SEM
0	59	60	61	43	48	41	0.15686	0.11111	0.19608	0.15468	0.02005	0.011574
5	77	79	80	47	48	49	0.24194	0.24409	0.24031	0.24211	0.00089	0.000517
10	76	77	70	52	53	57	0.1875	0.18462	0.10236	0.15816	0.02279	0.013157
15	85	88	87	58	60	63	0.18881	0.18919	0.16	0.17933	0.00789	0.004557
20	82	87	89	58	62	67	0.17143	0.16779	0.14103	0.16008	0.00783	0.004518
25	115	112	113	57	63	68	0.33721	0.28	0.24862	0.28861	0.02117	0.012225
30	106	107	110	64	74	79	0.24706	0.18232	0.16402	0.1978	0.02057	0.011874
35	67	73	74	42	49	52	0.22936	0.19672	0.1746	0.20023	0.01298	0.007497
40	97	94	95	70	77	72	0.16168	0.09942	0.13772	0.13294	0.0148	0.008547
45	154	158	156	98	100	104	0.22222	0.22481	0.2	0.21568	0.00643	0.003712
50	97	101	92	77	75	85	0.11494	0.14773	0.03955	0.10074	0.02615	0.015097
55	112	113	114	79	84	89	0.17277	0.14721	0.12315	0.14771	0.0117	0.006754
60	127	130	132	90	92	93	0.17051	0.17117	0.17333	0.17167	0.0007	0.000402
65	118	120	122	98	100	102	0.09259	0.09091	0.08929	0.09093	0.00078	0.00045

Table A.9.7 Detector at 60 deg

Poly-1			Signal Intensities				DOLP				
Angles		CO-polarised			Cross-Polaris	d1	d2	d3	Avg.	S.D	SEM
0	141	143	144	128	132	134	0.04833	0.04	0.03597	0.04143	0.00297	0.001715
5	151	152	154	135	133	131	0.05594	0.06667	0.0807	0.06777	0.005853	0.003379
10	180	181	169	136	139	140	0.13924	0.13125	0.09385	0.12145	0.011422	0.006595
15	172	174	177	141	143	137	0.09904	0.09779	0.12739	0.10807	0.007891	0.004556
20	159	154	152	132	136	138	0.09278	0.06207	0.04828	0.06771	0.01074	0.006201
25	156	165	159	142	139	145	0.04698	0.08553	0.04605	0.05952	0.010619	0.006131
30	197	198	195	92	102	100	0.36332	0.32	0.32203	0.33512	0.011524	0.006653
35	171	169	167	133	136	130	0.125	0.1082	0.12458	0.11926	0.004517	0.002608
40	161	164	159	118	120	124	0.15412	0.15493	0.12367	0.14424	0.008399	0.004849
45	168	172	165	159	152	157	0.02752	0.06173	0.02484	0.03803	0.009695	0.005597
50	177	181	183	161	160	159	0.04734	0.06158	0.07018	0.0597	0.005438	0.003139
55	168	164	170	157	160	162	0.03385	0.01235	0.0241	0.02343	0.005075	0.00293
60	177	181	185	167	164	158	0.02907	0.04928	0.07872	0.05235	0.011769	0.006795

10) Polysilicon solar panel with glass window

Table A.10.1 Detector at 10 deg

Poly-2			Signal Intensities				DOLP				
Angles		CO-polarised			Cross-Polar	d1	d2	d3	Avg.	S.D	SEM
20	97	91	103	92	87	88	0.02646	0.02247	0.07853	0.04249	0.01475	0.008514
22.5	128	120	116	96	102	98	0.14286	0.08108	0.08411	0.10268	0.01642	0.009478
25	136	129	140	94	107	96	0.18261	0.09322	0.18644	0.15409	0.02487	0.014357
27.5	152	136	138	108	112	116	0.16923	0.09677	0.08661	0.11754	0.02124	0.012262
30	158	160	159	101	96	104	0.22008	0.25	0.20913	0.2264	0.00997	0.005759
32.5	16.1	16.2	16.5	1.8	1.9	1.7	0.79888	0.79006	0.81319	0.80071	0.0055	0.003177
35	466	462	464	180	174	186	0.44272	0.45283	0.42769	0.44108	0.00596	0.003443
37.5	332	334	336	152	154	156	0.3719	0.36885	0.36585	0.36887	0.00143	0.000823
40	238	234	232	152	144	150	0.22051	0.2381	0.21466	0.22442	0.00575	0.00332
42.5	220	224	230	140	146	142	0.22222	0.21081	0.23656	0.2232	0.00608	0.003511
45	160	162	168	126	130	132	0.11888	0.10959	0.12	0.11616	0.00269	0.001555
47.5	150	148	142	120	126	128	0.11111	0.08029	0.05185	0.08108	0.01397	0.008066
50	160	162	158	140	144	138	0.06667	0.05882	0.06757	0.06435	0.00227	0.001309

Table A.10.2 Detector at 20 deg

Poly-2			Signal Intensities				DOLP				
Angles		CO-polarised			Cross-Polari	d1	d2	d3	Avg.	S.D	SEM
17.5	92	97	105	88	89	87	0.02222	0.043	0.0938	0.05299	0.017345	0.010014
20	116	114	112	98	92	97	0.08411	0.1068	0.0718	0.08756	0.008375	0.004835
22.5	360	380	370	262	264	282	0.15756	0.1801	0.135	0.15755	0.010643	0.006145
25	412	443	462	218	212	222	0.30794	0.3527	0.3509	0.33716	0.011939	0.006893
27.5	7.2	7.3	7.4	2.1	2.2	2.3	0.54839	0.5368	0.5258	0.537	0.005331	0.003078
30	15.8	15.9	16.2	1.7	1.8	1.9	0.80571	0.7966	0.7901	0.79746	0.003707	0.00214
32.5	1.3	1.4	1.6	0.99	0.99	0.9	0.13339	0.1706	0.28	0.19465	0.035928	0.020743
35	762	764	772	552	564	558	0.15982	0.1506	0.1609	0.15711	0.002668	0.00154
37.5	436	430	442	362	360	368	0.09273	0.0886	0.0914	0.0909	0.00099	0.000572
40	264	258	272	202	212	216	0.13305	0.0979	0.1148	0.11522	0.008293	0.004788
42.5	164	162	168	138	142	140	0.08609	0.0658	0.0909	0.08093	0.006285	0.003628
45	116	112	110	96	98	102	0.09434	0.0667	0.0377	0.06625	0.013343	0.007703

Table A.10.3 Detector at 30 deg

Poly-2			Signal Intensities				DOLP				
Angles		CO-polarised			Cross-Polaris	d1	d2	d3	Avg.	S.D	SEM
15	280	292	296	254	268	260	0.0487	0.0429	0.06475	0.0521	0.00534	0.003085
17.5	372	368	370	264	272	280	0.1698	0.15	0.13846	0.15276	0.00747	0.004315
20	432	440	436	288	296	292	0.2	0.1957	0.1978	0.19782	0.00102	0.000592
22.5	504	520	508	308	304	300	0.2414	0.2621	0.25743	0.25365	0.00513	0.002962
25	616	608	612	306	310	316	0.3362	0.3246	0.31897	0.3266	0.00415	0.002395
27.5	15.6	15.1	15.3	1.7	1.9	2.2	0.8035	0.7765	0.74857	0.77617	0.01294	0.007471
30	1.2	1.35	1.22	0.66	0.67	0.668	0.2903	0.3353	0.29237	0.306	0.01198	0.006914
32.5	466	475	489	280	262	254	0.2493	0.289	0.31629	0.28487	0.01587	0.009163
35	432	440	445	285	290	282	0.205	0.2055	0.22421	0.21157	0.00516	0.00298
37.5	350	345	330	272	254	265	0.1254	0.1519	0.10924	0.12886	0.01016	0.005864
40	255	250	260	228	212	225	0.0559	0.0823	0.07216	0.07011	0.00627	0.003619

Table A.10.4 Detector at 40 deg

Poly-2			Signal Intensities				DOLP				
Angles		CO-polarised			Cross-Polarise	d1	d2	d3	Avg.	S.D	SEM
15	92	94	92	88	86	90	0.02222	0.04444	0.01099	0.02589	0.00803	0.004634
17.5	250	212	225	116	122	118	0.36612	0.26946	0.31195	0.31584	0.02284	0.013186
20	770	752	734	232	238	229	0.53693	0.51919	0.5244	0.52684	0.0043	0.002481
22.5	16.1	15.9	16.2	1.6	1.4	1.3	0.81921	0.83815	0.85143	0.83626	0.00763	0.004407
25	8.2	8.6	8.3	1.1	1.2	1.3	0.76344	0.7551	0.72917	0.74924	0.00843	0.004865
27.5	2.4	2.2	2.5	0.91	0.92	0.9	0.45015	0.41026	0.47059	0.44367	0.01446	0.008351
30	1.1	1.2	1.3	0.55	0.59	0.52	0.33333	0.34078	0.42857	0.36756	0.02497	0.014416
32.5	690	625	632	262	264	280	0.44958	0.40607	0.38596	0.41387	0.01533	0.00885
35	556	548	552	312	316	308	0.28111	0.26852	0.28372	0.27778	0.00383	0.002212
37.5	392	394	402	310	312	302	0.11681	0.11615	0.14205	0.125	0.00696	0.004019
40	216	208	202	162	168	172	0.14286	0.10638	0.08021	0.10982	0.01483	0.008563
42.5	116	112	114	96	92	94	0.09434	0.09804	0.09615	0.09618	0.00087	0.000503

Table A.10.5 Detector at 50 deg

Poly-2			Signal Intensities				DOLP				
Angles		CO-polarised			Cross-Polarise	d1	d2	d3	Avg.	S.D	SEM
10	116	112	108	94	102	98	0.10476	0.04673	0.04854	0.06668	0.01555	0.00898
12.5	168	152	160	104	122	118	0.23529	0.10949	0.15108	0.16529	0.03021	0.017444
15	770	772	768	252	260	268	0.50685	0.49612	0.48263	0.4952	0.00572	0.003304
17.5	5.6	5.8	6.2	0.66	0.665	0.68	0.78914	0.79428	0.80233	0.79525	0.00313	0.001809
20	16.2	16.4	16.3	1.8	1.9	2.1	0.8	0.79235	0.77174	0.78803	0.00689	0.003978
22.5	1.2	1.4	1.3	0.44	0.432	0.448	0.46341	0.52838	0.48741	0.49307	0.01549	0.008941
25	680	675	692	256	262	260	0.45299	0.44077	0.45378	0.44918	0.00344	0.001986
27.5	514	512	502	220	232	230	0.40054	0.37634	0.37158	0.38282	0.00732	0.004227
30	312	308	322	202	212	216	0.21401	0.18462	0.19703	0.19855	0.00696	0.004016
32.5	118	112	116	104	108	110	0.06306	0.01818	0.02655	0.03593	0.01125	0.006496

Table A.10.6 Detector at 60 deg

Poly-2			Signal Intensities				DOLP				
Angles		CO-polarised			Cross-Polaris	d1	d2	d3	Avg.	S.D	SEM
5	430	442	444	384	392	376	0.05651	0.05995	0.08293	0.06646	0.00677	0.003909
7.5	580	590	600	442	436	434	0.13503	0.1501	0.16054	0.14856	0.00605	0.003491
10	708	692	694	440	432	436	0.23345	0.23132	0.22832	0.23103	0.00122	0.000702
12.5	1.16	1.12	1.2	0.52	0.52	0.53	0.38425	0.36253	0.38728	0.37802	0.00636	0.003674
15	16.1	16.2	15.9	1.2	1.3	1.4	0.86127	0.85143	0.83815	0.85028	0.00547	0.003158
17.5	1.568	1.564	1.55	0.42	0.42	0.42	0.5743	0.57661	0.5752	0.57537	0.00055	0.000318
20	462	474	470	160	162	165	0.48553	0.49057	0.48031	0.48547	0.00242	0.001395
22.5	452	455	448	152	157	158	0.49669	0.48693	0.47855	0.48739	0.00428	0.002471
25	362	338	342	140	143	145	0.44223	0.40541	0.40452	0.41738	0.01015	0.005858
27.5	275	280	282	260	258	254	0.02804	0.04089	0.05224	0.04039	0.00571	0.003296
30	232	235	248	212	214	216	0.04505	0.04677	0.06897	0.05359	0.00629	0.003631

11) Amorphous silicon solar panel with glass window

Table A.11.1 Detector at 10 deg

Amor-Si			Signal Intensities					DOLP				
Angles		CO-polarised			Cross-Polaris		d1	d2	d3	Avg.	S.D	SEM
17.5	104	102	106	98	99	101	0.0297	0.0149	0.02415	0.02293	0.00352	0.002032
20	163	158	152	136	138	133	0.0903	0.0676	0.06667	0.07485	0.00631	0.003645
22.5	216	222	217	182	188	183	0.0854	0.0829	0.085	0.08445	0.00063	0.000364
25	432	415	417	360	372	378	0.0909	0.0546	0.04906	0.06487	0.01071	0.006185
27.5	636	648	652	512	514	516	0.108	0.1153	0.11644	0.11326	0.00216	0.001245
30	962	945	956	652	648	651	0.1921	0.1864	0.18979	0.18943	0.00133	0.000771
32.5	5.2	5.4	5.6	3.6	3.2	3.1	0.1818	0.2558	0.28736	0.24166	0.02554	0.014744
35	15.9	16	15.7	1.9	1.6	1.3	0.7865	0.8182	0.84706	0.81725	0.01427	0.008242
37.5	735	736	714	532	534	563	0.1602	0.1591	0.11825	0.14584	0.01127	0.006506
40	411	416	419	312	398	390	0.1369	0.0221	0.03585	0.06496	0.02956	0.017065
42.5	216	225	221	202	210	215	0.0335	0.0345	0.01376	0.02725	0.00551	0.003181
45	148	139	144	132	134	136	0.0571	0.0183	0.02857	0.03468	0.00949	0.005476

Table A.11.2 Detector at 20 deg

Amor-Si			Signal Intensities					DOLP				
Angles		CO-polarised			Cross-Polaris		d1	d2	d3	Avg.	S.D	SEM
15	89	92	90	82	87	85	0.0409	0.0279	0.0286	0.03248	0.00346	0.001995
17.5	102	106	108	98	96	100	0.02	0.0495	0.0385	0.03599	0.00703	0.004057
20	132	136	139	111	108	104	0.0864	0.1148	0.144	0.11507	0.01358	0.007841
22.5	215	210	208	166	162	172	0.1286	0.129	0.0947	0.11746	0.00928	0.005356
25	292	296	298	230	231	236	0.1188	0.1233	0.1161	0.11941	0.00172	0.000996
27.5	412	416	419	308	306	304	0.1444	0.1524	0.1591	0.15195	0.00345	0.001991
30	4.9	4.2	4.6	3.1	3.3	3.4	0.225	0.12	0.15	0.165	0.0255	0.01472
32.5	15.9	15.8	15.7	1.9	2.1	1.8	0.7865	0.7654	0.7943	0.78206	0.00706	0.004074
35	5.6	5.7	5.8	3.8	3.9	3.7	0.1915	0.1875	0.2211	0.20001	0.00864	0.004988
37.5	812	816	819	740	738	736	0.0464	0.0502	0.0534	0.04999	0.00165	0.000952
40	542	538	514	492	495	498	0.0484	0.0416	0.0158	0.03526	0.0081	0.004676
42.5	316	318	317	298	301	306	0.0293	0.0275	0.0177	0.02481	0.00295	0.001705
45	162	164	168	148	151	152	0.0452	0.0413	0.05	0.04548	0.00206	0.00119

Table A.11.3 Detector at 30 deg

Amor-Si			Signal Intensities				DOLP				
Angles		CO-polarised			Cross-Polari		d1	d2	d3	Avg.	S.D	SEM
12.5	112	116	118	96	98	102	0.0769	0.0841	0.07273	0.07792	0.00271	0.001567
15	126	129	127	112	104	108	0.0588	0.1073	0.08085	0.08232	0.01144	0.006605
17.5	225	216	212	168	169	172	0.145	0.1221	0.10417	0.12376	0.00966	0.005576
20	332	329	331	278	277	272	0.0885	0.0858	0.09784	0.09073	0.00298	0.001718
22.5	772	768	770	498	492	490	0.2157	0.219	0.22222	0.21901	0.00153	0.000881
25	6.5	6.2	6.4	3.5	3.6	3.7	0.3	0.2653	0.26733	0.27754	0.00918	0.0053
27.5	15.9	15.8	15.7	1.9	2	1.7	0.7865	0.7753	0.8046	0.7888	0.00697	0.004026
30	3.3	3.4	3.5	1.3	1.4	1.5	0.4348	0.4167	0.4	0.41715	0.0082	0.004735
32.5	1.7	1.4	1.5	0.72	0.73	0.74	0.405	0.3146	0.33929	0.35293	0.02202	0.012716
25	292	293	298	148	152	154	0.3273	0.3169	0.31858	0.3209	0.00263	0.00152
37.5	168	164	160	136	134	139	0.1053	0.1007	0.07023	0.09206	0.00897	0.005181
40	113	116	119	108	112	104	0.0226	0.0175	0.06726	0.03581	0.0129	0.007446

Table A.11.4 Detector at 40 deg

Amor-Si			Signal Intensities					DOLP				
Angles		CO-polarised			Cross-Polar		d1	d2	d3	Avg.	S.D	SEM
7.5	128	132	134	116	112	108	0.0492	0.08197	0.10744	0.0795	0.01377	0.007949
10	246	240	238	198	192	196	0.1081	0.11111	0.09677	0.1053	0.00356	0.002058
12.5	318	320	319	280	284	278	0.0635	0.0596	0.06868	0.0639	0.00214	0.001238
15	512	508	506	396	392	390	0.1278	0.12889	0.12946	0.1287	0.00041	0.000237
17.5	1.1	1.2	1.3	0.99	0.98	0.97	0.0526	0.10092	0.14537	0.0996	0.02187	0.012624
20	5.2	5.6	5.3	3.1	3.2	3.3	0.253	0.27273	0.23256	0.2528	0.00947	0.005467
22.5	15.9	15.7	16	1.6	1.7	1.8	0.8171	0.8046	0.79775	0.8065	0.00464	0.002676
25	7.6	7.4	7.3	4.2	4.1	4.3	0.2881	0.28696	0.25862	0.2779	0.00788	0.004548
27.5	992	998	993	636	632	631	0.2187	0.22454	0.22291	0.222	0.00143	0.000824
30	461	468	452	292	298	211	0.2244	0.22193	0.3635	0.27	0.03819	0.022051
32.5	238	240	242	201	211	213	0.0843	0.0643	0.06374	0.0708	0.00552	0.003185
35	132	134	130	112	116	118	0.082	0.072	0.04839	0.0675	0.00813	0.004694

Table A.11.5 Detector at 50 deg

Amor-Si			Signal Intensities				DOLP				
Angles		CO-polarised			Cross-Polari	d1	d2	d3	Avg.	S.D	SEM
5	213	215	220	200	205	207	0.0315	0.0238	0.0304	0.0286	0.00196	0.001132
7.5	239	243	236	195	200	207	0.1014	0.0971	0.0655	0.088	0.00924	0.005337
10	173	179	168	127	133	132	0.1533	0.1474	0.12	0.1403	0.00839	0.004841
12.5	163	168	170	98	100	102	0.249	0.2537	0.25	0.2509	0.00117	0.000674
15	7.6	7.4	7.3	2.1	2.2	2.3	0.567	0.5417	0.5208	0.5432	0.0109	0.006294
17.5	15.7	15.8	15.9	1.2	1.24	1.28	0.858	0.8545	0.851	0.8545	0.00165	0.000952
20	5.6	5.3	5.2	2.3	2.4	2.5	0.4177	0.3766	0.3506	0.3817	0.01594	0.009204
22.5	177	174	175	134	135	141	0.1383	0.1262	0.1076	0.124	0.00728	0.004205
25	177	172	174	137	134	132	0.1274	0.1242	0.1373	0.1296	0.00321	0.001854
27.5	158	164	168	132	136	138	0.0897	0.0933	0.098	0.0937	0.00198	0.001144
30	145	142	138	127	131	135	0.0662	0.0403	0.011	0.0392	0.01302	0.007515

Table A.11.6 Detector at 60 deg

Amor-Si			Signal Intensities				DOLP				
Angles		CO-polarised			Cross-Polari	d1	d2	d3	Avg.	S.D	SEM
2.5	164	158	162	143	138	136	0.0684	0.06757	0.0872	0.07441	0.00525	0.003029
5	192	211	206	152	149	151	0.1163	0.17222	0.1541	0.14752	0.01345	0.007767
7.5	516	511	513	252	261	259	0.3438	0.32383	0.329	0.3322	0.00487	0.002812
10	7.2	7.3	7.6	2.1	2.2	2.3	0.5484	0.53684	0.5354	0.54019	0.00336	0.001942
12.5	16.1	16.2	16.3	1.1	1.2	1.3	0.8721	0.86207	0.8523	0.86214	0.00467	0.002697
15	5.6	5.9	5.7	1.6	1.7	1.9	0.5556	0.55263	0.5	0.53606	0.01474	0.008509
17.5	1.4	1.5	1.6	0.92	0.98	0.99	0.2069	0.20968	0.2355	0.21737	0.00744	0.004296
20	734	736	738	432	411	416	0.259	0.28335	0.279	0.27379	0.00612	0.003535
22.5	584	580	576	392	298	400	0.1967	0.32118	0.1803	0.23274	0.03631	0.020965
25	216	211	213	138	139	141	0.2203	0.20571	0.2034	0.20981	0.00433	0.002501
27.5	162	168	171	112	116	119	0.1825	0.1831	0.1793	0.18163	0.00096	0.000553
30	132	133	129	108	104	102	0.1	0.12236	0.1169	0.11308	0.00549	0.003172